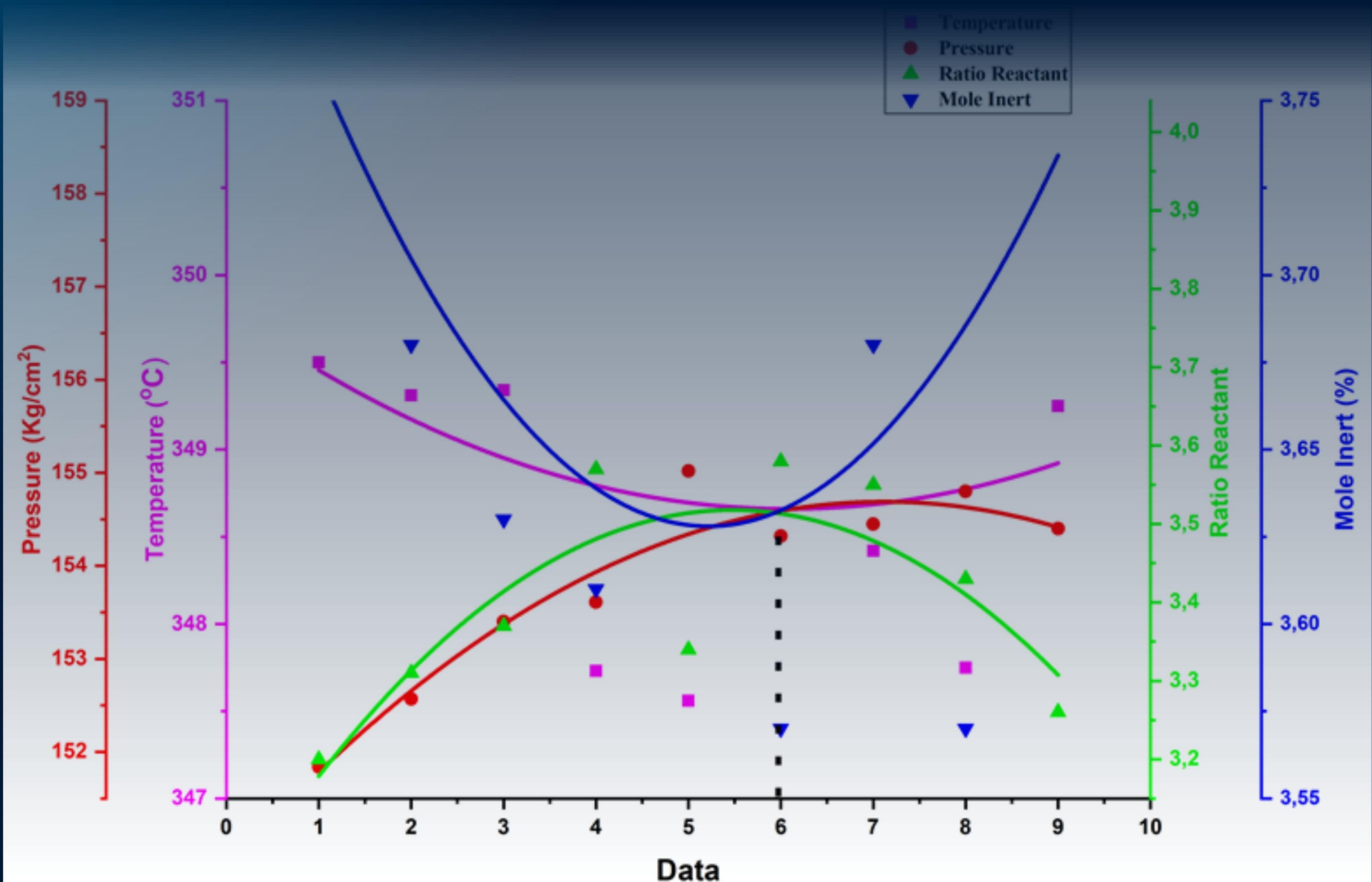
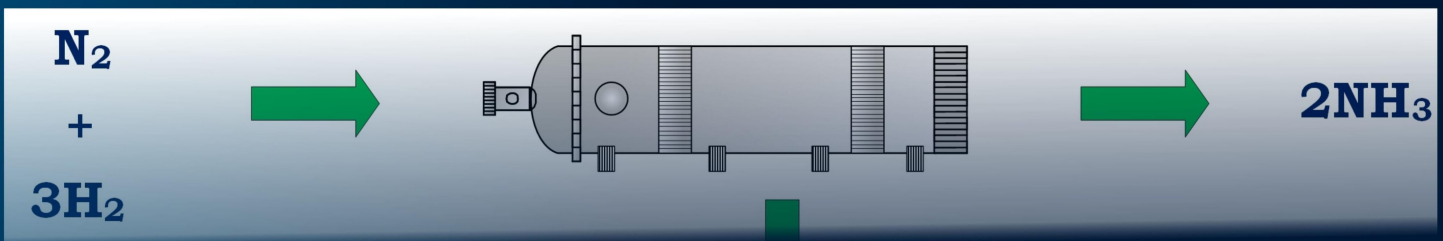




# CHEESA

*CHEMICAL ENGINEERING RESEARCH ARTICLES*



Performance of Ammonia Converter (Susmanto, et al)



# EDITORIAL BOARD

CHEESA: Chemical Engineering Research Articles

<b>Publisher</b>	Universitas PGRI Madiun	
<b>Editor in Chief</b>	Mohammad Arfi Setiawan Universitas PGRI Madiun, Indonesia	
<b>Associate (Handling) Editors</b>	Dr. Heri Septya Kusuma UPN Veteran Yogyakarta, Indonesia Dr. Nur Ihda Farikhatin Nisa Universitas PGRI Madiun, Indonesia Khoirul Ngibad Universitas Maarif Hasyim Latif, Indonesia Dyan Hatining Ayu Sudarni Universitas PGRI Madiun, Indonesia Ade Trisnawati Universitas PGRI Madiun, Indonesia	
<b>Editorial Advisory Board</b>	Prof. Munawar Iqbal University of Education, Lahore, Pakistan Emmanuel O. Oyelude C.K. Tadam University of Technology and Applied Sciences, Ghana Dr. Salfauqi Nurman Universitas Serambi Mekkah, Indonesia Rokiy Alfanaar Universitas Palangka Raya, Indonesia Wahyu Prasetyo Utomo Institut Teknologi Sepuluh Nopember, Indonesia Said Ali Akbar Universitas Serambi Mekkah, Indonesia	
<b>Assistant Editors</b>	Sri Wahyuningsih Universitas PGRI Madiun, Indonesia	
<b>Reviewer</b>	<p>Dr. Sivasamy Sethupathy Jiangsu University, China Prof. Dr. Yantus A.B. Neolaka Universitas Nusa Cendana, Indonesia Prof. Dr. Husni Husin Universitas Syiah Kuala, Indonesia Prof. Dr. Fronthea Swastawati Universitas Diponegoro, Indonesia Prof. Dr. Rieny Sulistijowati Universitas Negeri Gorontalo, Indonesia Prof. Dedy Suhendra, Ph.D Universitas Mataram, Indonesia Prof. Johnner P. Sitompul, Ph.D Institut Teknologi Bandung, Indonesia Prof. Dr. Poedji Loekitowati Hariani Universitas Sriwijaya, Indonesia Prof. Zuchra Helwani Universitas Riau, Indonesia</p>	<p>Prof. Mery Napitupulu Universitas Riau, Indonesia Prof. Dr. Yandi Syukri Universitas Islam Indonesia, Indonesia Rizqy Romadhona Ginting, Ph.D Institut Teknologi Kalimantan, Indonesia Mujtahid Kaavessina, Ph.D Universitas Sebelas Maret, Indonesia Muammar Fawwaz, Ph.D Universitas Muslim Indonesia, Indonesia Dyah Hesti Wardhani, Ph.D Universitas Diponegoro, Indonesia Ronny Purwadi, Ph.D Institut Teknologi Bandung, Indonesia Mochamad Zakki Fahmi, Ph.D Universitas Airlangga, Indonesia</p>



Volume 6 No 1, 2023

ISSN 2614-8757 (Print), ISSN 2615-2347 (Online)

Available online at: <http://e-journal.unipma.ac.id/index.php/cheesa>

Copyright © 2023



Agus Haryanto, Ph.D  
Universitas Lampung, Indonesia  
Erni Misran, Ph.D  
Universitas Sumatera Utara, Indonesia  
Dr. Maktum Muharja  
Universitas Jember, Indonesia  
Dr. Zuhdi Ma'sum  
Universitas Tribhuwana Tunggaladewi, Indonesia  
Dr. Mirna Apriani  
Politeknik Perkapalan Negeri Surabaya, Indonesia  
Dr. Rhenny Ratnawati  
Universitas PGRI Adi Buana Surabaya, Indonesia  
Dr. Agus Budianto  
Institut Teknologi Adhi Tama Surabaya, Indonesia  
Dr. Eng. Dewi Agustina Iryani  
Universitas Lampung, Indonesia  
Dr.-Ing. Anton Irawan  
Universitas Sultan Ageng Tirtayasa, Indonesia  
Dr. rer. nat. Deni Rahmat  
Universitas Pancasila, Indonesia  
Dr. Joko Waluyo  
Universitas Sebelas Maret, Indonesia  
Dr. Dian Kresnadipayana  
Universitas Setia Budi, Indonesia  
Dr. Rahmat Basuki  
Universitas Pertahanan, Indonesia  
Rita Dwi Ratnani  
Universitas Wahid Hasyim, Indonesia  
Ayu Ratna Permanasari  
Politeknik Negeri Bandung, Indonesia  
Felix Arie Setiawan  
Universitas Jember, Indonesia  
Iman Mukhaimin  
Politeknik Kelautan dan Perikanan Karawang, Indonesia  
Cucuk Evi Lusiani  
Politeknik Negeri Malang, Indonesia  
Ella Kusumastuti  
Universitas Negeri Semarang, Indonesia  
Ditta Kharisma Yolanda Putri  
Universitas Jember, Indonesia  
Renova Panjaitan  
UPN Veteran Jawa Timur, Indonesia  
Viona Natalia  
Universitas Sebelas Maret, Indonesia  
Nove Kartika Erliyanti  
UPN Veteran Jawa Timur, Indonesia

**Volume 6 No 1, 2023**

ISSN 2614-8757 (Print), ISSN 2615-2347 (Online)

Available online at: <http://e-journal.unipma.ac.id/index.php/cheesa>

Copyright © 2023

# ACKNOWLEDGMENT

## CHEESA: Chemical Engineering Research Articles

---

Our highest gratitude and appreciation go to the reviewers who have reviewed the submitted manuscripts and provided suggestions to us. The reviewers who contributed to this issue are,

1. Prof. Dr. Poedji Loekitowati Hariani
2. Dr. Sivasamy Sethupathy
3. Ronny Purwadi, Ph.D
4. Erni Misran, Ph.D
5. Dyah Hesti Wardhani, Ph.D
6. Dr. Zuhdi Ma'sum
7. Dr. Dian Kresnadipayana
8. Dr. Salfauqi Nurman
9. Dr. Rahmat Basuki
10. Wahyu Prasetyo Utomo
11. Ayu Ratna Permanasari
12. Rokiy Alfanaar
13. Cucuk Evi Lusiani
14. Nove Kartika Erliyanti

with the seriousness and thoroughness of the reviewers, help us to improve a quality and maintain the quality of writing in the CHEESA: Chemical Engineering Research Articles Volume 6 No 1, June 2023.

Our thanks also go to the various parties who have helped, so that this edition can be published online according to the specified time.

Editorial  
CHEESA

**Volume 6 No 1, 2023**

ISSN 2614-8757 (Print), ISSN 2615-2347 (Online)

Available online at: <http://e-journal.unipma.ac.id/index.php/cheesa>

Copyright © 2023

# TABLE OF CONTENTS

## CHEESA: Chemical Engineering Research Articles

CHEESA is a journal that becomes a media of study for chemical and chemical engineering. This journal serves as a media for publication of research in chemistry and chemical engineering aimed at academics, practitioners and community at large. Articles that were published in the CHEESA Journal have gone through editing according to established rules without changing the original manuscript.

### **Extraction of Basil Leaves Essential Oil using Microwave Assisted Hydrodistillation Method: Physical Characterization and Antibacterial Activity**

Ditta Kharisma Yolanda Putri<sup>\*</sup>, Salsabila Ananda Putri, Briantara Agung Nugraha, Boy Arief Fachri, Beki Palupi  
..... 1-12

### **Optimization of *Ulva* sp. Decomposition using H<sub>2</sub>SO<sub>4</sub> with Microwave-Assisted Hydrolysis Method as Feedstock of Bioethanol**

Beki Palupi<sup>\*</sup>, Muhammad Rizalluddin, Kiki Septianti, Istiqomah Rahmawati, Boy Arief Fachri, Meta Fitri Rizkiana, Helda Wika Amini  
..... 13-25

### **The Effect of H-Factor on Kappa Number and Viscosity in Continuous Digester**

Rizka Wulandari Putri<sup>\*</sup>, Rahmatullah, Faisal Siagian  
..... 26-33

### **Identification of Flavonoid Compounds in Ethanol Extract of Majapahit plant (*Crescentia cujete*) Leaves and their Potential as Anticancer**

Rahma Diyan Martha<sup>\*</sup>, Fatimah, Danar, Hesty Parbuntari  
..... 34-48

### **Optimization Production and Characterization of Bacterial Cellulose from Cornhusk**

Fikka Kartika Widyastuti<sup>\*</sup>, Ayu Chandra Kartika Fitri  
..... 49-55

### **Performance Analysis of Ammonia Converter in Ammonia Unit Factory**

Prahady Susmanto<sup>\*</sup>, Dino Dewantara, Teguh Widodo, Susi Susanti  
..... 56-62

### **Utilization of Activated Carbon/Magnesium(II) Composites in Decreasing Organic Materials**

Dheasi Rani Ullica, Titin Anita Zaharah<sup>\*</sup>, Imelda Hotmarisi Silalahi  
..... 63-75

**Volume 6 No 1, 2023**

ISSN 2614-8757 (Print), ISSN 2615-2347 (Online) Available  
online at: <http://e-journal.unipma.ac.id/index.php/cheesa>

Copyright © 2023

# Extraction of Basil Leaves Essential Oil using Microwave Assisted Hydrodistillation Method: Physical Characterization and Antibacterial Activity

Ekstraksi Minyak Atsiri Daun Kemangi menggunakan Metode Microwave Assisted Hydrodistillation: Uji Karakteristik Fisik dan Aktivitas Antibakteri

Ditta Kharisma Yolanda Putri<sup>1\*</sup>, Salsabila Ananda Putri<sup>1</sup>, Briantara Agung Nugraha<sup>1</sup>,  
Boy Arief Fachri<sup>1</sup>, Bakti Palupi<sup>1</sup>

<sup>1</sup>Universitas Jember, Chemical Engineering, Indonesia

## Article History

Received: 12<sup>th</sup> December 2022; Revised: 29<sup>th</sup> January 2023; Accepted: 11<sup>th</sup> February 2023;  
Available online: 30<sup>th</sup> May 2023; Published Regularly: June 2023

doi: [10.25273/cheesa.v6i1.14639.1-12](https://doi.org/10.25273/cheesa.v6i1.14639.1-12)

\*Corresponding Author.

Email:

dittakharisma@unej.ac.id

## Abstract

Basil oil can be obtained from basil leaves by non-extraction methods, namely Microwave Assisted Hydrodistillation (MAHD). Therefore, this research aims to determine the yield percentage, essential oil composition by GC-MS, physical characteristics, and antibacterial activity of basil essential oil. The highest yield of 0.3076% was obtained at the optimum condition, which included a microwave power of 300 W, a mass-to-volume solvent ratio (F/S) of 0.75 g/mL, a raw material size of  $\pm 1.75$  cm, and an extraction time of 90 min. The results of the analysis of variance showed that all process parameters used had a significant effect on the yield obtained. Basil oil exhibited a larger inhibition zone against *Escherichia coli* bacteria (16.38 mm) which tended to be stronger than *Staphylococcus aureus* (5.95 mm) and was classified as moderate. The main components contained in the basil oil were E-Citral (46.79%) and Z-Citral (38.17%). The physical characteristic test showed that the basil oil was soluble in 96% ethanol after a ratio of 1:9, with 1 ml of basil oil compared to 9 ml of ethanol. The density of basil oil at 0.961 g/mL also complied with the standard value according to the Essential Oil Association (EOA) of *Ocimum basilicum* Essential Oil. These results showed revealed that the parameter analyzed using oil yields at operating conditions produced the most optimum yield value.

**Keywords:** antibacterial; Basil oil; MAHD; physical characteristics test

## Abstrak

Minyak kemangi dapat diperoleh dari daun kemangi dengan metode ekstraksi non-konvensional yaitu Microwave Assisted Hydrodistillation (MAHD). Tujuan penelitian ini adalah untuk mengetahui persentase rendemen, komposisi minyak kemangi dengan GC-MS, uji karakteristik fisik, dan aktivitas antibakteri pada minyak kemangi. Rendemen tertinggi 0,3076% diperoleh pada daya 300 W, waktu 90 menit, ukuran daun  $\pm 1,75$  cm, serta rasio F/S 0,75 g/mL. Hasil analisis varian menyatakan bahwa semua parameter proses yang digunakan memiliki pengaruh yang signifikan terhadap rendemen yang dihasilkan. Minyak kemangi memiliki zona hambat lebih besar terhadap bakteri *Escherichia coli* (16,38 mm) yang cenderung lebih kuat dibandingkan *Staphylococcus aureus* (5,95 mm) yang tergolong sedang. Komponen utama yang terkandung dalam minyak kemangi yaitu E-Citral (46,79%) dan Z-Citral (38,17%). Uji karakteristik fisik menunjukkan bahwa minyak kemangi larut dengan etanol 96% saat perbandingan 1:9 yaitu 1 ml minyak kemangi dibandingkan 9 ml etanol. Densitas minyak kemangi 0,961 g/mL telah sesuai dengan standar nilai menurut Essential Oil Association (EOA) of *Ocimum basilicum* Essential Oil). Parameter analisis menggunakan hasil minyak pada kondisi operasi dengan nilai rendemen paling optimum.

**Kata kunci:** antibakteri; MAHD; minyak kemangi; uji karakteristik fisik

## Extraction of Basil Leaves Essential Oil using Microwave Assisted Hydrodistillation Method: Physical Characterization and Antibacterial Activity

### 1. Introduction

Basil is an indigenous vegetable that is quite dense, with a height of 100 cm [1] and is widely available across Indonesia, particularly in Jember, East Java. This vegetable belongs to the *Ocimum* genus, *Ocimum basilicum* L species, Magnoliopsida class, Lamiales orde, and Spermatophyta subdivision. Furthermore, basil is one of the indigenous products recognized by the Directorate General of Horticulture, according to the Decree of the Minister of Agriculture of Indonesia Number 511/Kpts/PD.310/9/2006.

Basil leaves contain phenolic compounds, saponins, flavonoids, and essential oils. In the health sector, basil can be used as an antipyretic, analgesic, antifungal, antiseptic, hepatoprotector, and immunomodulator [2]. The composition of basil oil consists of alcohol compounds, phenol (1–19% eugenol, iso-eugenol), oxides, phenolic ethers (3–31% methyl clavicol, 1-9% methyl eugenol), hydrocarbons, ketones, and esters [3]. Furthermore, the main component is the aldehyde group, citral, which acts as an antibacterial pathogen [4].

Due to its antibacterial properties, basil oil has the potential to be developed as a source of active ingredients for antibacterial products [5]. Pathogenic bacteria such as *Staphylococcus aureus*, which is a gram-positive bacteria, and *Escherichia coli*, a gram-negative, usually attack humans [6]. Therefore, an antibacterial activity test is conducted to determine the various kinds of antibacterial activities contained in basil oil.

The selection of the appropriate solvent for the extraction process is very important. In this research, water is used as the solvent because it has a high dielectric

constant, which optimizes microwave absorption [7]. The use of water as a solvent has the benefit of being a "green solvent" because it is relatively cheap, environmentally friendly, non-flammable, non-toxic, and allows for clean processing and pollution prevention [8].

The application of the "green technique" in essential oil extraction becomes more effective to overcome the drawbacks of conventional extraction methods, such as the long extraction time and increased energy consumption. The Microwave Assisted Hydrodistillation (MAHD) method is more effective because the process is short, produces a high yield, and minimizes the use of solvents [9]. According to Definiujemy [10], the use of MAHD with fresh basil and a 1 cm cut, 500 W power, 1000 ml aquadest volume, and a 5-7 hours time span produced a yield of 0.2948%. This research aims to conduct antibacterial activity tests, process variable differences, GC-MS analysis, and optimization using the Response Surface Methodology (RSM). Microwaves are used to heat and evaporate water from cells, causing the cells to swell, stretch, burst, and release metabolic components for solvent extraction. [11].

The extraction of basil leaves using a MAHD method was optimized with Box-Behnken Design (BBD) - Response Surface Methodology (RSM). The RSM was used to minimize costs, shorten the number of runs, optimize response, reduce research time, and as an improvement from previous research [12]. This technique can also be used to evaluate the relative significance of several factors influencing complex interactions between independent variables [13].

## Extraction of Basil Leaves Essential Oil using Microwave Assisted Hydrodistillation Method: Physical Characterization and Antibacterial Activity

### 2. Research Methods

#### 2.1 Tools and Materials

This research used several pieces of equipment, namely the Electrolux EMM-2007X type microwave, 20 L, 220 V, maximum power 800 W, wave frequency 2450 MHz, 1000 mL round bottom flask, modified clavenger (Figure 1), and condenser. The PTFE-coated microwave cavity measures 46.1 x 28 x 37.3 cm. The materials used were water, 96% ethanol, and fresh basil (*O. basilicum* L.) leaves with a water content of 85.8% obtained from Tanjung Market, Jember, East Java, Indonesia.

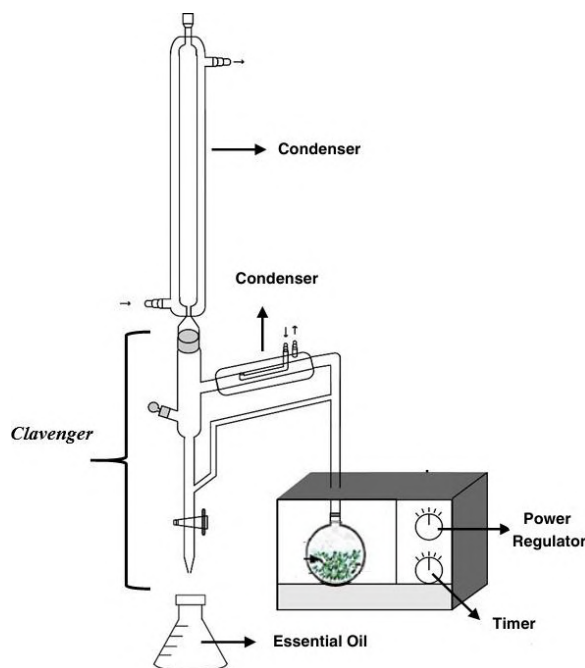


Figure 1. Modified Clavenger [14]

#### 2.2 Essential Oil Extraction Process

Fresh basil leaves were weighed using an analytical balance and cut according to their sizes of 0.5 cm, 1.75 cm, and 3 cm. The feed-to-solvent (F/S) ratio used was 0.25, 0.5, and 0.75 g/mL with a solvent volume of 200 mL. The extraction process was operated at a power of 150, 300, and 450 W for 30, 60, and 90 minutes, respectively. The extract was separated

using a separatory funnel on the clavenger and put into a 10 mL vial.

#### 2.3 Measurement of Essential Oil Yield

Yield is the ratio of the mass of oil produced to the mass of the raw material used (equation 1). The higher the yield obtained, the more basil oil is produced [15].

$$Yield = \frac{\text{mass of essential oil}}{\text{mass of raw material}} \times 100 \dots\dots(1)$$

#### 2.4 Physical Properties Analysis

The analysis of physical properties was carried out by analyzing the density of the sample using a pycnometer (equation 2).

$$\rho = \frac{m}{v} \dots\dots\dots(2)$$

The second analysis was the evaluation of solubility in alcohol, which is carried out by dripping ethanol on the sample.

#### 2.5 Essential Oil Composition Analysis

The GC-MS (Gas Chromatography and Mass Spectroscopy) test was used to determine the chemical content of basil oil. The compounds contained in the basil oil mixture were separated in the chromatography column. The advantages of this method included fast identification time, high sensitivity, good separation, and long-term use of tools [16].

#### 2.6 Antibacterial Activity Test

The method used in the antibacterial test was agar diffusion [17]. In this method, the basil extract was placed in a petri dish, each of which had been added with *E. coli* ATCC 25933 and *S. aureus* ATCC 25923. Subsequently, the petri dish was placed in an incubator for 24 hours at 36°C, and antibacterial activity was observed based on the zone of inhibition (halo diameter).

## Extraction of Basil Leaves Essential Oil using Microwave Assisted Hydrodistillation Method: Physical Characterization and Antibacterial Activity

### 2.7 Statistic Analysis

The optimization analysis used the RSM method, aided by the Design Expert 13 application. The RSM model used was the Box-Behnken Design with four process parameters, namely F/S ratio, microwave power, extraction time, and leaf size. A total of 29 experiments were carried out and the effect of the extraction parameters used on the extract yield was observed using analysis of variance (ANOVA) [18].

## 3. Results and Discussion

### 3.1 Effect of Process Parameters on Basil Oil Yield

#### 3.1.1 Effect of Microwave Power and Time on the Yield of Basil Oil

Microwave power in the extraction process functioned as a controller for the capacity of heat energy to be received by the material. The greater the power used, the higher the system temperature during extraction, thereby reducing the time needed to reach the boiling point of water [19]. In the research (Figure 2), using an F/S ratio of 0.75 g/mL, leaf size 1.75 cm, power 300 W, and time 90 minutes, produced a yield of 0.3076%. Meanwhile, with an F/S ratio of 0.75 g/mL, leaf size 1.75 cm, power 450 W, and time of 60 minutes, a yield of 0.247% was obtained. This indicated that longer extraction time and moderate microwave power produced higher yields [20]. This showed that the higher the power used, the greater the yield of oil obtained. However, the thermal degradation of the basil oil components and the materials used caused a decrease in the yield from 300 W to 450 W. An increase in extraction temperature also occurred at high power, which reduced solvent effectiveness in the absorption of the essential oil compounds in basil [21]. The time parameters used range

from 30 to 90 min, showing an increase in yield gain. The best yield was obtained at an F/S ratio of 0.75 g/mL, leaf size 1.75 cm, 300 W power, and 90 minutes of 0.3076%. This occurred because the longer extraction time caused the cell walls of basil leaves to break down, taking a long time for the solvent to extract the compound content in the leaves [22].

#### 3.1.2 Effect of F/S Ratio and Leaf Size on Basil Oil Yield

The F/S ratio was one of the important parameters in the extraction process. In this research (Figure 3), the basil oil extraction process that the greater mass of the material used produced a higher yield obtained. The use of an F/S ratio of 0.75 g/mL, leaf size 1.75 cm, power 300 W, and time of 90 minutes, obtained a yield of 0.3076%. Meanwhile, with an F/S ratio of 0.5 g/mL, leaf size 3 cm, power 300 W, and time 90 minutes, a yield of 0.237% was obtained. This showed that a greater F/S ratio and smaller leaf size produced a higher yield. In a previous research, a greater mass of the material, oil yield, and smaller leaf size produced a higher leaf surface area compared to the whole size [23].

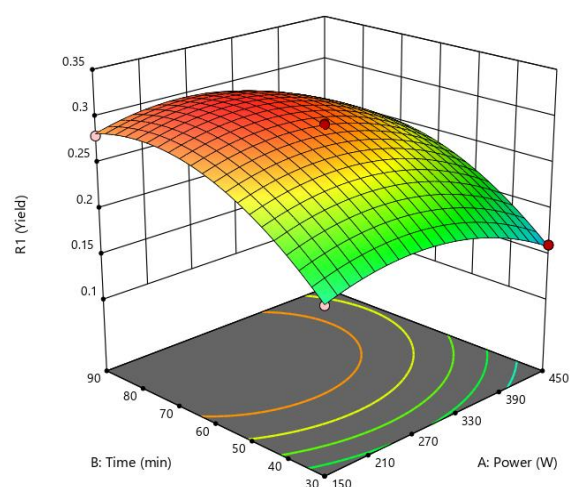


**Figure 2.** Effect of power and time on the yield of basil oil

### Extraction of Basil Leaves Essential Oil using Microwave Assisted Hydrodistillation Method: Physical Characterization and Antibacterial Activity

#### 3.1.3 Effect of Time and F/S Ratio on Basil Oil Yield

The parameters of time and F/S ratio showed a significant effect on the yield of basil oil produced. Increasing the extraction time also improved the extraction yield, while a higher F/S ratio produced more basil oil. The effect of time and ratio was proven by increasing the yield from 0.29% at an F/S ratio of 0.5 g/mL, with a time of 60 minutes to 0.3076% at an F/S ratio of 0.75 g/mL at 90 minutes, with all other parameters being kept constant. These values were the highest yield obtained from the experimental results (Figure 4). The ratio used was related to the density of the raw material when included in the distiller flask for optimal oil extraction and evaporation processes [14].

#### 3.1.4 Effect of Time and Leaf Size on Basil Oil Yield

The content of essential oils in plants was found in the sac vessels, glandular hairs, and oil glands [5]. In this research, the variation in leaf size was carried out to open the oil glands and facilitate the evaporation of essential oils. Therefore, as the leaf size became smaller, the surface area increased, making it easier to come into contact with moisture [24]. The effect of time and leaf size (Figure 5) was proven by decreasing the yield at 90 minutes with a leaf size of  $\pm 1.75$  cm from 0.3076% to 0.2525% obtained at 60 minutes with a leaf size of  $\pm 0.5$  cm using the parameters and processes. This was caused by the shorter time and the leaf enumeration factor, which was excessively small. Factors that caused a decrease in this yield were the release of oil during the enumeration process, oil left in the equipment, and the evaporation process [25]. Therefore, the longer the extraction

time and leaf size, the greater the yield of basil oil.

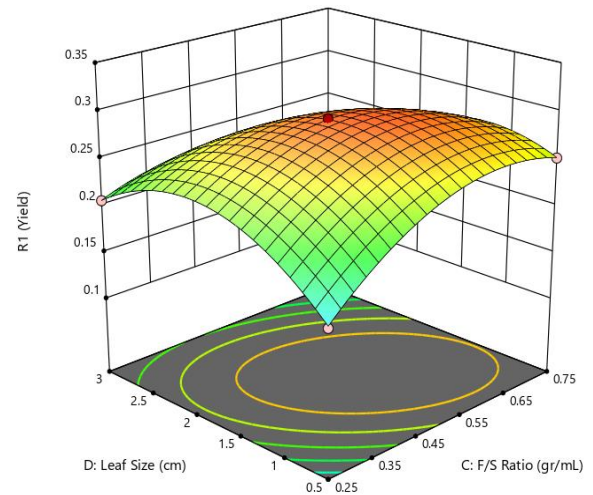


Figure 3. Effect of F/S ratio and leaf size on basil oil yield

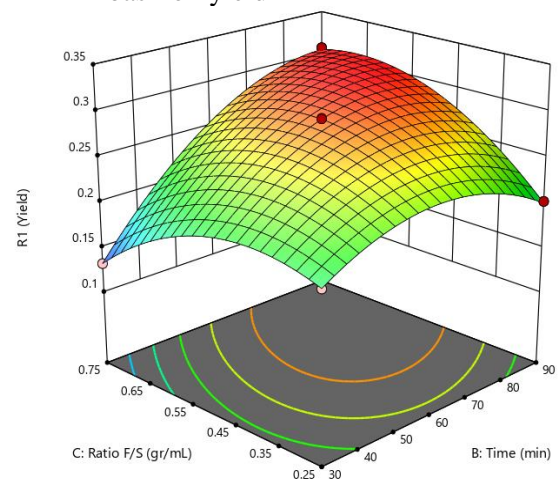


Figure 4. Effect of time and F/S ratio on basil oil yield

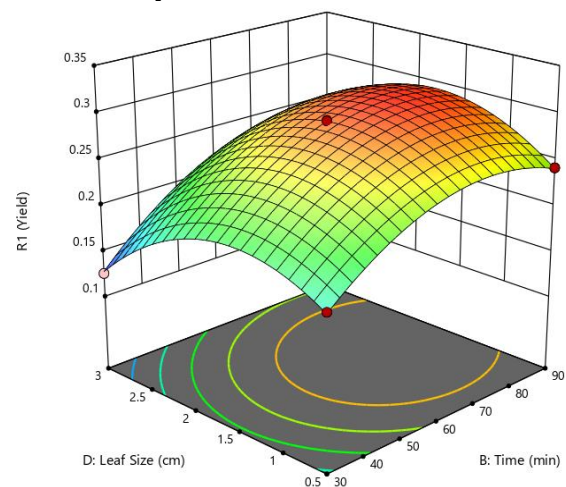


Figure 5. Effect of time and leaf size on basil oil yield

## Extraction of Basil Leaves Essential Oil using Microwave Assisted Hydrodistillation Method: Physical Characterization and Antibacterial Activity

### 3.2 Basil Oil Analysis

#### 3.2.1 Basil Oil Yield

The process of extracting basil oil using the MAHD method produced the smallest and largest yield of 0.1257% and 0.3076%, respectively, with clear yellow oil color. The diversity of yield values obtained was based on the existence of several different treatments between process variables. However, the variation in the yield of basil oil showed a significant difference. Table 1 showed a comparison of the largest and smallest basil oil yields with different parameters.

**Table 1.** The yield of the largest and smallest basil oil

Power (W)	Time (min)	F/S Ratio (g/mL)	Leaf Size (cm)	Yield (%)
300	30	0.5	± 3	0.1257
300	90	0.75	± 1.75	0.3076

#### 3.2.2 GC-MS Analysis

The components contained in basil oil were identified by Gas Chromatography–Mass Spectrometry (GC–MS) analysis. The results of basil oil analysis at 300 W, 90 minutes, 1.75 cm leaf size, and 0.75 g/mL F/S ratio were shown in Table 3, indicating that the basil oil contained 20 chemical constituents.

Based on GC-MS analysis (Figure 6), the components contained in basil oil consisted of five groups of compounds, namely monoterpenes 0.34%, sesquiterpenes 6.9%, oxygenated monoterpenes 91.56%, oxygenated sesquiterpenes 0.69%, and other oxygenated compounds 0.52%.

Oxygenated compounds had more influence on the aroma of essential oils than other components. The highest levels of basil oil were obtained in E-citral at 46.79% and Z-citral at 38.17%, which were the

constituent of the aldehyde group of citral. According to Putri and Rahmawati [24], the majority of the composition of the basil oil contained citral compounds, including E-Citral at 33.7 and Z-Citral at 27.9%.

#### 3.2.3 Antibacterial Activity

The inhibition activity of bacteria was determined by measuring the diameter of the inhibition zone formed. Based on the inhibition activity criteria of Lingga et al [26], inhibition zones formed between  $\geq 20$  mm were considered to have very strong inhibition, 10-20 mm as strong, 5-10 mm as moderate, and  $\leq 5$  mm as weak.

**Table 2.** Bacterial inhibition zone

Isolate	Inhibition Zone (mm)
<i>E. coli</i>	16.38
<i>S. aureus</i>	5.95

The inhibition zone values (Table 2) showed that the basil oil had a larger inhibition zone against *E. coli* bacteria, namely 16.38 mm. This indicated a stronger effect compared to *S. aureus*, which was only 5.95 mm and was classified as moderate. In this research, citral content was the main component of basil oil, which acted as a pathogenic antibacterial, thereby inhibiting the test bacteria. Aldehyde compounds can activate proteins by forming covalent cross-links with groups of functional organic matter in proteins [27].

Basil oil also contained flavonoids and phenolic compounds, which have different mechanisms of action against bacteria. The flavonoid compounds can damage bacterial membranes by forming complex compounds that dissolve with extracellular proteins. Meanwhile, phenol compounds can break peptidoglycan bonds when passing through the cell wall [28]. The variation in their mechanism also occurred due to differences in the sensitivity of the bacteria used.

**Extraction of Basil Leaves Essential Oil using Microwave Assisted Hydrodistillation Method: Physical Characterization and Antibacterial Activity**

*E. coli* bacteria are gram-negative, while *S. aureus* bacteria are gram-positive. Gram-negative bacteria have a hydrophilic side, namely amino acids, hydroxyls, and carboxyls, which caused them to be sensitive to polar compounds [29]. Hydrophilic molecules such as flavonoids and alkaloids more easily pass through lipopolysaccharides compared to hydrophobic [5]. Therefore, the use of water as a polar solvent for extraction caused *E. coli* bacteria to have a larger inhibition zone diameter than *S. aureus*.

In gram-negative bacteria, the peptidoglycan layer on the cell membrane

was thinner compared to gram-positive bacteria. The outer membrane of gram-negative bacteria was composed of phospholipids and lipopolysaccharides for antibacterial substances that interfered with the integrity of the cell membrane to easily affect gram-negative bacteria by dissolving the phospholipids. Phospholipids break down into glycerol, carboxylic acids, and phosphoric acids, causing the membrane to lose its shape and allowing uncontrollable entrance and exit of the cell, leading to disruption of metabolism by bacterial lysis [30].

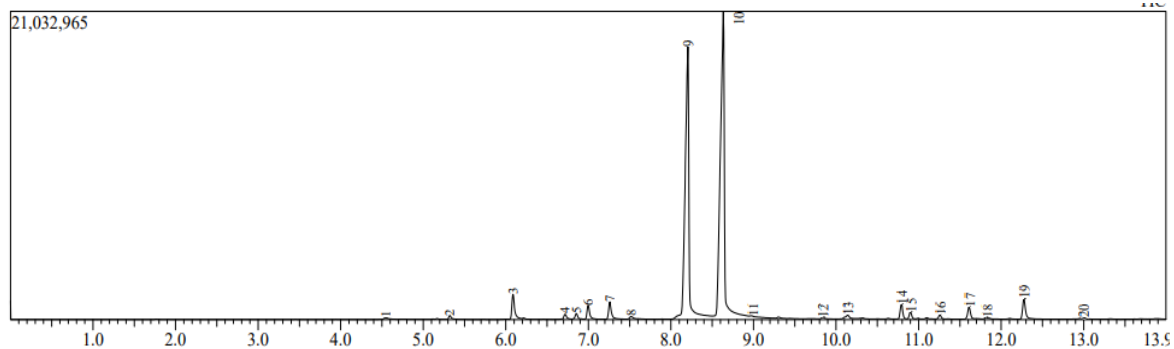


**Figure 6.** GC-MS analysis result

**Table 3.** GC-MS test result

Peak	Compound	Class	Retention Time	% Area
1	Methyl heptanone	OOM	4.548	0.18
2	β-Ocimene	M	5.322	0.34
3	LINALOOL-L	OM	6.087	2.67
4	Geranial	OM	6.718	0.50
5	Cyclohexene	S	6.854	0.54
6	Isogeraniol	OM	6.997	1.33
7	α-Sicositral	OM	7.259	1.77
8	α-Terpineol	OM	7.517	0.33
9	Z-Citral	OM	8.204	38.17
10	E-Citral	OM	8.635	46.79
11	trans-Myrtanyl acetate	OOC	8.985	0.15
12	Neryl acetate	OOC	9.839	0.19
13	β-Bisabolene	OS	10.140	0.55
14	trans-Caryophyllene	S	10.793	1.47
15	α-Bergamotene	S	10.902	0.67
16	α-Caryophyllen	S	11.258	0.42
17	Germacrene-D	S	11.610	1.26
18	Bicyclogermacrene	S	11.818	0.27
19	α-Humulene	S	12.275	2.27
20	(-)-Caryophyllene oxide	OS	12.994	0.14

## Extraction of Basil Leaves Essential Oil using Microwave Assisted Hydrodistillation Method: Physical Characterization and Antibacterial Activity

Gram-positive bacteria have a thicker peptidoglycan layer than gram-negative bacteria, which results in lower cell wall permeability. The sensitivity of bacteria to antibiotics also depends on differences in the arrangement of the cell wall. Therefore, it is more difficult for the active substance of essential oils to penetrate the cell membrane of gram-positive bacteria, leading to a less optimal antibacterial effect [31].

### 3.2.4 Physical Properties Analysis

Analysis of physical properties was carried out through visual observation or testing. According to the Essential Oil Association of *O. basilicum* Essential Oil, the average density of basil oil ranged from 0.952 to 0.973 g/mL. From the calculation results, the density of basil oil was 0.961 g/mL, which was in line with the standard value.

The thermogravimetric method was used for the alcohol solubility analysis of basil oil, with a ratio of 1:1, 1:5, and 1:9. To

achieve a ratio of 1:1, 1 mL of basil oil and 1 mL of 96% ethanol was mixed and the solubility was observed when pure basil oil dissolved, as described by a change in color to yellowish white. When the ratio was increased to 1:5, the color of the basil oil was still cloudy due to the presence of undissolved oil (Figure 7). Subsequently, the ratio was increased to 1:9, and the resulting color was getting clearer, indicating that the oil was perfectly mixed with alcohol. This showed that the better the oil quality, the more difficult the solubility. Generally, basil oil containing oxygenated monoterpenes was more soluble in alcohol compared to non-oxygenated monoterpenes [28].

### 3.2.5 Analysis of Variance (ANOVA)

Statistical analysis was used to prove that the process parameters employed in the extraction of basil affected the resulting yield. In Table 4, significant parameters were obtained when the p-value of the ANOVA method had a value less than 0.05.

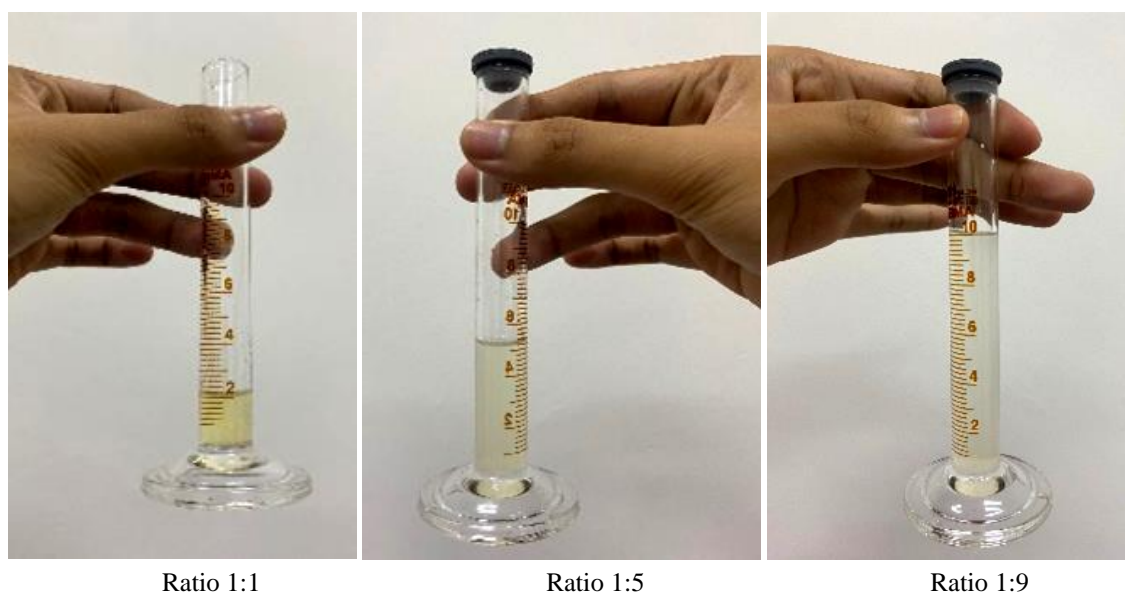


**Figure 7.** Comparison of the solubility of essential oils in alcohol

**Extraction of Basil Leaves Essential Oil using Microwave Assisted Hydrodistillation Method: Physical Characterization and Antibacterial Activity**

The regression equation of the model given was used to predict the actual results of the research. This indicated that the effect of process parameters, namely extraction time, microwave power, F/S ratio, and leaf size affected the yield of basil oil produced. However, the interaction of power and time did not significantly affect the yield.

$$\text{Yield} = 0.2916 + 0.0184A + 0.0433B + 0.0092C - 0.0135D + 0.0397AC + 0.0222AD + 0.0434BC + 0.0127BD - 0.0317CD - 0.0315A^2 - 0.0412B^2 - 0.0408C^2 - 0.0532D^2 \dots\dots\dots(3)$$

The equation 3 indicated that time was directly proportional to the yield response. The ratio parameter also showed the same relationship because the constant was positive. Meanwhile, the yield response was inversely proportional to the power and leaf size because the constants were negative [5]. This indicated that the yield

reduced as the size of the leaves decreased and more energy was used.

Table 5 showed that an R<sup>2</sup> value of 0.9992 was obtained. Since the value obtained was close to 1, the model was considered perfect and in line with the research results. The predicted R<sup>2</sup> value was 0.9958, which corresponded to the adjusted R<sup>2</sup> value of 0.9984, which showed a difference of less than 0.2. In the Figure 8, experimental data values spread around the line, indicating that there was a concordance between the models and the experimental data. Therefore, the regression model was considered suitable for use.

**Table 5.** Fit statistics ANOVA

<b>Std. Dev.</b>	0.0021	<b>R<sup>2</sup></b>	0.9992
<b>Mean</b>	0.2226	<b>Adjusted R<sup>2</sup></b>	0.9984
<b>C.V. %</b>	0.9523	<b>Predicted R<sup>2</sup></b>	0.9958
		<b>Adeq Precision</b>	116.6345

**Table 4.** ANOVA results

Source	Sum of Squares	df	Mean Square	F-value	p-value	
<b>Model</b>	0.0809	14	0.0058	1285.63	< 0.0001	significant
A	0.0040	1	0.0040	899.28	< 0.0001	
B	0.0225	1	0.0225	4999.55	< 0.0001	
C	0.0010	1	0.0010	227.69	< 0.0001	
D	0.0022	1	0.0022	487.94	< 0.0001	
AB	0.0000	1	0.0000	3.56	0.0801	not significant
AC	0.0063	1	0.0063	1401.32	< 0.0001	
AD	0.0020	1	0.0020	437.75	< 0.0001	
BC	0.0075	1	0.0075	1676.80	< 0.0001	
BD	0.0007	1	0.0007	144.72	< 0.0001	
CD	0.0040	1	0.0040	893.17	< 0.0001	
A <sup>2</sup>	0.0064	1	0.0064	1431.29	< 0.0001	
B <sup>2</sup>	0.0110	1	0.0110	2454.92	< 0.0001	
C <sup>2</sup>	0.0108	1	0.0108	2407.52	< 0.0001	
D <sup>2</sup>	0.0184	1	0.0184	4087.71	< 0.0001	
<b>Residual</b>	0.0001	14	4.493E-06			
Lack of Fit	0.0001	10	5.770E-06	4.44	0.0819	not significant
Pure Error	5.200E-06	4	1.300E-06			
<b>Cor Total</b>	0.0809	28				

A = Power; B = Time; C = F/S Ratio; D = Leaf Size

## Extraction of Basil Leaves Essential Oil using Microwave Assisted Hydrodistillation Method: Physical Characterization and Antibacterial Activity

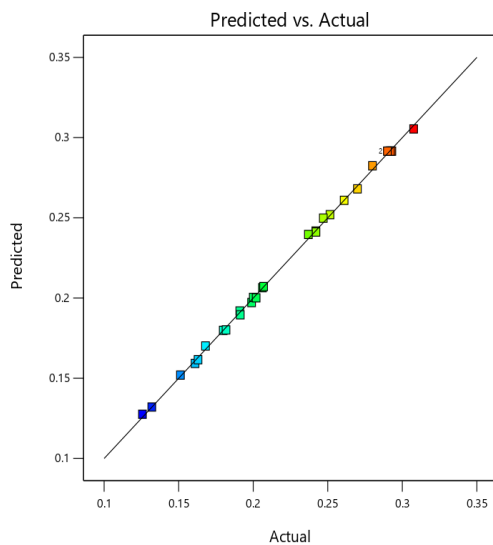


Figure 8. Predicted vs actual ANOVA

### 4. Conclusion

The optimum yield of basil oil was 0.3076% at 300 W power, 90 minutes, 1.75 cm leaf size, and an F/S ratio of 0.75 g/mL. The quality of basil oil was good, as indicated by its low solubility in 96% ethanol and a density value of 0.961 g/mL,

which was in line with the standard value according to the Essential Oil Association (EOA). The main components of basil oil extracted using the MAHD method were E-citral at 46.79% and Z-citral at 38.17%. The basil oil obtained was more effective against *E. coli* bacteria because it had a larger inhibition zone than *S. aureus*.

### 5. Acknowledgments

The authors are grateful to the LP2M Universitas Jember for providing funding through the Beginner Lecturer Internal Research Grant Program, which enabled the smooth execution of this research.

The authors are also grateful to the Chemical Engineering Laboratory of the Universitas Jember for providing the necessary laboratory facilities to complete this research.

### References

- [1] Putri, I. A., Fatimura, M., Husnah, & Bakrie, M. (2021). Pembuatan Minyak Atsiri Kemangi (*Ocimum Basilicum L.*) dengan Menggunakan Metode Distilasi Uap Langsung. *Jurnal Redoks*, 6(2), 149–156
- [2] Nazir, S., Wani, I. A., & Masoodi, F. A. (2017). Extraction optimization of mucilage from Basil (*Ocimum basilicum L.*) seeds using response surface methodology. *Journal of Advanced Research*, 8(3), 235–244. doi: 10.1016/j.jare.2017.01.003
- [3] Pratiwi, A., & Utami, L. B. (2018). Isolasi dan Analisis Kandungan Minyak Atsiri Pada Kembang Leson. *Bioeksperimen: Jurnal Penelitian Biologi*, 4(1), 42–47. doi: 10.23917/bioeksperimen.v4i1.5930
- [4] Qodri, U. (2020). Analisis kuantitatif minyak atsiri dari serai (*Cymbopogon sp*) sebagai aromaterapi. *Jurnal Farmasi Tinctura*, 1(2), 64–70
- [5] Malik, A. R., Sharif, S., Shaheen, F., Khalid, M., Iqbal, Y., Faisal, A., Botmart, T. (2022). Green synthesis of RGO-ZnO mediated *Ocimum basilicum* leaves extract nanocomposite for antioxidant, antibacterial, antidiabetic and photocatalytic activity. *Journal of Saudi Chemical Society*, 26(2), 101438. doi: 10.1016/j.jscs.2022.101438
- [6] Hashim, R., Husin, S. A., Ahmad, N., Bahari, N., Abu, N., Ali, R. M., Paul, S. C. (2022). Tricycle Project – One Health approach: Whole genome sequencing(WGS) of Extended-spectrum beta-lactamase (ESBL) producing *Escherichia (E.) coli* derived from human, food chain and environment. *International Journal of Infectious Diseases*, 116, S105–S106. doi: 10.1016/j.ijid.2021.12.249
- [7] Villar Blanco, L., González Sas, O., Sánchez, P. B., Domínguez Santiago, Á., & González de Prado, B. (2022). Congo red recovery from water using green extraction solvents. *Water Resources and Industry*, 27 December 2021. doi: 10.1016/j.wri.2021.100170
- [8] Filly, A., Fabiano-Tixier, A. S., Louis, C., Fernandez, X., & Chemat, F. (2016). Water as a green solvent combined with different techniques for extraction of essential oil from lavender flowers.

## Extraction of Basil Leaves Essential Oil using Microwave Assisted Hydrodistillation Method: Physical Characterization and Antibacterial Activity

- Comptes Rendus Chimie*, 19(6), 707–717. doi: 10.1016/j.crci.2016.01.018
- [9] Sharifvaghefi, S., & Zheng, Y. (2022). Microwave vs conventional heating in hydrogen production via catalytic dry reforming of methane. *Resources Chemicals and Materials*, 1(3-4), 290-307. doi: 10.1016/j.recem.2022.08.003
- [10] Anwar, A.K., Yuharmen., Zamri, A. (2017). Isolasi Minyak Atsiri Daun Kemangi (*Ocimum Sanctum* L) Cara Konvensional dan Microwave Serta Uji Aktivitas Antibakteri dan Antioksidan. *Repository UNRI* 4(1), 1–12. Retrieved from <http://repository.unri.ac.id/xmlui/handle/123456789/8714>
- [11] Yuliana, D. A., Nurhidayati, S., Aswan, A., & Febriana, I. (2020). Proses Pengambilan Minyak Atsiri dari Tanaman Nilam (*Progestemon cablin benth*) menggunakan Metode Microwave Hydrodistillation. *Jurnal Kinetika*, 11(03), 34–39.
- [12] Sarabia, L. A., & Ortiz, M. C. (2009). Response Surface Methodology. *Comprehensive Chemometrics*, 1(October 2004), 345–390. doi: 10.1016/B978-044452701-1.00083-1
- [13] Brooke, R., Fan, L., Khayet, M., & Wang, X. (2022). Heliyon A complementary approach of response surface methodology and an artificial neural network for the optimization and prediction of low salinity reverse osmosis performance. *Heliyon*, 8(September), e10692. doi: 10.1016/j.heliyon.2022.e10692
- [14] Erliyanti, N. K., Saputro, E. A., Yogaswara, R. R., & Rosyidah, E. (2020). Aplikasi Metode Microwave Hydrodistillation pada Ekstraksi Minyak Atsiri dari Bunga Kamboja (*Plumeria alba*). *Jurnal IPTEK*, 24(1), 37–44. doi: 10.31284/j.ipitek.2020.v24i1.865
- [15] Juul, L., Steinhagen, S., Bruhn, A., Jensen, S. K., Undeland, I., & Dalsgaard, T. K. (2022). Combining pressing and alkaline extraction to increase protein yield from *Ulva fenestrata* biomass. *Food and Bioprocess Technology*, 134, 80–85. doi: 10.1016/j.fbp.2022.05.006
- [16] Lacalle-Bergeron, L., Gotteris-Cerisuelo, R., Portolés, T., Beltran, J., Sancho, J. V., Navarro-Moreno, C., & Martinez-Garcia, F. (2021). Novel sampling strategy for alive animal volatolome extraction combined with GC-MS based untargeted metabolomics: Identifying mouse pup pheromones. *Talanta*, 235. doi: 10.1016/j.talanta.2021.122786
- [17] Da Cruz Almeida, E. T., da Silva, M. C. D., Oliveira, J. M. dos S., Kamiya, R. U., Arruda, R. E. dos S., Vieira, D. A., ... do Nascimento, T. G. (2017). Chemical and microbiological characterization of tinctures and microcapsules loaded with Brazilian red propolis extract. *Journal of Pharmaceutical Analysis*, 7(5), 280–287. doi: 10.1016/j.jpha.2017.03.004
- [18] Kusuma, H. S., Ansori, A., & Mahfud, M. (2021). Optimization of Synthesis of Methyl Acetate From Acetic Acid and Methanol Using Microwave-Assisted Esterification. *Journal of Chemical Technology and Metallurgy*, 56(4), 686–697.
- [19] Lopez-Avila, V., & Luque de Castro, M. D. (2014). *Microwave-Assisted Extraction. Reference Module in Chemistry, Molecular Sciences and Chemical Engineering*. Elsevier Inc. doi: 10.1016/b978-0-12-409547-2.11172-2
- [20] Hammad, E. A., & El-Sagheer, A. M. (2022). Comparative efficacy of essential oil nanoemulsions and bioproducts as alternative strategies against root-knot nematode, and its impact on the growth and yield of *Capsicum annum* L. *Journal of the Saudi Society of Agricultural Sciences*, (xxxx). doi: 10.1016/j.jssas.2022.06.002
- [21] Suganya, P., Jeyaprakash, K., Mallavarapu, G. R., & Murugan, R. (2015). Comparison of the chemical composition, tyrosinase inhibitory and anti-inflammatory activities of the essential oils of *Pogostemon plectranthoides* from India. *Industrial Crops and Products*, 69, 300–307. doi: 10.1016/j.indcrop.2015.02.045
- [22] Anh, T. T., Duyen, L. T., Hang, L. M., Lam, T. D., Bach, L. G., Nguyen, D. C., & Toan, T. Q. (2019). Effect of drying temperature and storage time on *Ocimum gratissimum* Linn. leaf essential oil from Central Highlands, Vietnam. *Materials Today: Proceedings*, 18, 4648–4658. doi: 10.1016/j.matpr.2019.07.449
- [23] Złotek, U., Mikulska, S., Nagajek, M., & Świeca, M. (2016). The effect of different solvents and number of extraction steps on the polyphenol content and antioxidant capacity of basil leaves (*Ocimum basilicum* L.) extracts. *Saudi Journal of Biological Sciences*, 23(5), 628–633. doi: 10.1016/j.sjbs.2015.08.002
- [24] Putri, D. K. Y & Rahmawati, A., (2020). Microwave Assisted-Extraction of Essential Oil From

**Extraction of Basil Leaves Essential Oil using Microwave Assisted Hydrodistillation Method: Physical Characterization and Antibacterial Activity**

- Fresh Basil (*Ocimum Basilicum L.*) Leaves. *Journal of Biobased Chemicals*, 1(1), 1–11. doi: 10.19184/jobc.v1i1.105
- [25] Lindriati, T., Herlina, H., Arbiantara, H., & Asrofi, M. (2020). Optimization of meat analog production from concentrated soy protein and yam (*Xanthosoma sagittifolium*) powder using pasta machine. *Food Research*, 4(3), 887–895. doi: 10.26656/fr.2017.4(3).357
- [26] Hawa, L. C., Dewi, S. R., Izza, N., & Wigati, L. P. (2016). Analisa Karakteristik Fisik Chips Umbi Talas (*Colocasia Esculenta L.*) Berbasis Machine Vision (Studi Pengeringan Dengan Tray Dryer). *J.Rekapan*, 10(1), 22–28.
- [27] Clarizka, C., Fulanah, D., Zullaikah, S., & Rachimoellah. (2015). Ekstraksi Minyak Daun Kemangi dengan Menggunakan Air Subkritis Untuk Pembuatan Hand sanitizer Cynthia. *Industrial Teknologi*, 1(1), 1–5.
- [28] Mahmoudi, H., Marzouki, M., M'Rabet, Y., Mezni, M., Ait Ouazzou, A., & Hosni, K. (2020). Enzyme pretreatment improves the recovery of bioactive phytochemicals from sweet basil (*Ocimum basilicum L.*) leaves and their hydrodistilled residue by-products, and potentiates their biological activities. *Arabian Journal of Chemistry*, 13(8), 6451–6460. doi: 10.1016/j.arabjc.2020.06.003
- [29] Rohana, I. (2019). Isolasi Dan Identifikasi Bakteri Endofit Dari Rimpang Temulawak (*Curcuma xanthorrhiza*) Sebagai Penghasil Senyawa Antibakteri Terhadap Bakteri *Pseudomonas aeruginosa* dan *Staphylococcus epidermidis*. *Journal of Chemical Information and Modeling*, 53(9), 1689–1699.
- [30] Silawati, S.O. (2018). Aktivitas Antibakteri Minyak Atsiri Daun Sirih Merah (*Piper crocatum Ruiz dan Pav*) Terhadap *Staphylococcus aureus* dan *Escherichia coli* secara In Vitro. Skripsi: Universitas Muhammadiyah Surakarta.
- [31] Ma, Y., Ye, K., Liu, P., Yuan, A., Chen, S., & He, Y. (2023). Effect of a Konjac glucomannan/chitosan antibacterial composite membrane microencapsulated with oregano essential oil on the quality of chilled pork. *Applied Food Research*, 3(1). doi: 10.1016/j.afres.2022.100249

# Optimization of *Ulva* sp. Decomposition using H<sub>2</sub>SO<sub>4</sub> with Microwave-Assisted Hydrolysis Method as Feedstock of Bioethanol

Optimasi Dekomposisi *Ulva* sp. Menggunakan H<sub>2</sub>SO<sub>4</sub> dengan Metode Microwave-Assisted Hydrolysis Sebagai Bahan Baku Pembuatan Bioetanol

Bekti Palupi<sup>1,2\*</sup>, Muhammad Rizalluddin<sup>1</sup>, Kiki Septianti<sup>1</sup>, Istiqomah Rahmawati<sup>1,2</sup>,  
Boy Arief Fachri<sup>1,2</sup>, Meta Fitri Rizkiana<sup>1,2</sup>, Helda Wika Amini<sup>1,2</sup>

<sup>1</sup>Universitas Jember, Department of Chemical Engineering, Indonesia

<sup>2</sup>Universitas Jember, Research Center for Biobased Chemical Product, Indonesia

## Article History

Received: 14<sup>th</sup> December 2022; Revised: 10<sup>th</sup> April 2023; Accepted: 06<sup>th</sup> May 2023;

Available online: 07<sup>th</sup> June 2023; Published Regularly: June 2023

doi: [10.25273/cheesa.v6i1.14682.13-25](https://doi.org/10.25273/cheesa.v6i1.14682.13-25)

\*Corresponding Author.

Email:

bekti.palupi@unej.ac.id

## Abstract

Bioethanol is a renewable energy used to reduce dependence on fossil fuels, which have negative impacts on the environment. Furthermore, *Ulva* sp. contains high levels of carbohydrates, making it potentially suitable as a raw material for bioethanol production. Therefore, this study aims to determine the optimal decomposition process using the microwave-assisted hydrolysis method with an acid solvent (H<sub>2</sub>SO<sub>4</sub>), by examining the effects of acid concentration, hydrolysis time, and microwave power. Optimization was carried out using several parameters such as hydrolysis time, microwave power, and the ratio of raw materials to solvents. The ANOVA test results showed that the hydrolysis variable parameter had a significant effect on the reducing sugar content obtained, evidenced by the R<sup>2</sup> value of 0.9892. The highest reducing sugar content of 19.71 mg/mL was produced under the operating conditions of 15 min hydrolysis time, 450 W microwave power, and 0.065 g/mL ratio of raw material to solvents.

**Keywords:** bioethanol; hydrolysis; microwave-assisted hydrolysis; reducing sugar; *Ulva* sp.

## Abstrak

Bioetanol merupakan bentuk energi terbarukan yang digunakan dalam mengurangi ketergantungan terhadap penggunaan bahan bakar fosil yang menimbulkan berbagai dampak negatif terhadap lingkungan. *Ulva* sp. mengandung karbohidrat yang tinggi sehingga berpotensi sebagai bahan baku produksi bioetanol. Penelitian ini bertujuan untuk mengidentifikasi konsentrasi asam, waktu hidrolisis, dan daya microwave untuk mendapatkan proses dekomposisi yang optimal menggunakan metode microwave-assisted hydrolysis dengan pelarut asam (H<sub>2</sub>SO<sub>4</sub>). Optimasi dilakukan dengan menggunakan beberapa parameter seperti waktu hidrolisis, daya microwave, dan rasio massa bahan baku terhadap volume pelarut. Hasil uji ANOVA menunjukkan bahwa parameter waktu, daya, serta rasio bahan dan pelarut pada proses hidrolisis berpengaruh signifikan terhadap kadar gula pereduksi yang diperoleh, yang didukung oleh nilai R<sup>2</sup> sebesar 0,9892. Kadar gula pereduksi tertinggi pada penelitian ini yaitu sebesar 19,71 mg/mL pada parameter kondisi operasi berupa waktu hidrolisis selama 15 menit, daya microwave 450 W, dan rasio massa bahan baku terhadap volume pelarut 0,065 g/mL.

**Kata kunci:** bioetanol; gula pereduksi; hidrolisis; microwave-assisted hydrolysis; *Ulva* sp.

## Optimization of *Ulva* sp. Decomposition using H<sub>2</sub>SO<sub>4</sub> with Microwave-Assisted Hydrolysis Method as Feedstock of Bioethanol

### 1. Introduction

As Indonesia continues to witness advancements and progress in multiple areas, including population growth, transportation sector expansion, and technological developments, the demand for fuel energy in the country has experienced a consistent rise year after year [1,2]. According to the World Energy Agency, the world's demand for energy will increase by up to 45% or approximately 1.6% annually by 2030. However, the primary energy supply is still dominated by the use of fossil fuel energy which contributes to increased carbon dioxide gas emissions and significant changes to climate instability [3-5]. Carbon emissions originating from the burning of carbon compounds such as carbon dioxide (CO<sub>2</sub>), diesel, and other fuels are the biggest contributors to climate change, leading to a rise in the earth's temperature [6]. To reduce dependence on fossil fuels, efforts must be made to develop biomass conversion into bioethanol [7-9].

Bioethanol is a form of renewable energy that has various advantages, such as a high octane rating, easy-to-obtain raw materials, and environmental friendliness [10, 11]. Meanwhile, macroalgae have been considered the 3<sup>rd</sup> generation of biomass for the production of bioethanol and other forms of biofuels due to their high carbohydrate content of up to 60% [12-14]. This innovation certainly supports government programs related to accelerating the development of new renewable energy with targets of fulfilling 23% and 31% of the total national energy demand in 2025 and 2050 respectively [15].

*Ulva* sp. commonly known as sea lettuce is a type of macroalgae commonly found in Indonesian waters [7, 16]. It has a

morphology consisting of small cells which are colonies in the form of branched filaments and its vegetative cell division occurs in more than one area. Furthermore, *Ulva* sp. belongs to the Chlorophyta division because it contains high chlorophyll content, evidenced by its green leaves [17,18]. It also contains carbohydrates, protein, lipids, and ash of up to 50.34%, 25.69%, 2.31%, and 21.66% respectively [19]. The high carbohydrate content has the potential to be used as a raw material for bioethanol through the role of bacterial and yeast microorganisms [20-22]. Several species of *Ulva* sp. with a high carbohydrate content include *Ulva fasciata* (43.0%), *Ulva lactuca* (54.3%), *Ulva pertusa* (52.3%), and *Ulva rigida* (53%) [23]. Bioethanol yields based on various biomass sources are presented in Table 1 [24].

**Table 1.** Bioethanol yield from various biomass sources

Biomass	Yield (L/ha)
Sorghum	3.050 - 4.070
Corn	3.460 - 4.020
Beet sugar	5.010 - 6.680
Cassava	3.310
Corn cob	3.460 - 4.020
Algae	46.760 - 140.290

One of the main steps in the conversion of macroalgal biomass into chemicals and biofuels is the deconstruction of complex carbohydrates into sugars [25, 26]. Reducing sugars include monosaccharides such as fructose, glucose, and galactose, as well as disaccharides namely maltose and lactose. However, they do not include polysaccharides such as starch and sucrose [27]. Hydrolysis is a step used to break down the algae cell wall and convert complex carbohydrates into simple sugars, which will then be fermented to produce

**Optimization of *Ulva* sp. Decomposition using H<sub>2</sub>SO<sub>4</sub> with Microwave-Assisted Hydrolysis Method as Feedstock of Bioethanol**

ethanol [28]. Conventional hydrolysis processes generally use concentrated strong acids [29, 30]. These strong acids, such as hydrochloric acid (HCl) or sulfuric acid (H<sub>2</sub>SO<sub>4</sub>), have several drawbacks, including negative impacts on the environment, long reflux times, and low yields due to very fast decomposition. [29, 31].

The relatively slow hydrolysis process can be overcome by using microwave assistance [32, 33]. The use of microwave irradiation can increase the rate of carbohydrate hydrolysis into glucose by 50-80% [34, 35]. Furthermore, microwave heating shortens the hydrolysis time and reduces energy consumption, making it effective in preventing the formation of other unwanted products [11, 31, 36]. Pretreatment of algae biomass using a

microwave at a power of 360 W for a relatively short time of 5-10 min exhibited optimal conditions for the release of organic compounds [37, 38]. Various previous studies regarding the hydrolysis of *Ulva* sp. are shown in Table 2.

Based on the background in Table 2, further study is needed on the production of biomass-based bioethanol raw material in the form of *Ulva* sp. commonly found in Indonesian waters. Therefore, this study aims to determine the optimal decomposition process of *Ulva* sp. with the Microwave-Assisted Hydrolysis (MAH) method using an acid solvent (H<sub>2</sub>SO<sub>4</sub>). Optimization was performed with parameters of hydrolysis time, microwave power, as well as the ratio of materials to solvents.

**Table 2.** Studies on Hydrolysis of *Ulva* sp.

Raw Materials	Methods and Results	Ref
<i>Ulva reticulata</i>	Acid hydrolysis with 2% H <sub>2</sub> SO <sub>4</sub> (150°C, 50 min) yielded a reducing sugar content of 27.30 g/L	[39]
<i>Ulva reticulata</i>	Acid hydrolysis with H <sub>2</sub> SO <sub>4</sub> 2% v/v (75–150°C, 30 min) yielded a reducing sugar content of 2.3–23.7 g/L	[21]
<i>Ulva lactuca</i>	Hydrothermal hydrolysis by autoclaving (121°C, 30 min) yielded a reducing sugar content of 2.9%	[40]
<i>Ulva lactuca</i>	Acid hydrolysis using H <sub>2</sub> SO <sub>4</sub> ( with concentrations of 2, 3,5, and 5%; for 60, 90, and 120 min, at 121°C) yielded a reducing sugar content of 29,050 mg/L	[41]
<i>Ulva rigrida</i>	Acid hydrolysis using H <sub>2</sub> SO <sub>4</sub> and HCl (0-10% v/v, autoclaved for 30, 45, and 60 min) yielded a reducing sugar content of 342 mg/g	[12]
<i>Ulva fasciata</i>	Enzymatic hydrolysis with cellulase 2% v/v in a volume of 20 mL of sodium acetate buffer (36 h incubation, 45°C, 150 rpm) yielded a reducing sugar yield of 206.82 ± 14.96 mg/g	[42]
<i>Ulva lactuca</i>	Acid hydrolysis with 4% H <sub>2</sub> SO <sub>4</sub> (80°C, 120 min) yielded a sugar yield of 155 mg/g	[43]
<i>Ulva</i> sp.	Acid hydrolysis with 2% H <sub>2</sub> SO <sub>4</sub> (autoclaved 121°C, 30 min) yielded a sugar yield of 225 mg/g	[26]
<i>Ulva</i> sp.	Acid hydrolysis with 4% H <sub>2</sub> SO <sub>4</sub> (121°C, 20 min) yielded a reducing sugar content of 21.1%	[19]
<i>Ulva</i> sp.	Hydrolysis with the addition of polyoxometalate (POM) in the microwave (4-10 min, 140°C) yielded a sugar content of 349-435 mg/g	[44]
<i>Ulva prolifera</i>	Enzymatic hydrolysis using <i>S. cerevisiae</i> at pH 4.8, temperature 50°C, 48 h, yielded reducing a sugar content of 0.42 g/g	[45]
<i>Ulva fasciata</i>	Enzymatic hydrolysis with cellulase (sodium acetate buffer pH 4.8, 45°C, 36 h) yielded a reducing sugar content of 20.6 g/L	[46]

## Optimization of *Ulva* sp. Decomposition using H<sub>2</sub>SO<sub>4</sub> with Microwave-Assisted Hydrolysis Method as Feedstock of Bioethanol

### 2. Research Methods

#### 2.1 Tools and Materials

The tools used in this study were a blender (Philips-HR2115), 100 mesh sieve (CBN), container, analytical balance (OHAUS-PX224), measuring cup (Pyrex), Erlenmeyer (Pyrex), round bottom flask (DURAN), condenser, microwave (Electrolux-EMM2308X), model 752AP UV-Vis spectrophotometer, metal spatula, dropping pipette, measuring pipette, vials, micropipette and tip, test tube and rack, cuvette. Meanwhile, the materials used were *Ulva* sp. (from the Cemara Indah Beach area, Situbondo, East Java), aquadest, sulfuric acid (H<sub>2</sub>SO<sub>4</sub>) 98% p.a (Smartlab), 3,5-dinitrosalicylic acid p.a 98% (Sigma Aldrich), anhydrous glucose p.a (Merck), potassium sodium tartrate (Kna-Tartrate) p.a (Pudak), and technical 2M NaOH solution (ROFA).

#### 2.2 Methods

The procedures followed included the pretreatment, the hydrolysis, and the analysis stage for reducing sugar levels, as well as statistical analysis using the Response Surface Methodology (RSM) as shown in Figure 1.

*Ulva* sp. pretreatment stage began with a washing process to remove sand and

other impurities. Subsequently, it was conventionally dried in direct sunlight for 2-3 days, until the mass reached a constant value and obtained a texture that could be easily crushed [47]. The water content used was 10%, then *Ulva* sp. was reduced in size by grinding using a blender. The sample was filtered using a 100 mesh sieve [41], yielding a powder with a uniform size of 0.147 mm.

Furthermore, the hydrolysis process was conducted using sulfuric acid (H<sub>2</sub>SO<sub>4</sub>). The series of tools used during the process included a microwave as shown in Figure 2. *Ulva* sp. powder was weighed with variations in the ratio of the mass to the volume of solvent between 0.03-0.1 [19, 21]. An analytical balance was used to measure the powder, and 100 mL of 2% (v/v) sulfuric acid solution (H<sub>2</sub>SO<sub>4</sub>) was added [39][21]. The hydrolysis process was carried out using a microwave with a power of 150-450 W [37] over a period of 5-15 min [38]. Afterward, the hydrolyzate results were cooled in the beaker glass until room temperature was reached. The hydrolyzate was then filtered using filter paper to separate the filtrate from the residue. The filtrate obtained was placed into a vial for further testing of reducing sugar levels.

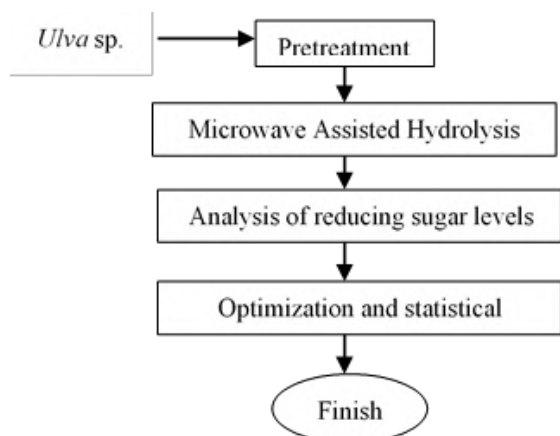


Figure 1. Study procedure

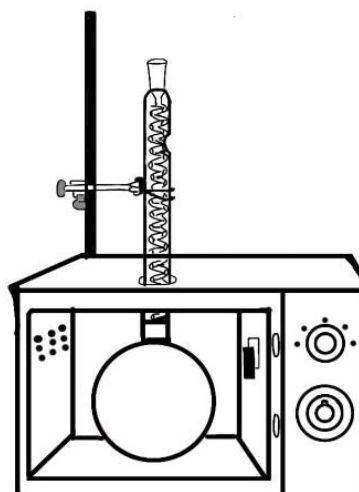


Figure 2. MAH process toolset

**Optimization of *Ulva* sp. Decomposition using H<sub>2</sub>SO<sub>4</sub> with Microwave-Assisted Hydrolysis Method as Feedstock of Bioethanol**

**2.3 Analysis of Reducing Sugar Levels**

The analysis of reducing sugar levels was carried out using a reagent in the form of 3,5-dinitrosalicylic acid (DNSA) and a spectrophotometer. Absorbance as a quantitative analysis was assessed based on the Lambert-Beer Law [48] which states that "The amount of visible light radiation (ultraviolet, infrared, etc.) absorbed or transmitted by a solution is an exponential function of the concentration of the substance and the thickness of the solution" [49]. The absorbance obtained showed the ratio of the absorbed light to the incident light intensity. The resulting absorbance value was directly proportional to the concentration of the substance contained in the sample [50].

DNSA is an aromatic compound that reacts with reducing sugar to form 3-amino 5-nitrosalicylic acid characterized by a reddish-orange color change [31]. The testing stages included sample preparation, preparing DNSA reagents, creation of glucose standard solutions and curves, as well as determining reducing sugar levels. The hydrolyzed sample was filtered using filter paper to separate it from the residue.

To prepare the DNSA reagent, 1 g of DNSA was added to 20 mL of 2M NaOH and then homogenized. Separately, 30 g of KNa Tartrate was dissolved in distilled water and the two solutions were homogenized using a hotplate with a magnetic stirrer. The solution was placed in a 100 mL volumetric flask and added with distilled water to the limit and further homogenized. The homogeneous solution was then placed in a 100 mL reagent bottle [51].

Standard glucose solutions were made in concentrations of 200, 300, 400, 500, 600, and 1000 ppm. A total of 0.5 mL of glucose solution was added to 0.5 mL of

DNSA reagent and 1 mL of distilled water in a test tube. The glucose solution was homogenized and heated in a water bath (boiling water) for 5 min. It was then cooled to room temperature, added with distilled water to a final volume of 5 mL, and homogenized. Absorbance values were measured using UV-Vis spectrophotometry at a wavelength ( $\lambda$ ) of 540 nm. Afterward, a standard curve was made to determine the linear regression equation which was used in determining the sample concentration [51].

The reducing sugar levels were tested by taking 3 mL of the sample solution into a test tube and adding 0.5 mL of DNSA reagent along with 1 mL of distilled water. The mixture was homogenized and heated in a water bath (boiling water) for 5 min. It was then cooled at room temperature, added with distilled water to a final volume of 5 mL, and then homogenized. Absorbance measurements were carried out using UV-Vis spectrophotometry at a wavelength ( $\lambda$ ) of 540 nm [39, 52].

**Table 3.** Variation of *Ulva* sp. hydrolysis data

No.	A (mins)	B (W)	C (g/mL)
1	10	150	0.1
2	5	150	0.065
3	10	450	0.1
4	15	150	0.065
5	5	300	0.03
6	15	450	0.065
7	10	300	0.065
8	10	300	0.065
9	10	150	0.03
10	5	300	0.1
11	15	300	0.1
12	15	300	0.03
13	10	300	0.065
14	10	450	0.03
15	5	450	0.065
16	10	300	0.065
17	10	300	0.065

**Optimization of *Ulva* sp. Decomposition using H<sub>2</sub>SO<sub>4</sub> with Microwave-Assisted Hydrolysis Method as Feedstock of Bioethanol**

2.4 Data analysis

Data analysis used the Design Expert software version 13, adapted to the Response Surface Methodology (RSM) approach and the Box-Behnken Design (BBD) model [53] for 17 runs. Table 3 shows that A is the hydrolysis time (min), B is the microwave power (W), and C is the ratio of the mass of the raw material to the volume of solvent (g/mL).

**3. Results and Discussion**

3.1 Results of Reducing Sugar Levels

To determine the reducing sugar levels, the standard glucose curve was initially derived to ascertain the most suitable linear regression equation. This curve was obtained by measuring the absorbance of standard solutions at various concentrations of 200, 300, 400, 500, 600, and 1000 ppm. Based on the curve in Figure 3, a linear regression equation was obtained for  $y = 0.0004x - 0.0117$ , with an R<sup>2</sup> value of 0.9937.

The results of reducing sugar levels obtained from the hydrolysis of *Ulva* sp. using the MAH method are presented in Table 4. As shown in the table A, B, and C represent the hydrolysis time, the microwave power, and the ratio of the mass of the raw material to the volume of the solvent. The highest reducing sugar content of 19.71 mg/mL was obtained at operating conditions of 15 min hydrolysis time, 450 W microwave power, and 0.065 g/mL ratio of raw material mass to solvent volume. Meanwhile, the lowest value of 1.67 mg/mL was obtained at similar operating conditions of 5 min, 300 W, and 0.1 g/mL respectively. Kolo et al. [21] produced a lower reducing sugar content compared to this study, with a value of 2.3 g/L or equivalent to 2.3 mg/mL when hydrolyzed using H<sub>2</sub>SO<sub>4</sub> at 75°C. This

variation was probably due to differences in operating conditions used in the hydrolysis process.

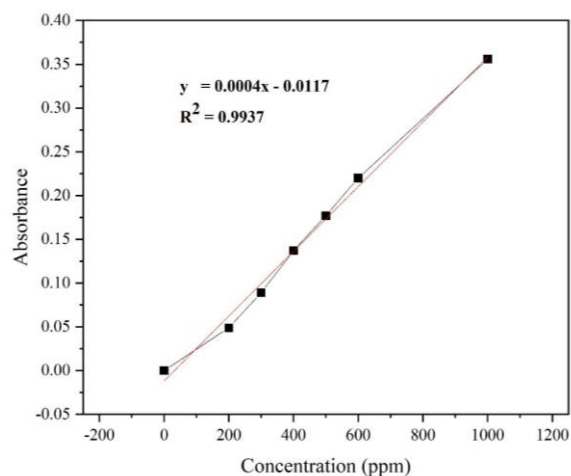


**Figure 3.** Glucose standard solution curve

**Table 4.** Reducing sugar levels in the filtrate hydrolyzed by *Ulva* sp.

No.	A (min)	B (W)	C (g/mL)	Reducing sugar levels (mg/mL)
1	10	150	0.100	3.31
2	5	150	0.065	4.37
3	10	450	0.100	5.04
4	15	150	0.065	7.3
5	5	300	0.030	4.73
6	15	450	0.065	19.71
7	10	300	0.065	5.24
8	10	300	0.065	5.37
9	10	150	0.030	3.68
10	5	300	0.100	1.67
11	15	300	0.100	7.74
12	15	300	0.030	18.81
13	10	300	0.065	5.24
14	10	450	0.030	19.23
15	5	450	0.065	4.16
16	10	300	0.065	6.89
17	10	300	0.065	6.22

3.2 The Effect of Parameters on Reducing Sugar Levels

Figure 4 is a graph showing the effect of each variable used in the hydrolysis process of *Ulva* sp. including hydrolysis time, microwave power, and mass ratio of raw materials to solvent volume on the reducing sugar content.

**Optimization of *Ulva* sp. Decomposition using H<sub>2</sub>SO<sub>4</sub> with Microwave-Assisted Hydrolysis Method as Feedstock of Bioethanol**

Based on the results, the concentration of reducing sugars was strongly influenced by hydrolysis time, as shown in Figures 4(a) and 4(b). There was an increase in the reducing sugar from 4.37 mg/mL to 7.3 mg/mL along with an extended hydrolysis time from 5 to 15 min, at similar microwave power and the ratio of material to solvent conditions.

Figure 4(a) shows that the highest reducing sugar yield was obtained after 15 min of hydrolysis time. This was consistent with Ngamput & Herrani [54] which used variations of hydrolysis time namely 15, 30, 45, and 60 min. The results obtained showed an increase in ethanol content. This was because the longer the hydrolysis

process, the more carbohydrates were degraded into reducing sugars (glucose) [41].

Figures 4(a) and 4(c) also show that the higher the microwave power, the greater the reducing sugar content produced. This was in accordance with the studies conducted by Kumar et al. [37] and Kavitha et al. [55] with varying microwave power of 90–630 W. The results showed that 2 phases of organic release occurred, namely in the range of 90-270 W (minor phase) and 360-630 W (major phase). In the major phase, there was a significant increase in the release of organic matter [37, 55].

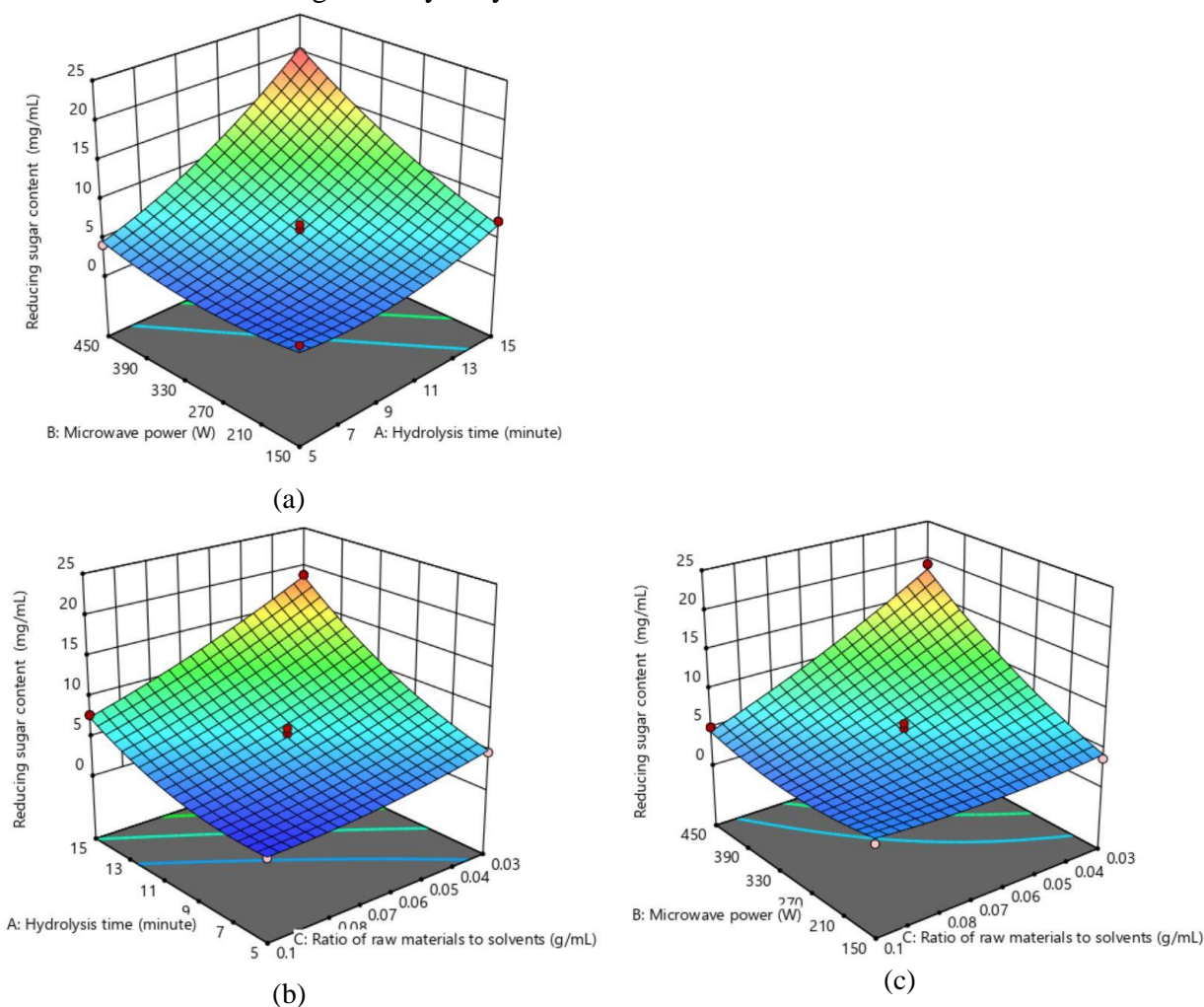


**Figure 4.** Variable relationship to reducing sugar content between (a) hydrolysis time (min) and microwave power (W); (b) raw material mass ratio to solvent volume (g/mL) and hydrolysis time (min); (c) raw material mass ratio to solvent volume (g/mL) and microwave power (W)

**Optimization of *Ulva* sp. Decomposition using H<sub>2</sub>SO<sub>4</sub> with Microwave-Assisted Hydrolysis Method as Feedstock of Bioethanol**

Based on Figures 4(b) and 4(c), the ratio of the raw material in the form of *Ulva* sp. to solvent (H<sub>2</sub>SO<sub>4</sub>) indicated that the higher the ratio, the lower the reducing sugar content produced. Hydrolysis treatment with a ratio of 0.03 g/mL (3 g *Ulva* sp. in 100 mL H<sub>2</sub>SO<sub>4</sub>) for 5 min yielded a reducing sugar content of 4.73 mg/mL. Meanwhile, in the treatment with a ratio of 0.1 g/mL solvent (10 g *Ulva* sp. in 100 mL H<sub>2</sub>SO<sub>4</sub>), the reducing sugar level was reduced to 1.67 mg/mL. This was attributed to the high ratio of ingredients which reduced the homogeneity of *Ulva* sp. powder in the MAH process. The insufficient amount of liquid and high viscosity caused by the high ratio of ingredients posed a challenge to the decomposition reaction, leading to a decrease in the yield of reducing sugars. These results were in line with Dave et al. [56] stating that a higher dose of macroalgae reduced its homogeneity with the solvent, thereby prolonging the hydrolysis time [57].

**3.3 Analysis of Variance (ANOVA)**

Analysis of variance was used to determine the effect of a combination of process variables on the resulting response [58]. The results obtained from the analysis are shown in Table 4. The parameters were considered significant when the p-value (probability) was <0.05 or α=5% according to a predetermined level of significance [58]. In this study, the p-value for the model was <0.001 indicating that the variable hydrolysis time, microwave power, and the ratio of raw material mass to solvent volume had an effect on the reducing sugar content obtained. Furthermore, the lack of fit demonstrated the level of deviation or inaccuracy of the model. The p-value for the lack of fit was > 0.05 indicating not significant results [59]. The p-value obtained for the lack of fit was 0.2483 (not significant) implying the suitability of the response to the model.

**Table 5.** ANOVA test results

Source	Sum of Squares	df	Mean square	F-value	p-value	
<b>Model</b>	526.41	9	58.49	70.91	< 0.0001	significant
A- Hydrolysis time	186.53	1	186.53	226.15	< 0.0001	
B- Microwave power	108.63	1	108.63	131.70	< 0.0001	
C-Ratio of raw materials to solvents	102.89	1	102.89	124.74	< 0.0001	
AB	39.82	1	39.82	48.27	0.0002	
AC	16.04	1	16.04	19.45	0.0031	
BC	47.75	1	47.75	57.89	0.0001	
A <sup>2</sup>	13.01	1	13.01	15.77	0.0054	
B <sup>2</sup>	7.51	1	7.51	9.10	0.0195	
C <sup>2</sup>	1.99	1	1.99	2.41	0.1642	
<b>Residual</b>	5.77	7	0.8248			
Lack of Fit	3.60	3	1.20	2.20	0.2301	not significant
Pure Error	2.18	4	0.5441			
<b>Cor Total</b>	532.18	16				

A = hydrolysis time; B = microwave power; C = raw material mass ratio to solvent volume

**Optimization of *Ulva* sp. Decomposition using H<sub>2</sub>SO<sub>4</sub> with Microwave-Assisted Hydrolysis Method as Feedstock of Bioethanol**

The R<sup>2</sup> value obtained was greater or closer to 1 indicating a better model [59]. The results of the ANOVA analysis presented in Table 5 show that R<sup>2</sup> was 0.9892, implying a significant relationship between hydrolysis time, microwave power, and the ratio of the mass of the raw material to the volume of solvent with the reducing sugar content obtained. The Adjusted R<sup>2</sup> and Predicted R<sup>2</sup> values were considered reasonable because the difference was <0.2.

**Table 6.** Fit Statistic

R <sup>2</sup>	Adjusted R <sup>2</sup>	Predicted R <sup>2</sup>	Adeq precision
0.9892	0.9752	0.8855	26.8875

Mathematically, the equation model for determining reducing sugar content is shown in Equation (1). A positive parameter coefficient indicated an increase in the value of the reducing sugar content, and vice versa. Based on the results, the ratio of the mass of the raw material to the volume of solvent did not significantly affect the reducing sugar content, as indicated by the negative equation coefficient.

The suitability between the experimental data and the model is demonstrated based on the porosity plot graph in Figure 5.

$$Y = 5.79 + 4.83A + 3.69B - 3.59C + 3.15AB - 2.00AC - 3.46BC + 1.76A^2 + 1.34B^2 + 0.6878C^2 \dots\dots\dots(1)$$

where,

Y = reducing sugar content (mg/mL)

A = hydrolysis time (min)

B = microwave power (W)

C = raw material mass ratio to solvent volume (g/mL)

**References**

[1] Paminto, A. K. (2020). Analisis Dan Proyeksi Kebutuhan Energi Sektor Transportasi Di Indonesia. *Jurnal Energi dan Lingkungan (Enerlink)*, 16(2), 51–54. doi: 10.29122/jel.v16i2.4801

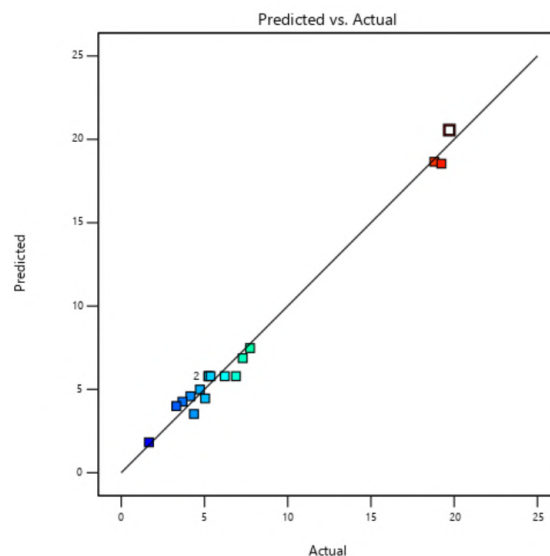


**Figure 5.** Comparison of model data with experimental data

**4. Conclusion**

In conclusion, the optimization of the hydrolysis process of *Ulva* sp. using the MAH method, with the Response Surface Methodology (RSM) model of the Box-Behnken Design (BBD), has demonstrated the significant impact of hydrolysis time (min), microwave power (W), and the ratio of the mass of the raw material to the volume of solvent (g/mL) on reducing sugar levels. This conclusion is further supported by the ANOVA test, which yielded an R<sup>2</sup> value of 0.9892. The highest reducing sugar content of 19.71 mg/mL was achieved by employing a hydrolysis time of 15 min, microwave power of 450 W, and a ratio of raw material mass to solvent volume of 0.065 g/mL.

**Acknowledgments**

The author is grateful to the Institute for Research and Community Service University of Jember for providing Beginner Lecturer Grants for this study.

**Optimization of *Ulva* sp. Decomposition using H<sub>2</sub>SO<sub>4</sub> with Microwave-Assisted Hydrolysis Method as Feedstock of Bioethanol**

- [2] Azhar, M., & Satriawan, D. A. (2018). Implementasi Kebijakan Energi Baru dan Energi Terbarukan Dalam Rangka Ketahanan Energi Nasional. *Administrative Law and Governance Journal*, 1(4), 398–412. doi: 10.14710/alj.v1i4.398-412
- [3] Pertamina. (2020). Pertamina Energy Outlook 2020, 1–128.
- [4] Khan, H., Khan, I., & Binh, T. T. (2020). The heterogeneity of renewable energy consumption, carbon emission and financial development in the globe: A panel quantile regression approach. *Energy Reports*, 6, 859–867. doi: 10.1016/j.egy.2020.04.002
- [5] Raheem, A., Prinsen, P., Vuppaladiyam, A. K., Zhao, M., & Luque, R. (2018). A review on sustainable microalgae based biofuel and bioenergy production: Recent developments. *Journal of Cleaner Production*, 181, 42–59. doi: 10.1016/j.jclepro.2018.01.125
- [6] Nugroho, D., & Rianto, A. (2022). Strategi Indonesia Dalam Mengurangi Emisi Karbon Dioksida (CO<sub>2</sub>) Di Masa New Normal. *Prosiding Ilmu Pemerintahan*, 1(1), 228–242.
- [7] Habibah, F., Budi, S., Kusuma, W., & Wijayati, N. (2016). Produksi Substrat Fermentasi Bioetanol dari Alga Merah *Gracilaria verrucosa*. *Indonesian Journal of Chemical Science*, 5(1), 36–41. Retrieved from <http://journal.unnes.ac.id/sju/index.php/ijcs>
- [8] Palupi, B., Fachri, B. A., Rahmawati, I., Rizkiana, M. F., & Amini, H. W. (2020). Pretreatment of tobacco stems as bioethanol raw material: The effect of temperature and time using chemical method. *AIP Conference Proceedings*, 2278(October). doi: 10.1063/5.0014558
- [9] Kostas, E. T., White, D. A., & Cook, D. J. (2020). Bioethanol Production from UK Seaweeds: Investigating Variable Pre-treatment and Enzyme Hydrolysis Parameters. *Bioenergy Research*, 13(1), 271–285. doi: 10.1007/s12155-019-10054-1
- [10] Aiman, S. (2014). Perkembangan Teknologi Dan Tantangan Dalam Riset Bioetanol Di Indonesia. *Jurnal Kimia Terapan Indonesia*. doi: 10.14203/jkti.v16i2.16
- [11] Yoo, G., Park, M. S., & Yang, J. W. (2015). *Chemical Pretreatment of Algal Biomass. Pretreatment of Biomass: Processes and Technologies*. Elsevier B.V. doi: 10.1016/B978-0-12-800080-9.00012-8
- [12] ElHarchi, M., Kachkach, F. Z., & ElMtili, N. (2018). Optimization Of Thermal Acid Hydrolysis For Bioethanol Production From *Ulva Rigida* With Yeast *Pachysolen Tannophilus*. *South African Journal of Botany*, 115, 161–169. doi: 10.1016/j.sajb.2018.01.021
- [13] Dave, N., Selvaraj, R., Varadavenkatesan, T., & Vinayagam, R. (2019). A critical review on production of bioethanol from macroalgal biomass. *Algal Research*, 42(June), 101606. doi: 10.1016/j.algal.2019.101606
- [14] Dominguez, H., & Loret, E. P. (2019). *Ulva lactuca*, A Source of Troubles and Potential Riches. *Marine Drugs*, 17(6). doi: 10.3390/md17060357
- [15] Pribadi, A. (2020). Forum Kehumasan Dewan Energi Nasional: Menuju Bauran Energi Nasional Tahun 2025. Retrieved from <https://ebtke.esdm.go.id/post/2021/04/09/2838/forum.kehumasan.dewan.energi.nasional.menuju.bauran.energi.nasional.tahun.2025>.
- [16] Ardinata, R. A. & Manguntungi, B. (2020). Inovasi Pemanfaatan Ekstrak Alga Hijau *Ulva* sp dari Pantai Luk, Sumbawa Sebagai Kandidat Antibakteri Terhadap *Salmonella thypi* dan *Staphylococcus aureus*. *Jurnal TAMBORA*, 4(3), 1–6. doi: 10.36761/jt.v4i3.785
- [17] Nur, O. (2014). Chlorophyta. *Implementation Science*, 39(1), 1–24.
- [18] Ramdan, M. R., & Nuraeni, E. (2021). Identifikasi Morfologi *Ulva intestinalis* dan *Acanthophora spicifera* di Kawasan Pantai Tanjung Layar, Sawarna, Bayah, Kabupaten Lebak, Banten. *Tropical Bioscience: Journal of Biological Science*, 1(1), 1–10.
- [19] Margareta, W., Nagarajan, D., Chang, J. S., & Lee, D. J. (2020). Dark fermentative hydrogen production using macroalgae (*Ulva* sp.) as the renewable feedstock. *Applied Energy*, 262(December 2019), 114574. doi: 10.1016/j.apenergy.2020.114574
- [20] Jaya, D., Setiyaningtyas, R., & Prasetyo, S. (2018). Pembuatan Bioetanol Dari Alga Hijau *Spirogyra* Sp Bioethanol Production From Green Algae *Spirogyra* sp. *Eksergi*, 15(1), 16–19.
- [21] Kolo, S. M. D., Presson, J., & Amfotis, P. (2021). Produksi Bioetanol Sebagai Energi Terbarukan Dari Rumpun Laut *Ulva Reticulata* Asal Pulau Timor. *ALCHEMY Jurnal Penelitian Kimia*, 17(2), 159. doi: 10.20961/alchemy.17.2.45476.159-167
- [22] Rilek, N. M., Hidayat, N. & Sugiarto, Y. (2017). Hidrolisis Lignoselulosa Hasil Pretreatment Pelepah Sawit (*Elaeis guineensis* Jacq) menggunakan H<sub>2</sub>SO<sub>4</sub> pada Produksi Bioetanol.

**Optimization of *Ulva* sp. Decomposition using H<sub>2</sub>SO<sub>4</sub> with Microwave-Assisted Hydrolysis Method as Feedstock of Bioethanol**

- 
- Industria: Jurnal Teknologi dan Manajemen Agroindustri*, 6(2), 76–82. doi: 10.21776/ub.industria.2017.006.02.3
- [23] Offei, F., Mensah, M., & Thygesen, A. (2018). Produksi Bioetanol Rumput Laut: Seleksi Proses Ulasan tentang Hidrolisis dan Fermentasi. doi: 10.3390/fermentasi4040099
- [24] Özçimen, D. & İnan, B. An overview of bioethanol production from algae. (2015). *Biofuels-Status and Perspective*, 141–162.
- [25] Greiserman, S., Epstein, M., Chemodanov, A., Steinbruch, E., Prabhu, M., Guttman, L., ...Golberg, A. (2019). Co-production of Monosaccharides and Hydrochar from Green Macroalgae *Ulva* (Chlorophyta) sp. with Subcritical Hydrolysis and Carbonization. *Bioenergy Research*, 12(4), 1090–1103. doi: 10.1007/s12155-019-10034-5
- [26] Jiang, R., Linzon, Y., Vitkin, E., Yakhini, Z., Chudnovsky, A., & Golberg, A. (2016). Thermochemical hydrolysis of macroalgae *Ulva* for biorefinery: Taguchi robust design method. *Scientific Reports*, 6(June), 1–14. doi: 10.1038/srep27761
- [27] Zelvi, M., Suryani, A., & Setyaningsih, D. (2017). Hidrolisis *Eucheuma Cottonii* Dengan Enzim K-Karagenase Dalam Menghasilkan Gula Reduksi Untuk Produksi Bioetanol. *Jurnal Teknologi Industri Pertanian*, 27(1), 33–42. doi: 10.24961/j.tek.ind.pert.2017.27.1.33
- [28] Kusmiyati, K., Heratri, A., Kubikazari, S., Hidayat, A., & Hadiyanto, H. (2020). Hydrolysis of microalgae spirulina platensis, chlorella sp., and macroalgae ulva lactuca for bioethanol production. *International Energy Journal*, 20(4), 611–620.
- [29] Aniriani, G. W., Apriliani, N. F., & Sulistiono, E. (2018). Hydrolysis of Polycoxarida Xylane Straw Using Strong Acid Acid Solution for Basic Materials of Bioetanol Production. *Jurnal Ilmiah Sains*, 18(2), 113–117.
- [30] Roni, K. A. (2015). Pembuatan Bioethanol dari Tanah Gambut dengan Proses Hidrolisis Asam Kuat. *Berkala Teknik*, 5(1), 801–813.
- [31] Kolo, S. M. D., & Edi, E. (2018). Hidrolisis Ampas Biji Sorgum dengan Microwave untuk Produksi Gula Pereduksi sebagai Bahan Baku Bioetanol. *Jurnal Saintek Lahan Kering*, 1(2), 22–23. doi: 10.32938/slk.v1i2.596
- [32] Rokhati, N. (2017). Pengaruh Pretreatment Iradiasi Microwave Pada Hidrolisis Kitosan Dengan Enzim Cellulase. *Jurnal Aplikasi Teknologi Pangan*, 6(1), 7–11. doi: 10.17728/jatp.212
- [33] Darojati, H. A. (2017). Prospek Pengembangan Teknologi Radiasi Sebagai Perlakuan Pendahuluan Biomassa Lignoselulosa. *Jurnal Forum Nuklir*, 11(2), 71. doi: 10.17146/jfn.2017.11.2.5313
- [34] Kolo, S. M. D., Wahyuningrum, D., & Hertadi, R. (2020). The Effects of Microwave-Assisted Pretreatment and Cofermentation on Bioethanol Production from Elephant Grass. *International Journal of Microbiology*, 2020. doi: 10.1155/2020/6562730
- [35] Kostas, E. T., Beneroso, D., & Robinson, J. P. (2017). The application of microwave heating in bioenergy: A review on the microwave pre-treatment and upgrading technologies for biomass. *Renewable and Sustainable Energy Reviews*, 77(November 2016), 12–27. doi: 10.1016/j.rser.2017.03.135
- [36] Santoso, B., Nabilla, A., Rahayu, S., Bondan, A.T., & Selpiana, S. (2020). Ekstraksi minyak biji ketapang menggunakan microwave pretreatment: pengaruh massa biji ketapang dan waktu radiasi. *Jurnal Teknik Kimia*, 26(2), 80–87. doi: 10.36706/jtk.v26i2.543
- [37] Kumar, M. D., Kaliappan, S., Gopikumar, S., Zhen, G., & Banu, J. R. (2019). Synergetic pretreatment of algal biomass through H<sub>2</sub>O<sub>2</sub> induced microwave in acidic condition for biohydrogen production. *Fuel*, 253(March), 833–839. doi: 10.1016/j.fuel.2019.05.066
- [38] Yu, K. L., Chen, W. H., Sheen, H. K., Chang, J. S., Lin, C. S., Ong, H. C., ...Ling, T. C. (2020). Production of microalgal biochar and reducing sugar using wet torrefaction with microwave-assisted heating and acid hydrolysis pretreatment. *Renewable Energy*, 156, 349–360. doi: 10.1016/j.renene.2020.04.064
- [39] Kolo, S. M. D., Obenu, N. M., dan Tuas, M. Y. C. (2022). Pengaruh Pretreatment Makroalga *Ulva Reticula* Menggunakan Microwave Irradiation Untuk Produksi Bioetanol, 16(2), 212–219. doi: <https://doi.org/10.24843/JCHEM.2022.v16.i02.p12>
-

**Optimization of *Ulva* sp. Decomposition using H<sub>2</sub>SO<sub>4</sub> with Microwave-Assisted Hydrolysis Method as Feedstock of Bioethanol**

- [40] Sandra, O. A., Nugroho, W. A., & Yulianingsih, R. (2015). Studi Pengaruh Pretreatment Hidrotermal Terhadap Fermentasi Simultan Pada Rumput Laut (*Ulva Lactuca*) Menjadi Bioetanol. *Jurnal Bioproses Komoditas Tropis*, 3(1), 68–72.
- [41] Poespowati, T., & Mahmudi, A. (2018). Optimization Of Acid Hydrolysis Process On Macroalga *Ulva Lactuca* For Reducing Sugar Production As Feedstock Of Bioethanol. *International Journal of Renewable Energy Research*, 8(1), 466–475. doi: 10.20508/ijrer.v8i1.7069.g7322
- [42] Trivedi, N., Gupta, V., Reddy, C. R. K., & Jha, B. (2013). Enzymatic Hydrolysis And Production Of Bioethanol From Common Macrophytic Green Alga *Ulva Fasciata* Delile. *Bioresource Technology*, 150, 106–112. doi: 10.1016/j.biortech.2013.09.103
- [43] Wu, Z. Z., Li, D. Y., & Cheng, Y. S. (2018). Application of ensilage as a green approach for simultaneous preservation and pretreatment of macroalgae *Ulva lactuca* for fermentable sugar production. *Clean Technologies and Environmental Policy*, 20(9), 2057–2065. doi: 10.1007/s10098-018-1574-7
- [44] Tsubaki, S., Oono, K., Hiraoka, M., Ueda, T., Onda, A., Yanagisawa, K., & Azuma, J. I. (2014). Hydrolysis of green-tide forming *Ulva* spp. by microwave irradiation with polyoxometalate clusters. *Green Chemistry*, 16(4), 2227–2233. doi: 10.1039/c3gc42027b
- [45] Li, Y., Cui, J., Zhang, G., Liu, Z., Guan, H., Hwang, H., ... Wang, P. (2016). Optimization Study On The Hydrogen Peroxide Pretreatment And Production Of Bioethanol From Seaweed *Ulva Prolifera* Biomass. *Bioresource Technology*, 214, 144–149. doi: 10.1016/j.biortech.2016.04.090
- [46] Hebbale, D., Bhargavi, R., & Ramachandra, T.V. (2019). Saccharification of macroalgal polysaccharides through prioritized cellulase producing bacteria. *Heliyon*, 5(3), e01372. doi: 10.1016/j.heliyon.2019.e01372
- [47] Ramachandra, T.V., & Hebbale, D. (2020). Bioethanol from macroalgae: Prospects and challenges. *Renewable and Sustainable Energy Reviews*, 117(September 2019), 109479. doi: 10.1016/j.rser.2019.109479
- [48] Winahyu, D. A., Retnaningsih, A., & Aprilia, M. (2019). Penetapan Kadar Flavonoid Pada Kulit Batang Kayu Baru Dengan Metode Spektrofotometri UV-VIS. *Jurnal Analisis Farmasi*, 4(1), 29–36.
- [49] Putri, L. E. (2017). Penentuan Konsentrasi Senyawa Berwarna KMnO<sub>4</sub> Dengan Metoda Spektroskopi UV Visible. *Natural Science Journal*, 3(1), 391–398.
- [50] Gusnedi, R. (2013). Analisis Nilai Absorbansi dalam Penentuan Kadar Flavonoid untuk Berbagai Jenis Daun Tanaman Obat. *Pillar of Physics*, 2, 76–83.
- [51] Lastriyanto, A. & Aulia, A. I. (2021). Analisa Kualitas Madu Singkong (Gula Pereduksi, Kadar Air, dan Total Padatan Terlarut) Pasca Proses Pengolahan dengan Vacuum Cooling. *Jurnal Ilmu Produksi dan Teknologi Hasil Peternakan*, 9(2), 110–114. doi: 10.29244/jipthp.9.2.110-114
- [52] Galung, F. S. (2021). Analisis Kandungan Karbohidrat (Glukosa) Pada Salak Golla – Golla. *Journal of Agritech Science*, 5(1), 10–14.
- [53] Hidayat, I. R., Zuhrotun, A., & Sopyan, I. (2020). Design-Expert Software sebagai Alat Optimasi Formulasi Sediaan Farmasi. *Majalah Farmasetika*, 6(1), 99–120. doi: 10.24198/mfarmasetika.v6i1.27842
- [54] Ngamput, H. M. A., & Herrani, R. (2019). The Effect Of Differentiation Of Hydrolysis Time Towards Ethanol Levels Produced Through *Ulva Lactuca* Fermentation. *Journal of Physics: Conference Series*, 1241(1). doi: 10.1088/1742-6596/1241/1/012010
- [55] Kavitha, S., Rajesh Banu, J., Kumar, G., Kaliappan, S., & Yeom, I. T. (2018). Profitable ultrasonic assisted microwave disintegration of sludge biomass: Modelling of biomethanation and energy parameter analysis. *Bioresource Technology*, 254(December 2017), 203–213. doi: 10.1016/j.biortech.2018.01.072
- [56] Dave, N., Varadavenkatesan, T., Selvaraj, R., & Vinayagam, R. (2021). Modelling Of Fermentative Bioethanol Production From Indigenous *Ulva Prolifera* Biomass By *Saccharomyces Cerevisiae* Nfcc1248 Using An Integrated Ann-Ga Approach. *Science of the Total Environment*, 791, 148429. doi: 10.1016/j.scitotenv.2021.148429

**Optimization of *Ulva* sp. Decomposition using H<sub>2</sub>SO<sub>4</sub> with Microwave-Assisted Hydrolysis Method as Feedstock of Bioethanol**

---

- [57] Kim, D. H., Lee, S. B., & Jeong, G. T. (2014). Production of reducing sugar from *Enteromorpha intestinalis* by hydrothermal and enzymatic hydrolysis. *Bioresource Technology*, 161, 348–353. doi: 10.1016/j.biortech.2014.03.078
- [58] Sabathani, A., Widjanarko, S. B., & Yuwono, S. S. (2018). Optimasi Durasi Dan Rasio Bahan Per Pelarut Ekstrak Daun Pepaya Untuk Uji Aktivitas Antibakteri. *Jurnal Teknologi Pertanian*, 19(3), 193–206. doi: 10.21776/ub.jtp.2018.019.03.6
- [59] Ramadhani, R. A., Riyadi, D. H. S., Triwibowo, B., & Kusumaningtyas, R. D. (2017). Review Pemanfaatan Design Expert untuk Optimasi Komposisi Campuran Minyak Nabati sebagai Bahan Baku Sintesis Biodiesel. *Jurnal Teknik Kimia dan Lingkungan*, 1(1), 11. doi: 10.33795/jtkl.v1i1.5

# The Effect of H-Factor on Kappa Number and Viscosity in Continuous Digester

*Pengaruh H-Factor terhadap Kappa Number dan Viscosity pada Continuous Digester*

Rizka Wulandari Putri<sup>1\*</sup>, Rahmatullah<sup>1)</sup>, Faisal Siagian<sup>1)</sup>

<sup>1)</sup>Universitas Sriwijaya, Chemical Engineering, Faculty of Engineering, Indonesia

## Article History

Received: 14<sup>th</sup> February 2023; Revised: 05<sup>th</sup> May 2023; Accepted: 06<sup>th</sup> May 2023;

Available online: 15<sup>th</sup> June 2023; Published Regularly: June 2023

doi: [10.25273/cheesa.v6i1.15681.26-33](https://doi.org/10.25273/cheesa.v6i1.15681.26-33)

\*Corresponding Author.

Email:

[rizkawulandariputri@unsri.ac.id](mailto:rizkawulandariputri@unsri.ac.id)

## Abstract

One of the most important steps in pulping is the cooking process, which serves to separate the cellulose and hemicellulose from lignin and other by-products. During the cooking process in the digester, various factors must be considered to create high-quality pulp. Among these factors, the H-Factor plays a significant role due to its impact on the kappa number and viscosity in the pulping process. A high H-Factor can also damage the strength of the pulp. Therefore, this research aims to investigate the effect of the H-Factor and active alkali on pulp yield and quality. The active alkali used was in line with the desired production objectives, as insufficient levels of active alkali can lead to a low yield of pulp. Meanwhile, pulp quality standards in the Pulp and Paper Industry included kappa number of 12-18 in the digester process, an approximate viscosity of 23 mPa.s, and the selection of H-Factor based on the desired production target.

**Keywords:** active alkali; cooking process; H-Factor; kappa number; viscosity

## Abstrak

Salah satu langkah terpenting dalam proses pulping adalah proses pemasakan. Tujuan dari proses pemasakan ini adalah untuk memisahkan selulosa dan hemiselulosa dari lignin dan produk sampingan lainnya. Dalam proses pemasakan pada digester, banyak faktor yang harus diperhatikan untuk menciptakan kualitas pulp yang baik, yaitu H-Factor, karena sangat mempengaruhi bilangan kappa dan viskositas dalam proses pulping. H-Factor yang tinggi akan merusak kekuatan pulp. Penggunaan alkali aktif harus sesuai dengan tujuan produksi yang ingin dicapai. Ketika alkali aktif ini terlalu rendah maka yield pulp akan rendah. Kualitas pulp pada industri Pulp and Paper meliputi beberapa standar antara lain bilangan kappa adalah 12-18 pada proses digester, viskositas sekitar 23 mPa.s, dan H-Factor yang digunakan bergantung pada target produksi.

**Kata kunci:** alkali aktif; bilangan kappa; H-Factor; proses pemasakan; viskositas

## 1. Introduction

A major part of the pulp production process is the digester [1]. The digester has several parameters such as temperature and time, which are expressed in H-Factor during the cooking process. This H-Factor has a significant effect on pulp quality, namely the kappa number, and viscosity. The kappa number is used to express the

amount of lignin remaining in the pulp and the viscosity determines the strength of the pulp produced [2]. In this unit, temperature and residence time during cooking are among the parameters that determine pulp quality as well as the amount of time and chemicals consumed.

In the pulp production process, one important factor to be considered is the

**The Effect of H-Factor on Kappa Number and Viscosity in Continuous Digester**

relationship between time and temperature, which is expressed in the H-Factor [3]. When the H-Factor is excessively high, it can cause the chips to overcook, resulting in the reduction of the lignin content due to maximum degradation. This will bereave more cellulose fibers due to the degradation process that causes a decrease in pulp quality. However, a low H-Factor has a negative impact, as it indicates that the wood chips are not cooked well and need to be reprocessed, resulting in increased consumption of time and chemicals.

Several parameters including the H-Factor need to be considered to obtain high-quality pulp [4]. The H-Factor is one of the cooking variables that should be considered when processing wood chips in the digester unit due to its relationship with the strength of the pulp (viscosity) and the amount of lignin remaining in the chips (kappa number). Therefore, this research aims to examine the kappa number and viscosity values of the pulp obtained from the blow tank with varying H-Factor.

## 2. Research Methods

Several steps were taken to determine the effect of the H-Factor on the kappa number and viscosity of pulp in continuous digesters. These included literature research, data collecting, data processing, calculation of white liquor composition, and analysis of the effect of the H-Factor on kappa number and viscosity. The representation of the research steps is shown in Figure 1.

The required data for this research were obtained from observations made at the Digital Control System (DCS) in the Pulp and Paper industry. The data were collected based on the production results from May to July 2022 at PT. Tanjung

Enim Lestari Industry Pulp and Paper, Tanjung Enim, South Sumatera.

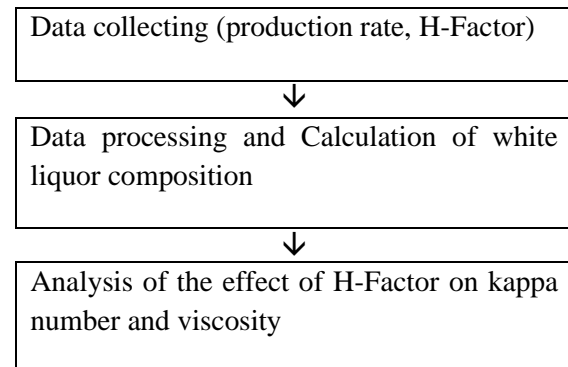


**Figure 1.** Flow chart of research

## 3. Result and Discussion

The two factors that influence chip maturity in solvents are time and temperature during cooking, which significantly affect pulp quality. Moreover, the H-factor represented the relationship between cooking time and temperature. This H-Factor aims to achieve a pulp viscosity standard of 23 mPa.s and a kappa number ranging from 12 to 18. These two parameters must meet the standards because when the viscosity is too high, it will create a pulp that is prone to breakage. For example, excessively high kappa numbers cause yellow spots in the pulp produced, while lower values result in the easy breakdown of cellulose fibers. [5]. In a Pulp and Paper Industry, the primary objective is to ensure pulp quality and meet production targets. To achieve this, the pulp digester unit must optimize the production rate that meets the kappa number with minimum chemical and energy inputs through the arrangement of the H-Factor [6].

### 3.1 Effect of H-Factor on Production Rate

In this research, the H-Factor used in the digester unit was determined by the production rate. It ensured the attainment of effective temperature and residence time

## The Effect of H-Factor on Kappa Number and Viscosity in Continuous Digester

during chip cooking and produced optimal pulp quality. Table 1 provided the data on production levels with their respective H-Factors.

Table 1 showed the best data for each production target based on the quality parameters of viscosity, brightness, and kappa number, which were close to the standardized values. The higher the production rate, the greater the H-Factor used and the more optimal the pulp quality. Based on the observation data in Table 1, the best pulp production was obtained at the target of 1500 ADT/d with an H-Factor of 1175. This resulted in a kappa number of 15.8, a viscosity of 20.5 mPa.s, and a brightness value of 29.5% ISO. These values fulfilled the required pulp quality standards in the Pulp and Paper industry. Moreover, the use of a higher or optimal H-Factor used caused a greater degradation of lignin, yielding a higher brightness value, with optimum kappa number, and viscosity [7].

The use of a low H-Factor in high production resulted in a non-optimal kappa number and pulp viscosity which required higher active alkali consumption and production cost [7].

### 3.2 Effect of H-Factor on Kappa Number and Viscosity

The H-Factor used in the cooking stage played crucial in determining the value of the kappa number and viscosity of the pulp. Based on previous research, a

higher or optimized H-Factor used will result in greater lignin degradation, indicating more effective temperature and residence time during chip cooking [8].

Figures 2 (a) and (b) showed the contrasting relationship between H-Factor and both the kappa number and viscosity. The results revealed that as the H-Factor increased, there was a corresponding decrease in the value of kappa number and viscosity, indicating a significant degradation in lignin. Kappa numbers standard obtained ranged from 12 to 18 and no statistically significant differences were observed.

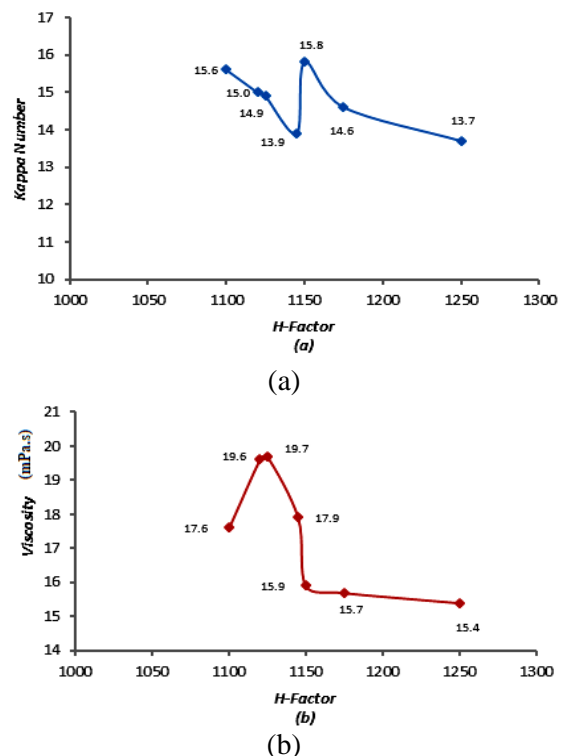


**Figure 2.** (a) Relationship between H-Factor and Kappa Number, (b) Relationship between H-Factor and Viscosity at a Production rate of 1200 ADT/d

**Table 1.** H-Factor at each production level

Date	Production Rate (ADT/d)	H-Factor	Viscosity (mPa.s)	Kappa Number	Brightness (%ISO)
09/05/22	1200	1125	19.7	14.9	27.7
03/07/22	1300	1145	19.4	15.7	29.4
02/06/22	1400	1175	20.4	15.8	29.4
04/05/22	1500	1175	20.5	15.8	29.5
26/06/22	1600	1150	19.1	15.0	29.0

**The Effect of H-Factor on Kappa Number and Viscosity in Continuous Digester**

The kappa number increased at an H-Factor of 1150 and decreased at the highest H-Factor. These results showed that H-Factor served as a useful tool to predict and control the rate of delignification, even when employing different combinations of pulping time and temperature. The viscosity increased with H-Factor due to the removal of hemicellulose and the weakening of cellulose in the extractive step. However, the viscosity decreased due to cooking treatments [9].

Figures 3 (a) and (b) showed the inversely proportional relationship between H-Factor and both the kappa number, and viscosity. Based on the results, the higher the H-Factor used, the lower the value of

the kappa number. This indicated that more lignin was degraded during the cooking process.

The kappa number was influenced by the cooking liquid ratio and control parameters such as H-Factor or increased cooking time. When using a low active alkali with a long cooking time or vice versa, the factor was influenced by the moisture content of the wood.

In this production, a decrease in viscosity was observed at the H-Factor of 1600. The initial increase in viscosity was due to a decrease in hemicellulose content or a high degree of polymerization (DP) of the pulp in the remaining cellulose fraction.

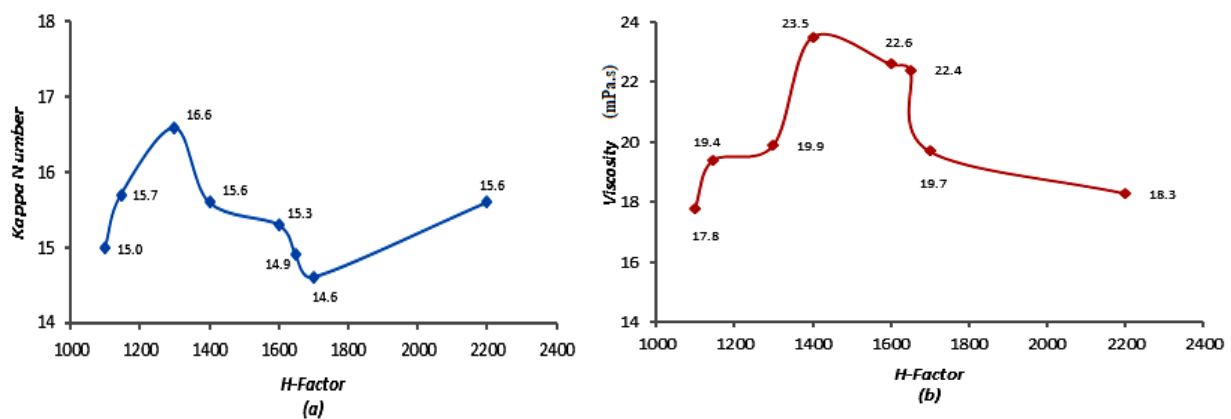


**Figure 3.** (a) Relationship between H-Factor and Kappa Number, (b) Relationship between H-Factor and Viscosity at a Production rate of 1300 ADT/d

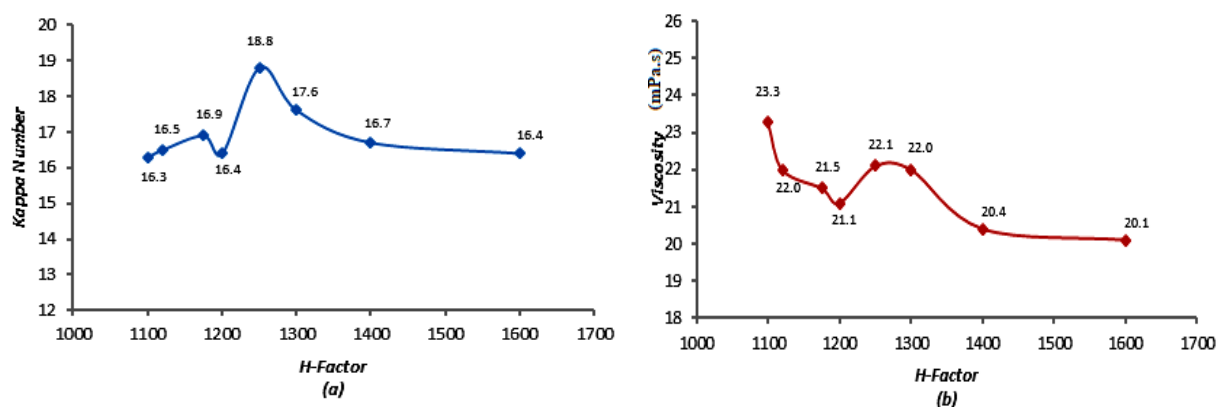


**Figure 4.** (a) Relationship of H-Factor and Kappa Number, (b) Relationship of H-Factor and Viscosity at a Production rate of 1400 ADT/d

**The Effect of H-Factor on Kappa Number and Viscosity in Continuous Digester**

The maximum viscosity with extraction severity indicated that the use of a high H-Factor resulted in fiber breakage due to increased accessibility of cooking liquor to crystalline cellulose. Therefore, to maintain fiber strength and crystallinity at this level of extraction, the cooking liquor should be weaker [9].

Figures 4 (a) and (b) showed that the relationship between H-Factor and both kappa number and viscosity was inversely proportional. This indicated that the higher the H-Factor used, the lower the value of the kappa number. However, in the H-Factor of 1250, the kappa number had increased slightly. This was not in line with the theory, where a higher H-Factor caused a decrease in the kappa number. For the H-Factor of 1250 that contrast with theory, high kappa numbers occurred due to the low active alkali charge used in the cooking process [9], as indicated by the large number of rejects produced. The low active alkali charge made the kappa number still significantly high. The use of excessively low active alkali charge also produced more rejects of undesired pulp [10]. This rejection was caused by uncooked wood chips in the digester because the incomplete delignification process decreased pulp quality. Therefore,

the use of active alkali loading should be considered to obtain the best pulp quality [9]. In this research, the viscosity value increased at H-Factor 1250.

Most of the increase in viscosity increase can be traced to the removal of hemicellulose and high cellulose content. The removal of the hemicellulose increased the crystallinity index of pulp fibers in the softwood fibers [9].

Figure 5 (a) showed that there was no continuity between the theory of the H-Factor and the kappa number. Furthermore, the relationship between H-Factor and kappa number was directly proportional.

Pascoal, et al stated that variations in time during cooking with a constant temperature affected the value of the kappa number. This was because a longer cooking time caused a reduction in the value of the kappa number and vice versa [11]. The cooking time was also directly proportional to H-Factor. Therefore, it can be concluded that the increase in kappa number in Figure 5 (a) was caused by high cooking temperature with low time. A decrease in kappa value was in line with the increasing H-Factor and cooking temperature, leading to more degradation of lignin.

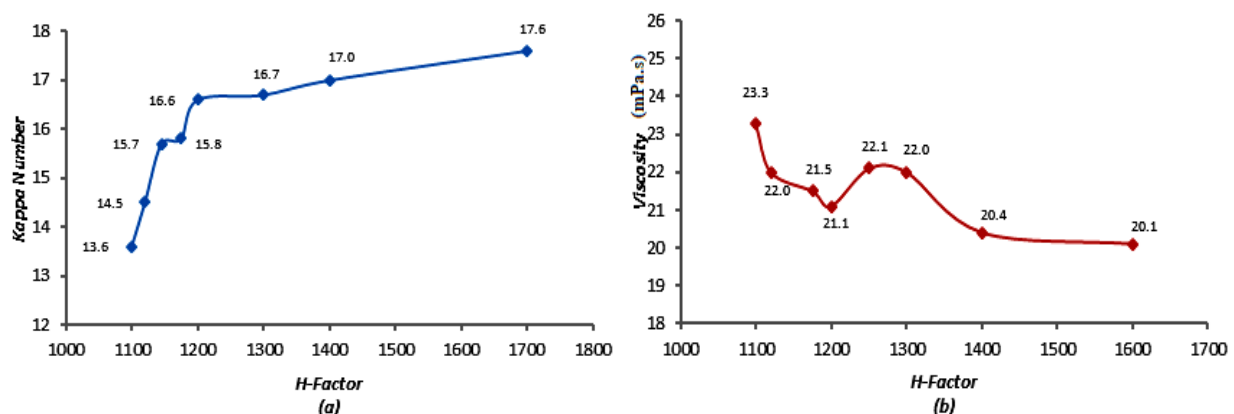


**Figure 5.** (a) Relationship of H-Factor and Kappa Number, (b) Relationship of H-Factor and Viscosity at a Production rate of 1500 ADT/d

**The Effect of H-Factor on Kappa Number and Viscosity in Continuous Digester**

The main objective of cooking is to reduce the lignin content, as measured by the kappa number as a standard. An increase in active alkali content leads to a decrease in pulp yield. Therefore, the higher the active alkali content used during the cooking process, the lower the pulp yield. Every 1% increase in active alkali content will also reduce pulp yield by 0.15% due to the high degree of delignification [12].

The relationship between H-Factor and viscosity shown in Figure 5 (b) was inversely proportional. The results showed that the higher the H-Factor used, the lower the viscosity value achieved. This result was in line with related research data, where the H-Factor value was inversely proportional to the viscosity value [7]. However, at lower H-Factor variations of 1100, 1120, and 1145 there was a high viscosity value. Viscosity was a function of cellulose fiber degradation in the pulping process (Tappi T-230). In this context, temperature ranging from 150 to 170°C was the main driving force for degrading the cellulose pulp structure by the associated viscosity decrease. The viscosity increased with H-Factor due to the removal of hemicellulose and short-chain cellulose in the extractive step,

which further decreased as a result of more severe cooking treatments.

The high viscosity at low white liquor ratios can be attributed to good interfiber connections. Meanwhile, a limited amount of white liquor weakened the cellulose bond. [13]. The high pulp viscosity was expected to improve pulp quality, pulp strength, tensile strength, and ease of treatment.

Figures 6 (a) and (b) showed that the relationship between H-Factor and kappa number was inversely proportional. This indicated that the higher the H-Factor used, the lower the kappa number. Similarly, previous research stated that the H-Factor value was inversely proportional to the viscosity value and kappa number [7].

The H-Factor in the cooking process affected the kappa number and viscosity of the pulp. Based on the data, a higher production rate led to an increase in the H-Factor used. However, excessively high temperatures and cooking time can damage cellulose, leading to low pulp yield [14]. To ensure the desired chip maturity, the relationship between temperature and time must be maintained, as shown in the H-Factor. This balance is necessary to achieve the desired kappa number and pulp viscosity.

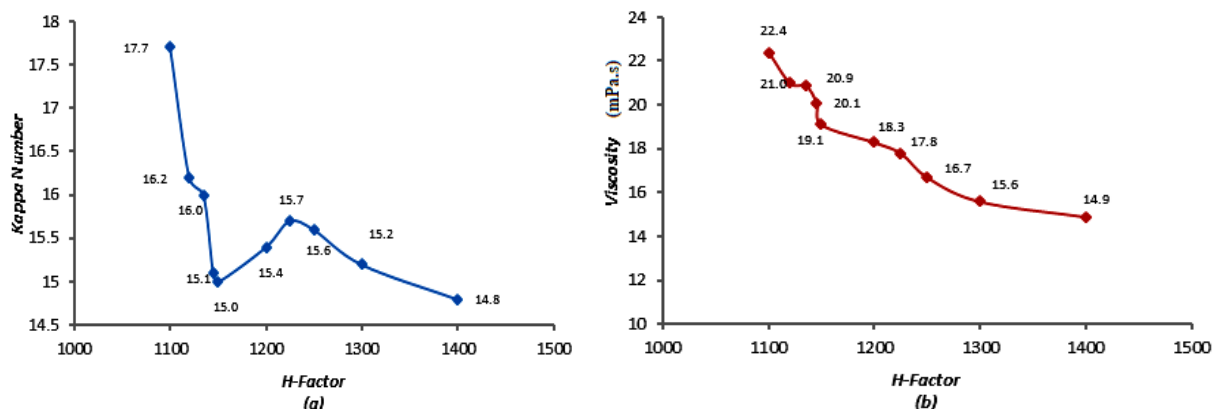


**Figure 6.** (a) Relationship of H-Factor and Kappa Number, (b) Relationship of H-Factor and Viscosity at a Production rate of 1600 ADT/d

**The Effect of H-Factor on Kappa Number and Viscosity in Continuous Digester**

The H-Factor is a variable that needs to be controlled to obtain the kappa number of the pulp produced. When the kappa number value exceeds the standardization, it can increase the H-Factor and vice versa [15].

In a cooking process system (digestion), many parameters must be considered to obtain the best results, with temperatures ranging from 150 to 170°C. A good quality pulp with a high white liquor content can be obtained by controlling the H-Factor with a short cooking time. However, this approach requires a high price for chemicals. The H-Factor is used as a variation of time and temperature to describe the cooking conditions and optimize the process without any wasted energy. The equal distribution of the white liquor throughout the cooking section enables the chips to cook at the appropriate temperature and time.

**4. Conclusion**

The best pulp production at the target of 1500 Adt/d was obtained at an H-Factor value of 1175 with a kappa number parameter of 15.8, a viscosity of 20.5 mPas, and a brightness value of 29.5% ISO. This indicated that higher production levels led to a greater H-Factor, thereby producing the optimal pulp quality. The results met the TAPPI standard such as 1-100 of kappa number (TAPPI/ANSI T 236 om-13) and viscosity of 7 – 27 mPa.s (TAPPI T 230 om-08). The H-Factor was also influenced by the active alkali charge of white liquor. The relationship between H-Factor and kappa number and viscosity was inversely proportional. This was shown by a decrease in viscosity and kappa number due to a higher H-Factor value. The H-Factor was used as a time adjustment at various cooking temperatures and condition estimation, in case of deviations from the operating standards.

**References**

- [1] Sheoran, M., Goswami, S., Pant, H. J., Biswal, J., Sharma, V. K., Chandra, A., Dash, A. (2016). Measurement of residence time distribution of liquid phase in an industrial-scale continuous pulp digester using radiotracer technique. *Applied Radiation and Isotopes*, 111, 10–17. doi: 10.1016/j.apradiso.2016.01.025
- [2] Segura, T. E. S., dos Santos, J. R. S., Sarto, C., & da Silva, J. F. G. (2016). Effect of Kappa Number Variation on Modified Pulping of Eucalyptus. *BioResources*, 11(4), 9842–9855. doi: 10.15376/BIORES.11.4.9842-9855
- [3] Li, J., Hu, H., & Chai, X. (2017). The kinetic modeling of carbonate formation during kraft pulping of eucalyptus wood. *AIChE Journal*, 63(5), 1489-1493. doi: 10.1002/aic.15681
- [4] Sim, K., Youn, H. J., Cho, H., Shin, H., & Lee, H. L. (2012). Improvements in pulp properties by alkali pre-extraction and subsequent kraft pulping with controlling h-factor and alkali charge. *BioResources*, 7(4), 5864–5878. doi: 10.15376/biores.7.4.5864-5878
- [5] Bahri, S. (2017). Pembuatan Pulp dari Batang Pisang. *Jurnal Teknologi Kimia Unimal*, 4(2), 36. doi: 10.29103/jtku.v4i2.72
- [6] Mercangoz, M., & Doyle, F. J. (2006). Characterizing the process from the digester to the paper machine. *IEEE Control Systems*, 26(4), 30–39. doi: 10.1109/MCS.2006.1657874
- [7] Małachowska, E., Dubowik, M., Boruszewski, P., Łojewska, J., & Przybysz, P. (2020). Influence of lignin content in cellulose pulp on paper durability. *Scientific Reports*, 10(1), 1–12. doi: 10.1038/s41598-020-77101-2
- [8] Sinaga, I. (2008). *Pengaruh H-Faktor terhadap Viskositas dan Bilangan Kappa Unbleach Diunit Digester di Pt Toba Pulp Lestari Tbk. Porsea*. Institusi Universitas Sumatera Utara.
- [9] Núñez, N., Martín-Alfonso, J. E., Eugenio, M. E., Valencia, C., Díaz, M. J., & Franco, J. M.

## The Effect of H-Factor on Kappa Number and Viscosity in Continuous Digester

---

- (2012). Influence of eucalyptus globulus kraft pulping severity on the rheological properties of gel-like cellulose pulp dispersions in castor oil. *Industrial and Engineering Chemistry Research*, 51(29), 9777–9782. doi: 10.1021/ie301014v
- [10] Ardina, V., Irawan, B., Prajitno, D. H., & Roesyadi, A. (2018). Active alkali charge effect on kraft pulping process of acacia mangium and eucalyptus pellita. In *AIP Conference Proceedings*, 1-6. doi: 10.1063/1.5054440
- [11] Pascoal, N., C., Evtuguin, D. V., Furtado, F. P., & Mendes, S. A. P. (2002). Effect of pulping conditions on the ECF bleachability of Eucalyptus globulus kraft pulps. *Industrial and Engineering Chemistry Research*, 41, 6200-6206. doi: 10.1021/ie020263x
- [12] Luo, X., Liu, J., Zhan, H., Cao, S., Huang, L., & Chen, L. (2013). Prediction model and in-digester control of residual alkali content in black liquor during kraft pulping of eucalyptus. *Journal of Biobased Materials and Bioenergy*, 7 (5), 559-565. doi: 10.1166/jbmb.2013.1391
- [13] Santos, R. B., Jameel, H., Chang, H. M., & Hart, P. W. (2012). Kinetics of hardwood carbohydrate degradation during kraft pulp cooking. *Industrial and Engineering Chemistry Research*. 51, 12192-12198. doi: 10.1021/ie301071n
- [14] Supraptiah, E., Ningsih, A., S., Sofiah, & Apriandini, R. (2014). Pengaruh Rasio Cairan Pemasak (AA Charge) Pada Proses Pembuatan Pulp dari Kayu Sengon (*Albizia Falcataria*) Terhadap Kualitas Pulp. *Kinetika*, 5(1), 14–21.
- [15] Resalati, H., Kermanin, H., Fadavi, F., & Feizmand, M. (2012). Effect of Hot-Water and Mild Alkaline Extraction on Soda-Aq Pulping of Wheat Straw. *Lignocellulose*, 1(1), 71-80.

# Identification of Flavonoid Compounds in Ethanol Extract of Majapahit plant (*Crescentia cujete*) Leaves and their Potential as Anticancer

Identifikasi Senyawa Flavonoid Ekstrak Etanol Daun Tanaman Majapahit (*Crescentia cujete*) dan Potensinya sebagai Antikanker

Rahma Diyan Martha<sup>1\*</sup>, Fatimah<sup>2)</sup>, Danar<sup>3)</sup>, Hesty Parbuntari<sup>4)</sup>

<sup>1)</sup>STIKes Karya Putra Bangsa, Department of Pharmacy, Indonesia

<sup>2)</sup>STIKes Karya Putra Bangsa, Department of Health Analyst, Indonesia

<sup>3)</sup>Universitas Negeri Malang, Department of Chemistry, Indonesia

<sup>4)</sup>Universitas Negeri Padang, Department of Chemistry, Indonesia

## Article History

Received: 05<sup>th</sup> October 2022; Revised: 08<sup>th</sup> June 2023; Accepted: 15<sup>th</sup> June 2023;

Available online: 25<sup>th</sup> June 2023; Published Regularly: June 2023

doi: [10.25273/cheesa.v6i1.14056.34-48](https://doi.org/10.25273/cheesa.v6i1.14056.34-48)

\*Corresponding Author.

Email:

rahmadiyan@stikes-kartrasa.ac.id

## Abstract

The Majapahit plant is commonly found in Indonesia but is rarely used due to a lack of information about its potential. One of the secondary metabolites commonly found in this plant are flavonoids. Therefore, this study aims to determine the distribution of flavonoid compounds in the Majapahit plant, particularly their potential as anticancer activity. Leaf material from Majapahit plants was extracted using the maceration technique, while the flavonoid compounds in the extract were identified using LCMS (Shimadzu LCMS-8040 LC/MS). The identification results showed that about 97 compounds were detected, including 14 flavonoids. The flavonoid compounds found include Quercetin, Chlorogenic acid, Kaempferol 3-O rhamnoside, Acacetin 7-rutinoside, Fortunellin, Kaempferol 3-[6''-(3-hydroxy-3-methyl glutaryl) glucoside], Didymin, Diosmin, Hesperidin, Rutin, Citrusoside C, Citrusoside D, Narirutin 4'-glucoside, and Kaempferol 3-[6''-(3-hydroxy-3-methylglutaryl)glucoside] -7-glucoside. The highest composition of the identified flavonoid compounds was found in Kaempferol 3-O rhamnoside, with a 3.90%

**Keywords:** ethanol extract; flavonoids; Majapahit plant leaves; LCMS

## Abstrak

Tanaman Majapahit banyak ditemukan di Indonesia, tetapi kurang dapat dimanfaatkan oleh masyarakat Indonesia, karena kurangnya informasi mengenai potensi tanaman tersebut. Senyawa metabolit sekunder yang ditemukan salah satunya yaitu flavonoid. Tujuan penelitian ini adalah untuk mengetahui sebaran senyawa flavonoid ekstrak etanol daun tanaman majapahit yang berpotensi sebagai antikanker. Metode yang digunakan untuk ekstraksi daun tanaman majapahit yaitu maserasi, sedangkan identifikasi senyawa flavonoid pada ekstrak daun tanaman majapahit menggunakan LCMS (Shimadzu LCMS-8040 LC/MS). Identifikasi menggunakan LCMS (Shimadzu LCMS-8040 LC/MS) diketahui sekitar 97 senyawa yang terdeteksi, termasuk didalamnya 14 senyawa flavonoid. Senyawa flavonoid yang ditemukan, yaitu; Quercetin, Chlorogenic acid, Kaempferol 3-O rhamnoside, Acacetin 7-rutinoside, Fortunellin, Kaempferol 3-[6''-(3-hydroxy-3-methyl glutaryl) glucoside], Didymin, Diosmin, Hesperidin, Rutin, Citrusoside C, Citrusoside D, Narirutin 4'-glucoside, dan Kaempferol 3-[6''-(3-hydroxy-3-methylglutaryl)glucoside] -7-glucoside. Salah satu senyawa golongan flavonoid yang terdeteksi, senyawa Kaempferol 3-O rhamnoside yang memiliki komposisi tertinggi yaitu 3,90%.

**Kata kunci:** daun tanaman majapahit; ekstrak etanol; flavonoid; LCMS

## Identification of Flavonoid Compounds in Ethanol Extract of Majapahit plant (*Crescentia cujete*) Leaves and their Potential as Anticancer

### 1. Introduction

Indonesia is renowned for its abundant natural resources, including a biodiversity of animal and plant species. This biodiversity produces numerous types and quantities of chemical compounds that play a crucial role in supporting life, particularly for humans, such as medicines and antibiotics. One of the chemical compounds that can serve this purpose is a group of secondary metabolites commonly found in plants, including Majapahit.

Majapahit is a native plant to South America [1] but it can also be found in Indonesia. It is a member of the citrus family and is distinguished by enormous, bitter-tasting green fruits, which contributes to its underutilization by Indonesian people. Majapahit receives little attention and is mostly regarded as an ornamental plant. Therefore, it is crucial to conduct a study on the benefits of the plant, with a specific focus on the leaves and constituent compounds, such as flavonoids.

Flavonoids are secondary metabolites abundantly produced in natural substances. These compounds are concentrated in the leaves, particularly in full exposure sunlight area [2] because they function as UV radiation filters [3]. Flavonoids can be found in the lower and upper epidermis cells as well as the stomata of leaves.

Within plants, flavonoids have various roles, including serving as secondary antioxidants in tissue defense against abiotic and biotic stressors [4], promoting growth, such as auxins [1], and providing color to plants, which can indicate their stress level [5].

The maceration method (soaking) was used to extract Majapahit plant leaves because it requires relatively simple

equipment and is a straightforward process. Compounds in the extract were identified using LCMS (Shimadzu LCMS-8040 LC/MS), which provided information about their structure [6]. Previous studies have been conducted on various parts of the Majapahit plant, including toxicity analysis and anticancer potential of the leaves using maceration with methanol solvent of BSLT [7], identification of potential anticancer compounds and in silico prediction on the stem bark [8], as well as detection and identification of flavonoid compounds in the ethanol extract of the bark using LCMS [9]. The novelty of this study is predicated on the identification and classification of flavonoid compounds, which are secondary metabolites in the ethanol extract of Majapahit plant leaves. Furthermore, it aimed to examine the fragmentation patterns of the flavonoid compounds with the highest composition.

### 2. Research Methods

#### 2.1 Tools and Materials

The main materials used were Majapahit plant leaves, 96% ethanol, methanol, and water, while the materials for the phytochemical test included an alkaline reagent.

The tools used included a maceration tube, a Buchi brand rotary evaporator, and an LCMS (Liquid Chromatography Mass Spectrometry) device, specifically the Shimadzu LCMS-8040 LC/MS model, which was conducted at the Muhammadiyah University of Malang.

#### 2.2 Extraction of Majapahit Plant Leaves

Fresh Majapahit plant leaves were washed thoroughly with running water and then dried. Drying was carried out without direct exposure to sunlight. Subsequently,

## Identification of Flavonoid Compounds in Ethanol Extract of Majapahit plant (*Crescentia cujete*) Leaves and their Potential as Anticancer

The leaves were then sieved through an 80-mesh sieve after being coarsely crushed in a blender. Around 100 grams. sieved material was then macerated with 600 ml of 96% ethanol. This process was carried out in a maceration tube and left for 3 days. The extraction process result was filtered using filter paper and yielded the extract of Majapahit plant leaves. The extract was concentrated using a rotary evaporator.

### 2.3 Qualitative Test for the Extract of Majapahit Plant Leaves

About 1 mL of the ethanol extract from Majapahit plant leaves was taken and placed into a test tube. Furthermore, 3-5 drops of the alkaline reagent were added and the result was observed. A positive result would produce a yellow color in the sample.

### 2.4 Identification of Compounds with LCMS

The concentrated extract obtained from the extraction process was dissolved in methanol at a concentration of 20 ppm with a ratio of 2 mg concentrated extract to 10 mL of methanol. Furthermore, 1  $\mu$ L of the sample was taken and injected into the LCMS-8040 instrument equipped with a binary pump. The eluents used in this process were water and 90% methanol. The LC (Liquid Chromatography) eluent connected to the Quadrupole Time-of-Flight (QTOF) mass spectrometer was set at a total flow rate of 0.5 mL/minute. The mass spectrometry (MS) used was the QTOF system with positive ionization mode.

## 3. Results and Discussion

### 3.1 Extraction of Majapahit Plant Leaves

The extraction process of Majapahit plant leaves was conducted using the soaking or maceration method. This extraction employed a semi-polar solvent of 96% ethanol to extract both non-polar and polar compounds. The 96% ethanol was used to inhibit the growth of yeast and mold during the maceration process due to its lower toxicity compared to other organic solvents [10].

In the maceration method, re-maceration was carried out to obtain a higher yield of the extract, ensuring that the compounds present in the *simplicia* were fully extracted. The obtained extract shown in Figure 1 was then concentrated using a rotary evaporator. This process aimed to reduce direct contact between the extract and continuous heat, preventing the degradation or alteration of the constituent compounds.



**Figure 1.** Concentrated Extract of Majapahit Plant Leaves

### 3.2 Qualitative Test for the Extract of Majapahit Plant Leaves

The phytochemical analysis was conducted to determine the presence or absence of secondary metabolites in the Majapahit plant, particularly in their leaves. An alkaline reagent was implemented in the procedure to establish the presence of flavonoid compounds.

## Identification of Flavonoid Compounds in Ethanol Extract of Majapahit plant (*Crescentia cujete*) Leaves and their Potential as Anticancer

Samples containing flavonoids were identified by the appearance of a yellow color as shown in Figure 2.



**Figure 2.** Phytochemical Test of Flavonoid Compounds

### 3.3 Identification of Compounds with LCMS

The extract of Majapahit plant leaves was discovered to contain 14 chemicals that were thought to be flavonoids based on the identification by LCMS. The compounds included quercetin, chlorogenic acid, kaempferol 3-O rhamnoside, acacetin 7-rutinoside, fortunelin, kaempferol 3-[6''-(3-hydroxy-3-methyl glutaryl) glucoside], didymin, diosmin, hesperidin, rutin, citrusoside C, citrusoside D, narirutin 4'-glucoside, and kaempferol 3-[6''-(3-hydroxy-3-methylglutaryl)glucoside]-7-glucoside (Table 1).

As shown in Table 1, the mass spectrum of chlorogenic acid, kaempferol 3-O rhamnoside, kaempferol 3-[6''-(3-hydroxy-3-methyl glutaryl) glucoside], hesperidin, and rutin have the highest content with values of 3.06%, 3.90%, 3.19%, 3.77%, and 3.43% respectively, compared to other flavonoid compounds.

Therefore, the fragmentation patterns of these compounds were determined and the results are presented in Table 2.

The mass spectrum of chlorogenic acid showed peaks at  $m/z$  306, 305, and 304. The molecular ion ( $M^+$ ) at  $m/z$  306 released an H radical, resulting in 2 consecutive fragments at  $m/z$  305 and 304. The molecular ion ( $M^+$ ), as well as the base peak, was observed at  $m/z$  304, corresponding to the molecular weight of the target compound, Chlorogenic acid.

Similarly, the mass spectrum of kaempferol 3-O rhamnoside exhibited peaks at  $m/z$  433, 432, and 431. The molecular ion ( $M^+$ ) at  $m/z$  433 released an H radical, culminating in the generation of 2 consecutive fragments at  $m/z$  432 and 431. The molecular ion ( $M^+$ ), as well as the base peak, was observed at  $m/z$  431, corresponding to the molecular weight of the target compound, kaempferol 3-O rhamnoside.

In the case of kaempferol 3-[6''-(3-hydroxy-3-methyl glutaryl) glucoside], the mass spectrum showed other peaks such as  $m/z$  594, 593, and 592. The molecular ion ( $M^+$ ) at  $m/z$  594 released an H radical, resulting in 2 consecutive fragments at  $m/z$  593 and 592. The molecular ion ( $M^+$ ), as well as the base peak, was observed at  $m/z$  592, representing the molecular weight of the target compound, kaempferol 3-[6''-(3-hydroxy-3-methyl glutaryl) glucoside].

The mass spectrum of hesperidin exhibited peaks at  $m/z$  612, 611, and 610. The molecular ion ( $M^+$ ) at  $m/z$  612 released an H radical, leading to the generation of 2 consecutive fragments at  $m/z$  611 and 610. The molecular ion ( $M^+$ ), as well as the base peak, was observed at  $m/z$  610, corresponding to the molecular weight of the target compound, hesperidin.

## Identification of Flavonoid Compounds in Ethanol Extract of Majapahit plant (*Crescentia cujete*) Leaves and their Potential as Anticancer

For rutin, the mass spectrum showed peaks at  $m/z$  612, 611, and 610. The molecular ion ( $M^+$ ) at  $m/z$  612 released an H radical, resulting in 2 consecutive fragments at  $m/z$  611 and 610. The molecular ion ( $M^+$ ), as well as the base peak, was observed at  $m/z$  610, corresponding to the molecular weight of the target compound, rutin.

The presence of flavonoid compounds in Majapahit plant leaves as shown in Table 1, confirmed its potential as an anti-cancer agent. Kaempferol 3-O rhamnoside was detected at a retention time of 21.429 minutes in the LCMS instrument. A previous study showed that kaempferol 3-O rhamnoside extracted from *Schima wallichii* Kort leaves can inhibit MCF-7 breast cancer cells [11].

Acacetin 7-rutinoside has been found to induce apoptosis in cancer cells [12], while quercetin has chemopreventive effects on prostate cancer [13]. Quercetin can also act as an anti-metastatic agent in gastrointestinal cancer [14]. In a previous study, hesperidin induced apoptosis in MSTO-211H pleural mesothelioma cells [15]. Another study also showed that hesperidin can induce colon, breast, lung, and liver cancer [16].

In lung cancer cells, rutin has been shown to reduce cell migration and adhesion, leading to inhibited proliferation and decreased ROS production [17].

Acacetin 7-rutinoside, also known as linarin, has the ability to induce apoptosis in human prostate cancer cells, indicating its potential as an anti-cancer agent [12]. Meanwhile, narirutin 4'-glucoside can inhibit the proliferation of HL-60 leukemia cells [1].

Kaempferol 3-[6''-(3-hydroxy-3-methylglutaryl) glucoside]-7-glucoside and kaempferol 3-[6'-(3-hydroxy-3-methylglutaryl)glucoside] are known to be anti-cancer agents and are derivatives of kaempferol [18]. Kaempferol reportedly inhibited the growth of breast cancer cells [19]. Moreover, diosmin demonstrated great potential against prostate cancer cells and exhibited genotoxic effects, suppressing the proliferation and viability of HepG2 hepatocarcinoma cell cultures [20]. Didymin has potential against neuroblastoma cells as it can kill both p-53 wild-type and drug-resistant p-53 mutant cells [21].

### 4. Conclusion

In conclusion, LCMS analysis of Majapahit plant leaves revealed the presence of 14 different flavonoid chemicals. 12 of these were discovered to have remarkable anticancer potential. Kaempferol 3-O rhamnoside had the highest concentration compared to other flavonoid compounds.

### References

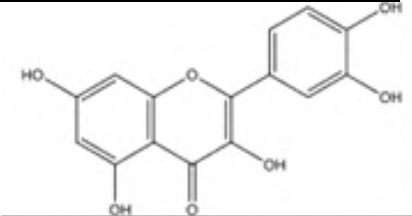
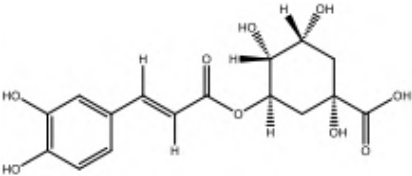
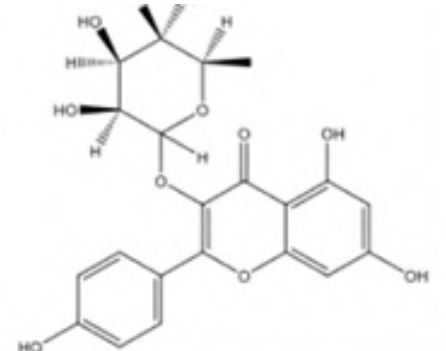
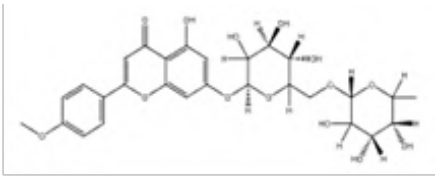
- [1] Agati, G., Azzarello, E., Pollastri, S., & Tattini, M. (2012). Flavonoids as antioxidants in plants: Location and functional significance. *Plant Science*, 196(November), 67–76. doi: 10.1016/j.plantsci.2012.07.014
- [2] Tattini, M., Gravano, E., Pinelli, P., Mulinacci, N., Romani, A. (2000). Flavonoids Accumulate in Leaves and Glandular Trichomes of *Phillyrea latifolia* Exposed to Excess Solar Radiation. *Phytol*, 148, 69–77.
- [3] Wollenweber E, D. V. (1981). *Occurrence and distribution of free flavonoid aglycones in plants*.
- [4] Kumar, S., & Pandey, A. K. (2013). Chemistry and biological activities of flavonoids: An overview. *The Scientific World Journal*, 2013. doi: 10.1155/2013/162750

**Identification of Flavonoid Compounds in Ethanol Extract of Majapahit plant (*Crescentia cujete*) Leaves and their Potential as Anticancer**

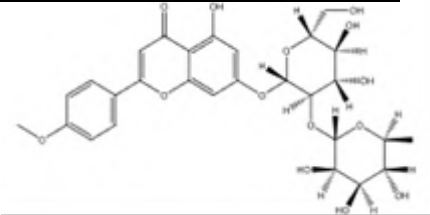
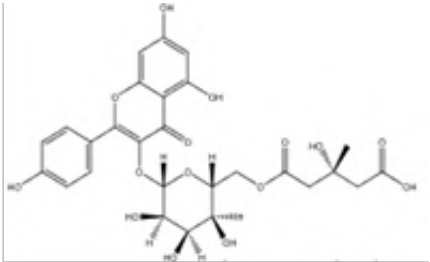
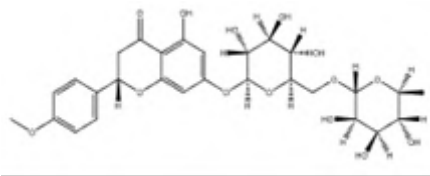
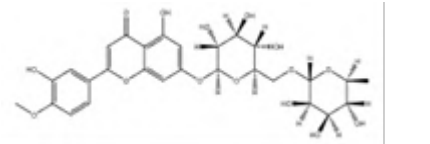
- 
- [5] Peixoto, H., Roxo, M., Krstin, S., Rohrig, T., Richling, E., Wink, M. (2016). An anthocyanin-rich extract of acai (*Euterpe precatoria* Mart.) increases stress resistance and retards aging-related markers in *Caenorhabditis elegans*. *J. Agric. Food Chem*, 64, 1283–1290.
- [6] Saibaba, S. V., Kumar, M. S., & Shanmuga, P. (2016). Mini Review on LC/MS Techniques. *Journal of Pharmacy and Pharmaceutical Science*, 5(4), 2381–2395.
- [7] Fatimah, F., Martha, R. D., & Danar, D. (2022). Analisis toksisitas dan potensi antikanker ekstrak metanol daun Majapahit (*Crescentia cujete*) dengan metode Brine Shrimp Lethality Test. *Jurnal Penelitian Sainstek*.
- [8] Fatimah, F., Martha, R. D., Danar, D., Zummah, A., Anggraini, I. M. D., & Kusumawati, A. (2023). Identification of Anticancer Potential Compounds and its In Silico Prediction of The Cytotoxic Activity in Majapahit (*Crescentia cujete* L.) Stem Bark. In *AIP Conference Proceedings*. doi: 10.1063/5.0112833
- [9] Fatimah, F., Martha, R. D., & Kusumawati, A. (2020). Deteksi dan Identifikasi Senyawa Flavonoid Ekstrak Etanol Kulit Batang Tanaman Majapahit (*Crescentia cujete*) dengan LCMS. *CHEESA: Chemical Engineering Research Articles*, 3(2), 88. doi: 10.25273/cheesa.v3i2.7688.88-98
- [10] Saifudin, F & Rahayu, V. (2011). *Standarisasi Bahan Obat Bahan Alam*.
- [11] Lewinska, A., Siwak, J., Rzeszutek, I. & Wnuk, M. (2015). Diosmin Induces Genotoxicity and Apoptosis in DU145 Prostate Cancer Cell Line. *Toxicology in Vitro*, 29(3), 417–425.
- [12] Singh, R. P., Agrawal, P., Yim, D., Agarwal, C. & Agarwal, R. (2005). Acacetin Inhibits Cell Growth and Cell Progression, and Induces Apoptosis in Human Prostate Cancer Cells: Structure-Activity Relationship with Linarin and Linarin Acetate. *Carcinogenesis*, 26(4), 845–854.
- [13] Kim, W. K., Bang, M. H., Kim, E. S., Kang, N. E., Jung, K. C., Cho, H. J., & Park, J. H. Y. (2005). Quercetin decreases the expression of ErbB2 and ErbB3 proteins in HT-29 human colon cancer cells. *Journal of Nutritional Biochemistry*, 16(3), 155–162. doi: 10.1016/j.jnutbio.2004.10.010
- [14] Araújo, J. R., Gonçalves, P., & Martel, F. (2011). Chemopreventive effect of dietary polyphenols in colorectal cancer cell lines. *Nutrition Research*, 31(2), 77–87. doi: 10.1016/j.nutres.2011.01.006
- [15] Lee, K. A., Lee, S. H., Lee, Y. J., Baeg, S. M., & Shim, J. H. (2012). Hesperidin induces apoptosis by inhibiting Sp1 and its regulatory protein in MSTO-211H cells. *Biomolecules and Therapeutics*, 20(3), 273–279. doi: 10.4062/biomolther.2012.20.3.273
- [16] Devi, K. P., Rajavel, T., Nabavi, S. F., Setzer, W. N., Ahmadi, A., Mansouri, K., & Nabavi, S. M. (2015). Hesperidin: A promising anticancer agent from nature. *Industrial Crops and Products*, 76, 582–589. doi: 10.1016/j.indcrop.2015.07.051
- [17] Sghaier, M. B., Pagano, A., Mousslim, M., Ammari, Y., Kovacic, H. & Luis, J. (2016). Rutin Inhibits Proliferation, Attenuates Superoxide Production, and Decreases Adhesion and Migration of Human Cancerous Cells. *Biomedicine & Pharmacotherapy*, 84, 1972–1978.
- [18] Imran, M., Salehi, B., Sharifi-Rad, J., Gondal, T. A., Saeed, F., Imran, A., ... Estevinho, L. M. (2019). Kaempferol: A key emphasis to its anticancer potential. *Molecules*, 24(12), 1–16. doi: 10.3390/molecules24122277
- [19] ben Sghaier, M., Pagano, A., Mousslim, M., Ammari, Y., Kovacic, H., & Luis, J. (2016). Rutin inhibits proliferation, attenuates superoxide production and decreases adhesion and migration of human cancerous cells. *Biomedicine and Pharmacotherapy*, 84, 1972–1978. doi: 10.1016/j.biopha.2016.11.001
- [20] Perumal, S., & Langeswaran, K. (2019). Diosmin anti-tumor efficacy against hepatocellular carcinoma ., 1–10.
- [21] Singhal, S. S., Singhal, S., Singhal, P., Singhal, J., Horne, D., & Awasthi, S. (2017). Didymnin: An orally active citrus flavonoid for targeting neuroblastoma. *Oncotarget*, 8(17), 29428–29441. doi: 10.18632/oncotarget.15204
-

### Identification of Flavonoid Compounds in Ethanol Extract of Majapahit plant (*Crescentia cujete*) Leaves and their Potential as Anticancer

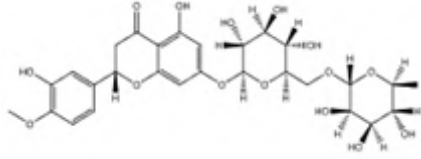
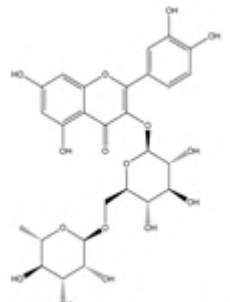
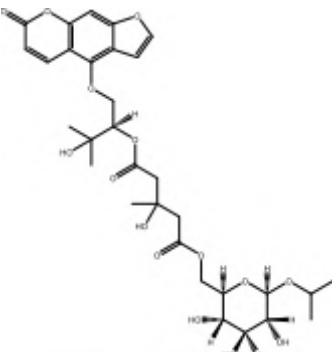
**Table 1.** LCMS Results of Flavonoid Compounds from the Extract of Majapahit Plant Leaves

No	Compounds	Retention Time (min)	Composition (%)	Analysis	Structure
1	<i>Quercetin</i>	11.427	1.96925	Chemical formula: C <sub>15</sub> H <sub>10</sub> O <sub>7</sub> Molecular weight: 302.0427 m/z : 302.0427 (100%)	
2	<i>Chlorogenic acid</i>	12.421	3.06210	Chemical formula: C <sub>16</sub> H <sub>18</sub> O <sub>9</sub> Molecular weight: 354.0951 m/z : 354.0951 (100%)	
3	<i>Kaempferol 3-O rhamnoside</i>	21.429	3.90389	Chemical formula: C <sub>21</sub> H <sub>20</sub> O <sub>10</sub> Molecular weight: 431.0984 m/z : 431.0984 (100%)	
4	<i>Acacetin 7-rutinosid</i>	33.702	2.69590	Chemical formula: C <sub>28</sub> H <sub>32</sub> O <sub>14</sub> Molecular weight: 592.5500 m/z : 592.1792 (100%)	

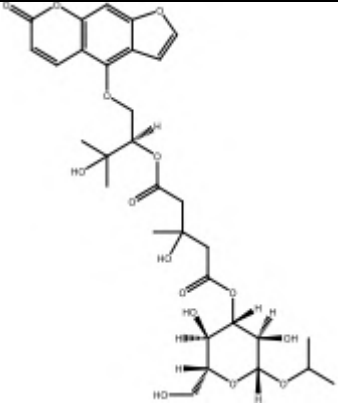
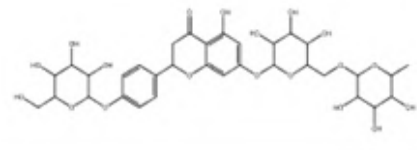
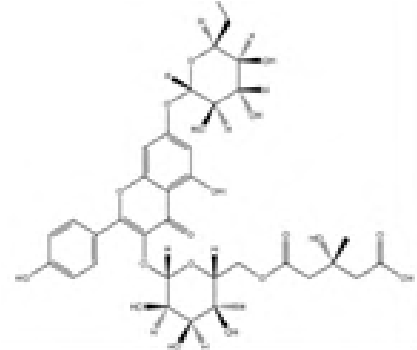
**Identification of Flavonoid Compounds in Ethanol Extract of Majapahit plant (*Crescentia cujete*) Leaves and their Potential as Anticancer**

No	Compounds	Retention Time (min)	Composition (%)	Analysis	Structure
5	<i>Fortunelin</i>	33.722	1.69004	Chemical formula: C <sub>28</sub> H <sub>32</sub> O <sub>14</sub> Molecular weight: 592.1792 m/z : 592.1792 (100%)	
6	<i>Kaempferol 3-[6''-(3-hydroxy-3-methyl glutaryl) glucoside]</i>	33.729	3.19042	Chemical formula: C <sub>27</sub> H <sub>28</sub> O <sub>15</sub> Molecular weight: 592.5060 m/z : 592.1428(100%)	
7	<i>Didymin</i>	34.004	1.70507	Chemical formula: C <sub>28</sub> H <sub>34</sub> O <sub>14</sub> Molecular weight: 594.5060 m/z : 594.1428(100%)	
8	<i>Diosmin</i>	35.504	1.84236	Chemical formula: C <sub>28</sub> H <sub>32</sub> O <sub>15</sub> Molecular weight: 608.5490 m/z : 608.5490 (100%)	

**Identification of Flavonoid Compounds in Ethanol Extract of Majapahit plant (*Crescentia cujete*) Leaves and their Potential as Anticancer**

No	Compounds	Retention Time (min)	Composition (%)	Analysis	Structure
9	<i>Hesperidin</i>	35.507	3.77466	Chemical formula: C <sub>28</sub> H <sub>34</sub> O <sub>15</sub> Molecular weight: 610.5650 m/z : 610.1741 (100%)	
10	<i>Rutin</i>	35.517	3.43252	Chemical formula: C <sub>27</sub> H <sub>30</sub> O <sub>16</sub> Molecular weight: 610.1534 m/z : 610.1534 (100%)	
11	<i>Citrusoside C</i>	39.064	1.25323	Chemical formula: C <sub>31</sub> H <sub>40</sub> O <sub>15</sub> Molecular weight: 652.2367 m/z : 654.2367 (100%)	

**Identification of Flavonoid Compounds in Ethanol Extract of Majapahit plant (*Crescentia cujete*) Leaves and their Potential as Anticancer**

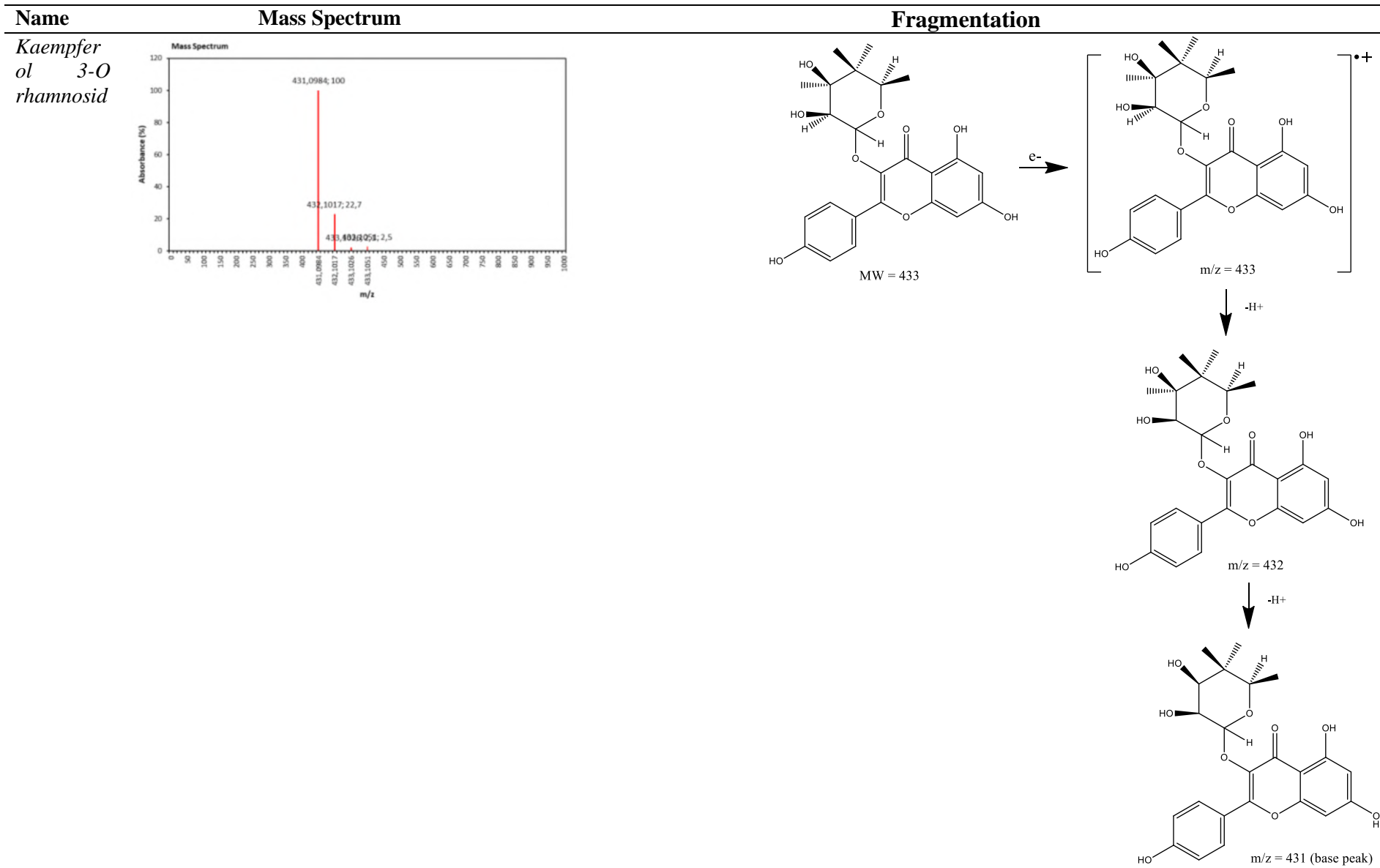
No	Compounds	Retention Time (min)	Composition (%)	Analysis	Structure
12	<i>Citrusosid D</i>	39.067	1.48975	Chemical formula: C <sub>31</sub> H <sub>40</sub> O <sub>15</sub> Molecular weight: 652.6460 m/z : 654.2434 (100%)	
13	<i>Narirutin 4'-glucosid</i>	46.301	2.21045	Chemical formula: C <sub>33</sub> H <sub>42</sub> O <sub>19</sub> Molecular weight: 742.2320 m/z : 742.2320 (100%)	
14	<i>Kaempferol 3-[6''-(3-hydroxy-3-methylglutaryl)glucosid] -7-glucoside</i>	46.564	2.60072	Chemical formula: C <sub>33</sub> H <sub>38</sub> O <sub>20</sub> Molecular weight: 754.6470 m/z : 754.1956 (100%)	

**Identification of Flavonoid Compounds in Ethanol Extract of Majapahit plant (*Crescentia cujete*) Leaves and their Potential as Anticancer**

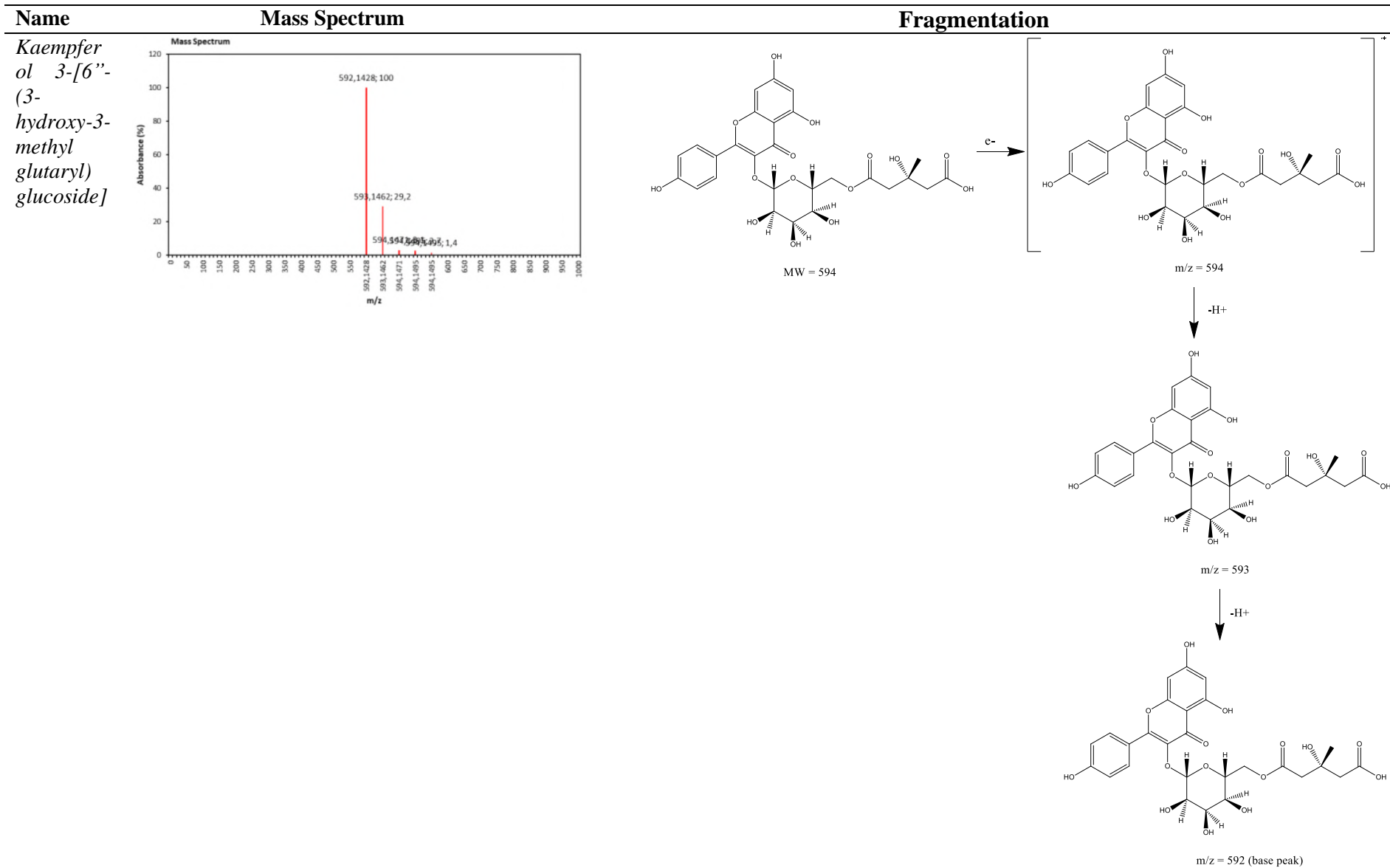
**Table 2.** Mass Spectrum and Fragmentation of Compounds with the Highest Composition

Name	Mass Spectrum	Fragmentation
<i>Chlorogenic acid</i>		<p>MW = 356</p> <p><math>m/z = 356</math></p> <p><math>m/z = 355</math></p> <p><math>m/z = 354</math> (base peak)</p>

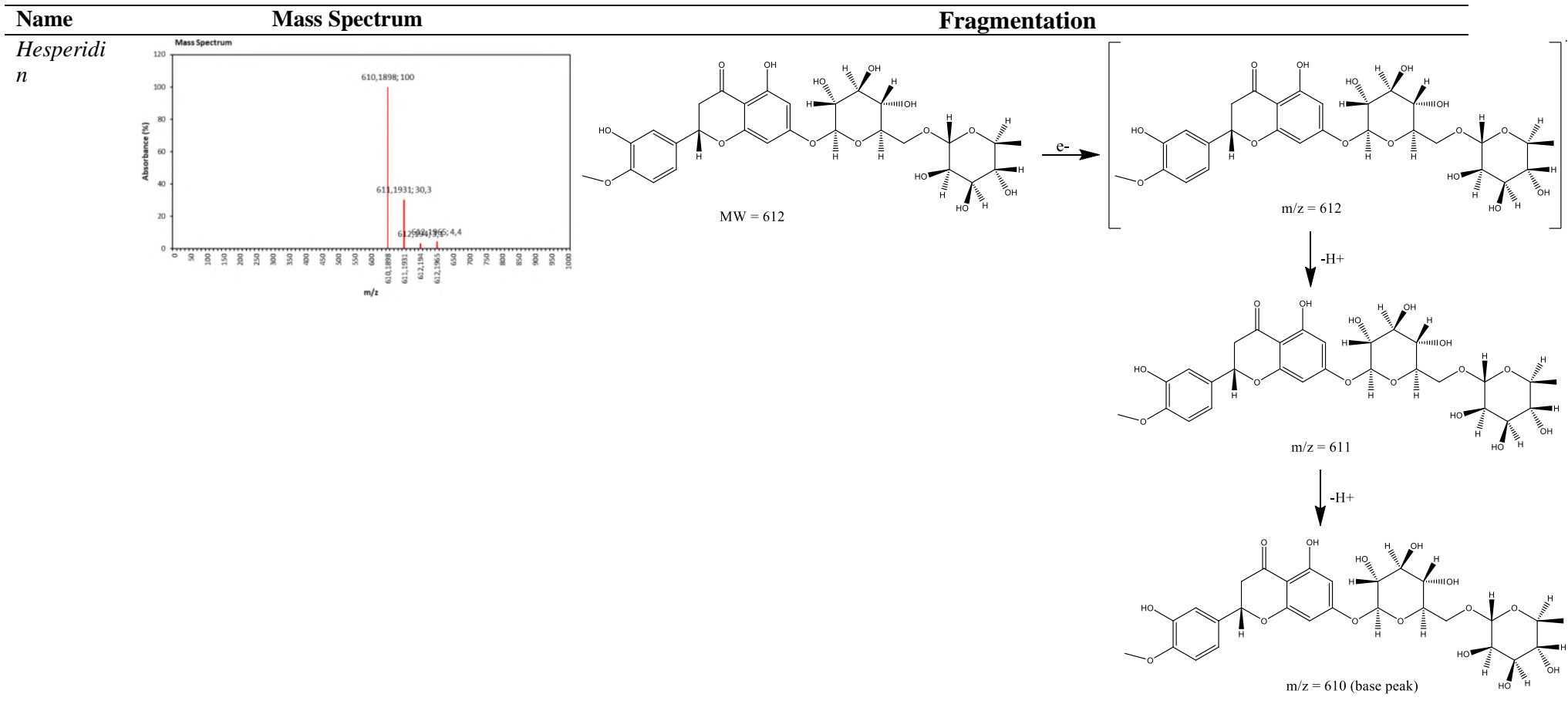
**Identification of Flavonoid Compounds in Ethanol Extract of Majapahit plant (*Crescentia cujete*) Leaves and their Potential as Anticancer**



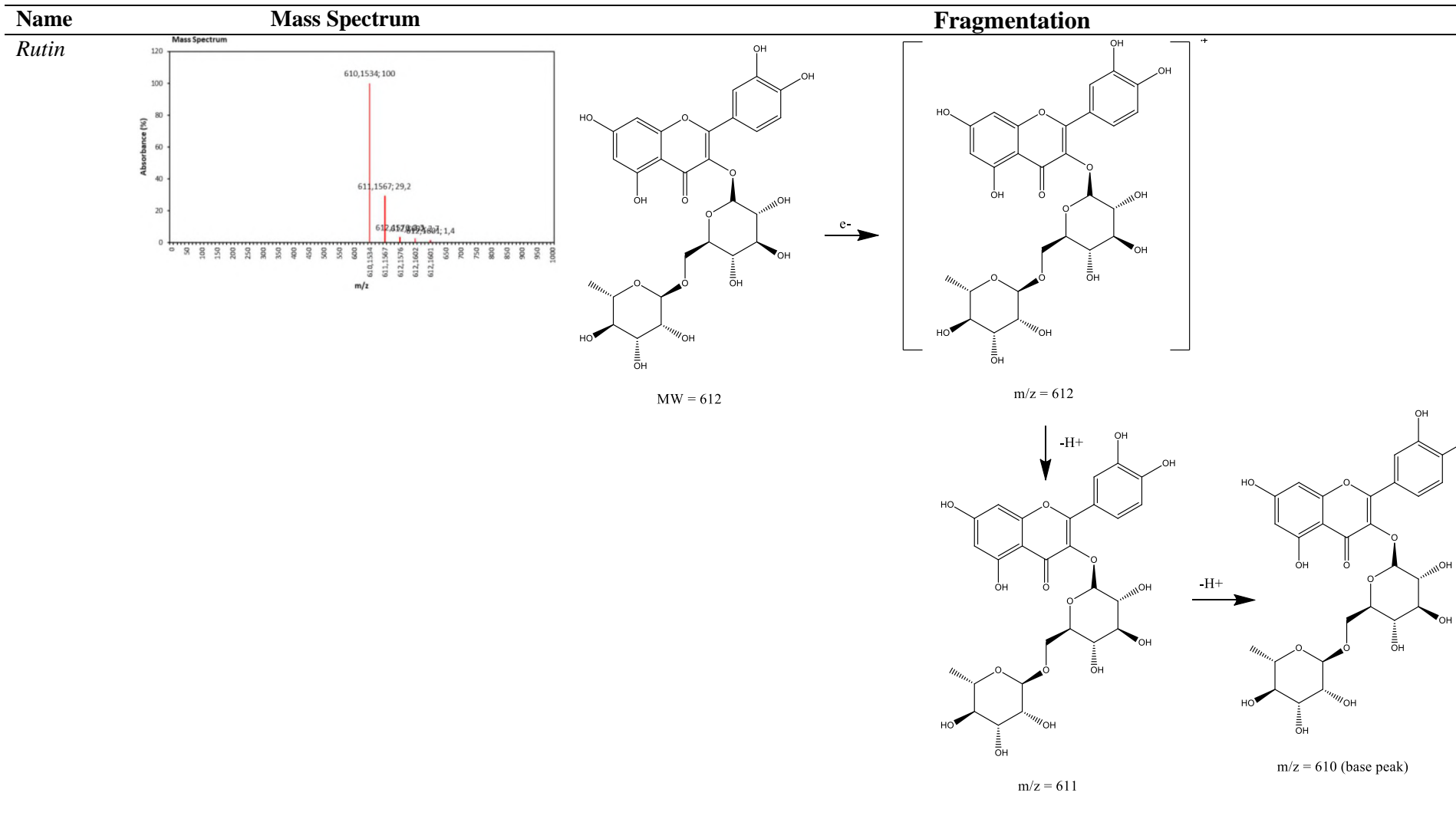
**Identification of Flavonoid Compounds in Ethanol Extract of Majapahit plant (*Crescentia cujete*) Leaves and their Potential as Anticancer**



Identification of Flavonoid Compounds in Ethanol Extract of Majapahit plant (*Crescentia cujete*) Leaves and their Potential as Anticancer



Identification of Flavonoid Compounds in Ethanol Extract of Majapahit plant (*Crescentia cujete*) Leaves and their Potential as Anticancer



# Optimization Production and Characterization of Bacterial Cellulose from Cornhusk

*Optimasi Produksi dan Karakterisasi Selulosa Bakteri dari Klobot Jagung*

**Fikka Kartika Widyastuti<sup>1\*)</sup>, Ayu Chandra Kartika Fitri<sup>1)</sup>**

<sup>1)</sup>*Universitas Tribhuwana Tunggaladewi, Faculty of Engineering, Chemical Engineering Study Program, Indonesia*

## Article History

Received: 13<sup>th</sup> January 2022; Revised: 17<sup>th</sup> July 2023; Accepted: 17<sup>th</sup> July 2023;

Available online: 13<sup>th</sup> August 2023; Published Regularly: June 2023

doi: [10.25273/cheesa.v6i1.11781.49-55](https://doi.org/10.25273/cheesa.v6i1.11781.49-55)

\*Corresponding Author.

Email:

[fikka.kartika@unitri.ac.id](mailto:fikka.kartika@unitri.ac.id)

## Abstract

Cornhusks are agricultural wastes with low economic value that will cause environmental pollution if not appropriately handled. Cornhusk waste can be processed as raw material for bacterial cellulose (nata) since it contains 44% cellulose. This study aims to optimize bacterial cellulose production from cornhusks and determine the effect of cornhusk mass and fermentation duration on the characteristics of the nata produced. The primary process for producing bacterial cellulose from cornhusks was fermentation by *Acetobacter xylinum*. The nata characterization carried out in this study includes thickness, yield, crude fiber, and moisture content, as well as statistical analysis to determine whether there was significant effect of variations in cornhusk mass and fermentation duration on bacterial cellulose production. Based on the results of optimizing the production of nata from cornhusks, the optimal mass of cornhusks was of 25 grams with fermentation duration of 17 days. Based on the characterization and data analysis results, variation on the cornhusks mass and duration of the fermentation had a significant effect on fiber content, yield, and tensile strength of bacterial cellulose from cornhusks. On the other hand, the variations on cornhusks mass and the duration of fermentation did not significantly affect the moisture content and thickness of bacterial cellulose from cornhusks.

**Keywords:** cornhusk; fermentation; nata; optimization

## Abstrak

Klobot jagung merupakan limbah pertanian yang bernilai ekonomis rendah dan akan menyebabkan pencemaran lingkungan jika tidak ditangani dengan tepat. Limbah kulit jagung dapat diolah sebagai bahan baku selulosa bakteri (nata) karena mengandung 44% selulosa. Penelitian ini bertujuan untuk mengoptimalkan produksi selulosa bakteri dari klobot jagung dan untuk mengetahui pengaruh massa klobot jagung dan lama fermentasi terhadap karakteristik nata yang dihasilkan. Proses utama dalam memproduksi selulosa bakteri dari klobot jagung adalah fermentasi dengan *Acetobacter xylinum*. Karakterisasi nata yang dilakukan pada penelitian ini meliputi ketebalan, rendemen, serat kasar, dan kadar air, serta analisis statistik untuk mengetahui ada tidaknya pengaruh variasi massa klobot jagung dan lama fermentasi terhadap produksi selulosa bakteri atau nata. Berdasarkan hasil optimasi produksi nata dari klobot jagung diperoleh massa klobot jagung yang optimal adalah 25 gram dengan lama fermentasi 17 hari. Berdasarkan hasil karakterisasi dan analisis data, variasi massa klobot jagung dan lama fermentasi berpengaruh nyata terhadap kadar serat dan rendemen selulosa bakteri dari klobot jagung. Sedangkan variasi massa klobot jagung dan lama fermentasi tidak berpengaruh nyata terhadap kadar air dan ketebalan selulosa bakteri yang dihasilkan.

**Katakunci:** kulit jagung; fermentasi; nata; pengoptimalan

## 1. Introduction

The most abundant natural polymer in the world is cellulose. Cellulose obtained from the synthetic process of acetic acid bacteria is commonly known as bacterial cellulose [1,2]. Bacterial cellulose is a nanomaterial produced by various strains of *Acetobacter* species including *Pseudomonas*, *Achromobacter*, *Alcaligene*, *Aerobacter*, and *Azotobacter* [3]. Bacterial cellulose or natural hydrogels have better properties than hydrogels produced from synthetic polymers. For instance, bacterial cellulose shows high water content (98-99%), good liquid absorption, wet strength, high chemical purity and can be safely sterilized without changing its structure and properties in the slightest [4].

Bacterial Cellulose (BC) has always attracted the interest of scientists because it has a high level of purity, biodegradability, biocompatibility, and ease of polymerization [5,6]. BC can be applied to engineering skin tissue and bone, to barrier technology and electricity, to electrochemistry, and to sensing applications [7–11]. Although BC has excellent potential, its high production costs limit its industrial-scale applications.

Kurniawan et al. [12] had created a new BC from chayote fruit and bamboo shoots. The BC has excellent mechanical properties such as tensile strength, elongation and water absorption capacity. Despite this fact, there have been efforts to evaluate the possibility of utilizing other agricultural wastes for carbon sources in BC production, including corn products, coffee cherry husk (CCH), date fruits, and banana peel. The findings were parallel with research evidence showing that corn steep liquor was rich in nutrients such as carbon and nitrogen, which supplied organic content during BC production [5,13].

Sulistiyanana [14] also found that light yellow corn extract can be used as an ingredient for making nata de corn with the

optimum condition for 14 days of fermentation. The characterization of nata de corn from light yellow corn substrate includes the yield of 46.82%, the water content of 93.13%, and fiber content of 1.31%. This value had met the quality standards of nata according to SNI No. 01-4317-1996. Among the substrates that have been widely used in previous studies, the use of agricultural waste biomass can be an alternative for the use of food ingredients that will disrupt food security.

That is why, active research investigating the cost-effectiveness of BC synthesis from different waste products has been conducted and elaborated. Many agricultural wastes are rich in carbon and nitrogen content; therefore, utilizing them as substrates can produce high concentrations of microbial cellulose by optimizing the culture conditions [15].

One of the agricultural waste biomasses that can be used as a substrate is cornhusks. Cornhusk is an abundant agricultural waste and is widely used as a raw material for handicrafts, bio-ethanol production, pulp alternatives, etc. The cornhusk is the part of the plant that protects the corn kernels, is bright green when young, and dries on the trees as it ages. Communities commonly use cornhusk waste as animal feed, but the usage is still limited. Because of their limited use, cornhusks still have little economic value.

Therefore in the present work, it is necessary to find out if cornhusks could be used as raw material to manufacture bacterial cellulose and to determine the optimal conditions required for the production of bacterial cellulose in terms of the results of the characterization of its physical and chemical properties.

## Optimization Production and Characterization of Bacterial Cellulose from Cornhusk

### 2. Research Methods

#### 2.1 Materials

Materials used in this research were cornhusk (obtained from the traditional market Landungsari-Malang), *Acetobacter xylinum* starter in liquid medium of coconut water (from Laboratory of Process Engineering, Agricultural Industry Technology Study Program, UNITRI), pro analysis urea, pro analysis glucose, glacial acetic acid (Merck 100%), and aquadest. Characterization tests were done at Laboratory of Chemistry - UNITRI and at Laboratory of Animal Husbandry - UMM.

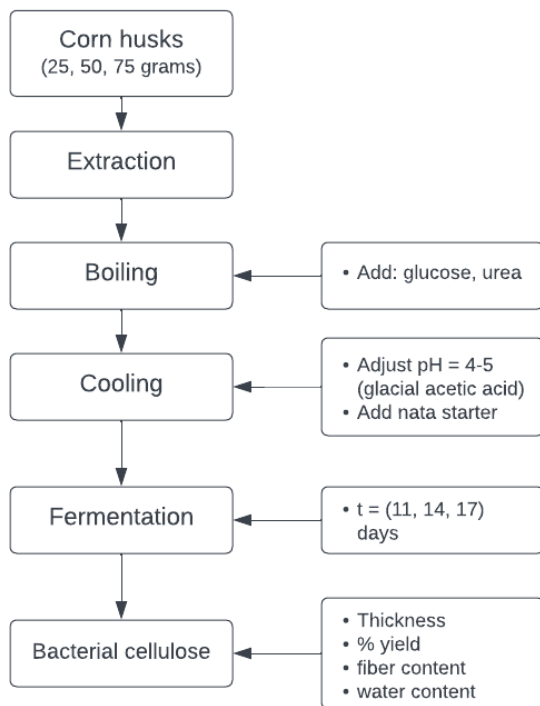


Figure 1. Research Method Flowchart

#### 2.2 BC Production from Cornhusk Extract

Raw materials (cornhusks) were weighed as much as 25, 50, and 75 grams and then was blended with 1 liter of distilled water. Hot maceration was done after the cornhusk was boiled and filtered to get the cornhusk extract. Then, 100 grams of glucose and 4 grams urea were added and stirred while brought to a-boil. The mixture was then adjusted to pH 4 by adding glacial acetic acid. When pH 4 has been reached, the mixtures of 250-300 mL (each)

were poured into a sterile plastic box containers and then for every 100 mL of the mixture was added 20 ml of nata starter. All of them were stored for fermentation at room temperature with variation of fermentation duration of 11, 14, and 17 days. The same procedures were applied for each cornhusk mass variation. BC/nata were harvested and cleaned using running water and sterilized by soaking it in hot water.

#### 2.3 Characterization of BC from Cornhusk

The next step was to characterize the physical properties (thickness and yield) and chemical properties (fiber and water content). The thickness of the cellulose produced by *A. xylinum* was measured using a vernier caliper at three different points. The yield of bacterial cellulose from cornhusks was determined based on the ratio between the weight of the nata and the weight of the medium. The determination of crude fiber content was based on SNI ISO 5498: 2015, while the determination of water content was done by using the thermogravimetric method according to SNI-01-2354.2-2006.

### 3. Result and Discussion

#### 3.1 Optimization of Cornhusk BC Production

Figure 2 showed that the fiber content of nata was affected by the duration of fermentation and the mass of the cornhusk substrate. Among the three mass variations of cornhusks, the smallest mass of 25 grams actually had the highest nata fiber content compared to the others. Meanwhile, the duration of the 17-day fermentation had resulted in high

## Optimization Production and Characterization of Bacterial Cellulose from Cornhusk

fiber content for all three variations of cornhusk mass.

When compared to each fermentation duration, all of them had the same curve patterns; especially on the fiber content was decrease for the cornhusk mass of 25 grams to 75 grams. Therefore, the optimal condition in cornhusk bacterial cellulose production was one with the highest 25 grams fiber content and 17 days fermentation duration.

In the production of BC, fermentation duration had a determining effect on the formation of nata or BC. Too long fermentation would cause *A. xylinum* bacteria went to the death phase due to a lack of nutrients and depletion, causing cells to lose a lot of energy reserves. According to Putriana & Aminah [16], fermentation duration had caused bacteria growth slowing down due to reduced sugar levels and the emergence of acid as metabolite of the fermentation process. Types of incubation time in the production of nata were 6-12 days, 14 days, 16 days, and 21 days.

### 3.2 Characterization and Results of Statistical Analysis

The data on the characterization of BC from cornhusks with the variable in the cornhusks mass and the fermentation duration, including fiber content, moisture content, yield, and thickness are summarized in Table 1.

The factorial ANOVA test was carried out to test whether there were differences in the

average for the mass of corn-husk, the duration of fermentation, and interactions between corn-husk mass and fermentation duration on the variables measured (fiber content, moisture content, yield, and thickness).

If the ANOVA factorial analysis results showed a significant difference, then a further test (if the treatment being compared was more than 2), namely the Tukey test, then a different notation would be given if the two treatments were in different subsets, which means that the two were significantly different. Meanwhile, the same notation would be given if they were in the same subset, which was not significantly different.

The highest average thickness score in treatment A2B2 (mass of cornhusks 50 gr, fermentation duration 14 days) was 0.8750, and the lowest average thickness score in treatment A3B1 (mass of cornhusks 75 gr, fermentation duration 11 days) was 0.3400. To see whether the difference in the mean between the treatment groups was significant or not, a factorial ANOVA analysis was carried out.

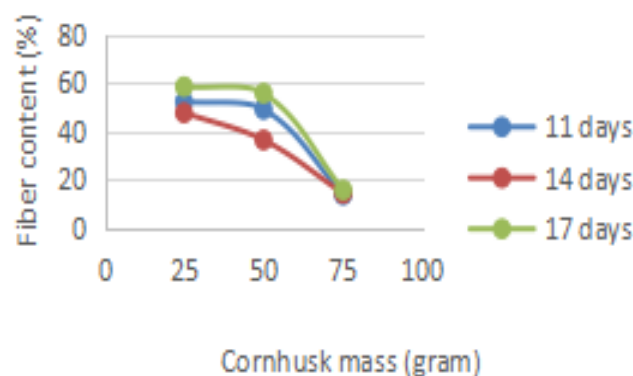


**Figure 2.** The correlation between cornhusk mass and fermentation duration to the fiber content

## Optimization Production and Characterization of Bacterial Cellulose from Cornhusk

Table 1. BC Characterization Results Data

No	Cornhusk mass (gram)	Fermentation Duration (days)	Fiber Content (%)	Moisture content (%)	Yield (%)	Average Thickness (cm)
1	25	11	52.39	98.62	30.05	0.50
		14	49.18	98.64	37.27	0.65
		17	13.69	94.29	38.36	0.63
2	50	11	47.75	98.44	40.59	0.67
		14	36.45	97.97	53.08	0.87
		17	14.26	93.97	54.25	0.85
3	75	11	58.60	98.89	19.83	0.34
		14	55.88	98.90	23.12	0.44
		17	15.69	95.93	23.69	0.41

Table 2. The Anova Factorial Analysis Results of Average Thickness Parameter

Treatment	Average	SD	Notation	Average A (Mass)	Average B (Fermentation Duration)
A1B1	0.5000	0.35355	a	A1 (25 gram) =	B1 (11 days of fermentation) = 0.5033
A1B2	0.6500	0.28284	a	0.5938 <b>ab</b>	<b>a</b>
A1B3	0.6313	0.14142	a		
A2B1	0.6700	0.14142	a		
A2B2	0.8750	0.07071	a	0.8004 <b>b</b>	<b>a</b>
A2B3	0.8563	0.05657	a		
A3B1	0.3400	0.28284	a		
A3B2	0.4375	0.14142	a	0.3967 <b>a</b>	<b>a</b>
A3B3	0.4125	0.11314	a		
<b>F (p-value)</b>					
Nata	6.014 (0.022)*				
Fermentation duration	0.986 (0.410)				
Nata * Fermentation duration	0.050 (0.994)				

From the results of the ANOVA factorial test in Table 2, it demonstrated that:

- There was a significant average difference based on treatment factor A (mass of cornhusks) on the variable mean thickness number measured, it can be seen from the p-value which is smaller than 0.050 ( $0.022 < 0.050$ ). The highest average thickness of the 50 grams cornhusk mass was significantly different from the 75 grams cornhusk mass, but the 50 grams cornhusk mass was not significantly different from the 25 grams cornhusk mass.
- There was an insignificant average difference based on treatment factor B (fermentation duration) to the measured

average thickness number variable, it can be seen from the p-value which is greater than 0.050 ( $0.410 > 0.050$ ). The average thickness of the average number of fermentation duration was not significantly different from the average number is not too much different.

- There was an insignificant average difference based on the interaction of treatment factors A (mass of cornhusk) and B (fermentation duration) on the variable number of average thicknesses measured, it can be seen from the p-value which is greater than 0.050 ( $0.994 > 0.050$ ).

## Optimization Production and Characterization of Bacterial Cellulose from Cornhusk

---

The average thickness score on the interaction of cornhusk mass treatment and fermentation duration was not significantly different, as seen from the average number between treatments which was not much different.

The conclusions from the results of the factorial ANOVA test for all characterization parameters were:

- a) The treatment of cornhusk mass and fermentation duration and their interactions had a significant effect on fiber content, with the significance value of the ANOVA test results being significant ( $p < 0.05$ )
- b) Fermentation duration had a significant effect on water content with the significance value of the ANOVA test results being significant ( $p < 0.05$ ). While the treatment of cornhusk mass and its interaction with fermentation duration did not significantly affect the water content with the significance value of the ANOVA test results was not significant ( $p > 0.05$ ).
- c) Treatment of cornhusk mass and fermentation duration and their interactions had a significant effect on the yield, with the significance value of the ANOVA test results ( $p < 0.05$ ).
- d) The treatment of cornhusk mass had a significant effect on water content with the significance value of the ANOVA test results ( $p < 0.05$ ). While the fermentation duration treatment and its interaction with the mass of cornhusk did not significantly affect the water content, the significance

value of the ANOVA test results was not significant ( $p > 0.05$ ).

### 4. Conclusion

As found in this research, the optimal corn-husk mass was 25 grams with fermentation duration of 17 days. Both corn-husk mass and fermentation duration were significantly affected fiber content and yield, but did not show significant effect to the moisture content and thickness of bacterial cellulose. The results of this study were expected to provides an overview of the optimal conditions in the production of bacterial cellulose from cornhusks and this research can serve as a ground point for the development of the manufacture of bacterial cellulose, especially in terms of the application of bacterial cellulose from cornhusks as a natural source of cellulose.

### Acknowledgments

Thank you to the UNITRI Research and Community Service Institute (LPPM) for giving authors the opportunity to get the 2021 UNITRI Research Grant Program - Batch II with number of MoU 05/TB-LPPM/TU-220/VI/2021.

### References

- [1] Li, S., Warzywoda, J., Wang, S., Ren, G., & Fan, Z. (2017). Bacterial cellulose derived carbon nanofiber aerogel with lithium polysulfide catholyte for lithium-sulfur batteries. *Carbon*, 124, 212–218.
- [2] Jozala, A. F., de Lencastre-Novaes, L. C., Lopes, A. M., de Carvalho Santos-Ebinuma, V., Mazzola, P. G., Pessoa-Jr, A., ... Chaud, M. V. (2016). Bacterial nanocellulose production and application: a 10-year overview. *Applied microbiology and biotechnology*, 100, 2063–2072.
- [3] Barud, H. S., Regiani, T., Marques, R. F. C., Lustri, W. R., Messadeq, Y., & Ribeiro, S. J. L. (2011). Antimicrobial Bacterial Cellulose-Silver Nanoparticles Composite Membranes. *Journal of Nanomaterials*, 8(6), 1–8. doi: <https://doi.org/10.1155/2011/721631>

**Optimization Production and Characterization of Bacterial Cellulose from Cornhusk**

- 
- [4] Maneerung, T., Tokura, S., & Rujiravanit, R. (2008). Impregnation of silver nanoparticles into bacterial cellulose for antimicrobial wound dressing. *Carbohydrate Polymers*, 72(1), 43–51. doi: <https://doi.org/10.1016/j.carbpol.2007.07.025>
- [5] Joshi, S., Goyal, S., & Reddy, M. S. (2018). Corn steep liquor as a nutritional source for bio cementation and its impact on concrete structural properties. *Journal of Industrial Microbiology and Biotechnology*, 45(8), 657–667. doi: 10.1007/s10295-018-2050-4
- [6] Abrial, H., Pratama, A. B., Handayani, D., Mahardika, M., Aminah, I., Sandrawati, N., ... Ilyas, R. A. (2021). Antimicrobial Edible Film Prepared from Bacterial Cellulose Nanofibers/Starch/Chitosan for a Food Packaging Alternative. *International Journal of Polymer Science*, 2021, 6641284. doi: 10.1155/2021/6641284
- [7] Abrial, H., Chairani, M. K., Rizki, M. D., Mahardika, M., Handayani, D., Sugiarti, E., ... Ilyas, R. A. (2021). Characterization of compressed bacterial cellulose nanopaper film after exposure to dry and humid conditions. *Journal of Materials Research and Technology*, 11, 896–904. doi: 10.1016/J.JMRT.2021.01.057
- [8] Cazón, P., Velazquez, G., & Vázquez, M. (2020). Characterization of mechanical and barrier properties of bacterial cellulose, glycerol and polyvinyl alcohol (PVOH) composite films with eco-friendly UV-protective properties. *Food Hydrocolloids*, 99, 105323. doi: 10.1016/J.FOODHYD.2019.105323
- [9] Lin, C.-M., Chang, Y.-C., Cheng, L.-C., Liu, C.-H., Chang, S. C., Hsien, T.-Y., ... Hsieh, H.-J. (2020). Preparation of graphene-embedded hydroxypropyl cellulose/chitosan/polyethylene oxide nanofiber membranes as wound dressings with enhanced antibacterial properties. *Cellulose*, 27(5), 2651–2667. doi: 10.1007/s10570-019-02940-w
- [10] Kamiński, K., Jarosz, M., Grudzień, J., Pawlik, J., Zastawnik, F., Pandyra, P., & Kołodziejczyk, A. M. (2020). Hydrogel bacterial cellulose: a path to improved materials for new eco-friendly textiles. *Cellulose*, 27(9), 5353–5365. doi: 10.1007/s10570-020-03128-3
- [11] Galdino, C. J. S., Maia, A. D., Meira, H. M., Souza, T. C., Amorim, J. D. P., Almeida, F. C. G., ... Sarubbo, L. A. (2020). Use of a bacterial cellulose filter for the removal of oil from wastewater. *Process Biochemistry*, 91, 288–296. doi: 10.1016/J.PROCBIO.2019.12.020
- [12] Kurniawan, F., Sulistiyana, I. U., & Ulfin, I. (2014). New bacterial cellulose membranes from chayote fruit and bamboo shoots. *Int. J. Appl. Chem*, 10(2), 101–112.
- [13] Xiao, X., Hou, Y., Liu, Y., Liu, Y., Zhao, H., Dong, L., ... Luo, G. (2013). Classification and analysis of corn steep liquor by UPLC/Q-TOF MS and HPLC. *Talanta*, 107, 344–348. doi: 10.1016/J.TALANTA.2013.01.044
- [14] Sulistiyana. (2020). Analisis Kualitas Nata De Corn Dari Ekstrak Jagung Kuning Muda Dengan Variasi Lama Fermentasi. *Indonesian Journal of Chemical Research*, 8(1), 79-84. doi: 10.30598/10.30598/ijcr.2020.8-sul
- [15] Pang, M., Huang, Y., Meng, F., Zhuang, Y., Liu, H., Du, M., ... Cai, Y. (2020). Application of bacterial cellulose in skin and bone tissue engineering. *European Polymer Journal*, 122, 109365. doi: 10.1016/J.EURPOLYMJ.2019.109365
- [16] Putriana, I., & Aminah, S. (2013). Physical quality, Dietary Fiber and Organoleptic Characteristic from Nata de Cassava Based time of Fermentation. *Jurnal Pangan dan Gizi*, 4(07).

## Research Article

# Performance Analysis of Ammonia Converter in Ammonia Unit Factory

Evaluasi Kinerja Ammonia Converter Pada Pabrik Unit Amonia

Prahady Susmanto<sup>1\*)</sup>, Dino Dewantara<sup>1)</sup>, Teguh Widodo<sup>2)</sup>, Susi Susanti<sup>1)</sup>

<sup>1)</sup>Universitas Sriwijaya, Faculty of Engineering, Chemical Engineering, Ogan Ilir 30662, Indonesia

<sup>2)</sup>PT PUSRI IIB, Operations Department, Palembang 30118, Indonesia

## Article History

Received: 17<sup>th</sup> October 2022; Revised: 24<sup>th</sup> January 2023; Accepted: 09<sup>th</sup> February 2023;

Available online: 21<sup>th</sup> August 2023; Published Regularly: June 2023

doi: [10.25273/cheesa.v6i1.14157.56-62](https://doi.org/10.25273/cheesa.v6i1.14157.56-62)

\*Corresponding Author.

Email:

prahady.susmanto@ft.unsri.ac.id

## Abstract

An ammonia converter is a catalyzed reactor that facilitates the synthesis of NH<sub>3</sub> (ammonia) from hydrogen (H<sub>2</sub>) and nitrogen (N<sub>2</sub>). Several studies have shown that the performance of this reactor significantly influences the operational efficiency and productivity of ammonia plants. Therefore, this study aims to evaluate the performance of an ammonia converter by assessing the effect of operating conditions on the reactant conversion and reaction products using design and actual data. The operating conditions examined included temperature, pressure, ratio of reactants, and inert mole utilized during the NH<sub>3</sub> synthesis process. The results showed that the highest NH<sub>3</sub> yield of 20.28% was achieved in actual data with 351.5°C temperature, 154.32 kg/cm<sup>2</sup> pressure, 3.58 raw material ratio, and 3.57% inert mole (sixth dataset). The performance efficiency of an ammonia converter can be assessed using temperature, reactant ratio, and inert moles, while the pressure factor was insignificant due to dataset fluctuations. Based on the evaluation results, the converter experienced a decrease in performance due to a discrepancy in the existing operating conditions between the design and actual data.

**Keywords:** Ammonia converter; operating conditions; reactor; yield

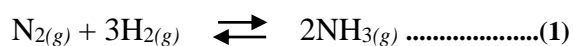
## Abstrak

Ammonia Converter adalah reaktor berkatalis yang berfungsi sebagai tempat proses pembentukan NH<sub>3</sub> (amonia) dari hidrogen (H<sub>2</sub>) dan nitrogen (N<sub>2</sub>). Reaktor ammonia converter sangat berpengaruh terhadap produktivitas dan efisiensi di pabrik amonia sehingga diperlukan analisis kinerja reaktor. Tujuan penelitian ini untuk mengevaluasi kinerja ammonia converter berdasarkan kondisi operasi terhadap hasil konversi reaktan dan produk reaksi yang dihasilkan dengan ditinjau dari data desain dan data aktualnya. Penelitian ini menganalisis kondisi operasi suhu, tekanan dan rasio reaktan serta inert yang dihasilkan dari proses sintesis NH<sub>3</sub> dengan membandingkan data aktual yang didapatkan dengan data desainnya. Hasil evaluasi menunjukkan kondisi operasi optimal yang dicapai oleh NH<sub>3</sub> converter dengan suhu 154,32°C, tekanan 154,32 kg/cm<sup>2</sup>, rasio reaktan 3,58 dan mol inert 3,57% dengan konversi H<sub>2</sub> 32,82%, konversi N<sub>2</sub> 35,11% dan yield NH<sub>3</sub> 20,28%. Hasil evaluasi menunjukkan efisiensi kinerja reaktor ammonia converter dapat ditinjau oleh suhu, rasio reaktan dan mol inert sedangkan faktor tekanan tidak dapat digunakan karena data aktualnya yang fluktuatif.

**Kata kunci :** Ammonia converter; kondisi operasi; reaktor; yield

**Performance Analysis of Ammonia Converter in Ammonia Unit Factory****1. Introduction**

Ammonia synthesis is a process that is often carried out in an ammonia converter unit. Within this unit, synthesis gases (N<sub>2</sub> and H<sub>2</sub>) obtained from the purification unit are reacted to obtain ammonia based products [1]. Furthermore, it is indigenously structured with three horizontal bed converters, which are designed using pressure wall materials at a cold temperature. The cold feed gas is passed through the annulus between the catalyst basket and the converter wall to maintain a low wall vessel temperature [2,3]. The converter unit also consists of a removable basket containing 4 fixed beds and 2 interchangers, with approximately 77.1 m<sup>3</sup> of promoted iron catalyst [3]. The volume of the catalyst within the beds varies, and it increases from the first to the third bed. This strategic volume augmentation helps to curtail the temperature elevation caused by the exothermic reaction occurring within the first bed (where the fastest reaction occurs). Consequently, the design preserves the converter's temperature within the desired range [3,4]. The ammonia formation is an exothermic equilibrium reaction using the Haber-Bosch process method, which is illustrated below [1]:



The performance of an ammonia converter is significantly influenced by several factors, including temperature, pressure, H<sub>2</sub>/N<sub>2</sub> ratio, and inert mole. Several studies have shown that temperature plays a dual role, impacting both the synthesis reaction rate and ammonia equilibrium. NH<sub>3</sub> synthesis occurs through an exothermic reaction, leading to the limitation of the operating temperature by chemical equilibrium. However, higher

levels concurrently enhance kinetic energy, leading to faster molecular collisions [5].

Pressure is a crucial factor that influences both the equilibrium of NH<sub>3</sub> and reaction rate, where higher levels often lead to increased yield. Changing the H<sub>2</sub>/N<sub>2</sub> ratio can lead to an increase or decrease in yield in an ammonia converter. Based on the plant design, an optimal H<sub>2</sub>/N<sub>2</sub> ratio typically ranges from 2.8-3.2 [2-4]. The primary operational variable used to control the hydrogen and nitrogen ratio is the composition of the introduced make-up or fresh feed gas.

Methane and argon are inert components commonly found within the syngas stream. These components are not harmful to the catalyst and do not undergo synthesis reactions. However, they have been reported to have a negative impact on reaction rates and equilibrium. A feasible approach that is often used to minimize inert concentration involves purging syngas in the loop [1,3,4]. Therefore, this study aims to analyze the performance of an ammonia converter in an NH<sub>3</sub> plant by comparing the yield obtained under actual and standard operating conditions. The parameters observed included temperature, pressure, reactant ratio, and the inert mole produced by the reactor.

**2. Research Methods**

The methodology used in this study included a literature review, observation, as well as data collection and processing. The dataset used for the ammonia converter analysis consisted of both design and actual data. The design dataset included the predetermined parameters established during the development of the unit [2,4]. Furthermore, these parameters consisted of inlet temperature, pressure, inert mole, and H<sub>2</sub>/N<sub>2</sub> reactant ratio.

**Performance Analysis of Ammonia Converter in Ammonia Unit Factory****3. Results and Discussion**

The actual data used for evaluating the performance of an ammonia converter were obtained from the operation conditions at the control room and laboratory of the PT PUSRI IIB unit in the form of log sheets. The conditions examined included the flow rate, %mol composition data for inlet and outlet, feed temperature, pressure, inter-bed temperature, inert mole, and H<sub>2</sub>/N<sub>2</sub> reactant ratio. Furthermore, the analysis was performed with mass balance calculations using Microsoft Excel to determine the conversion of N<sub>2</sub> and H<sub>2</sub>. It was also used to determine the yield of NH<sub>3</sub> products produced by comparing the design and actual data. The actual data from 6<sup>th</sup> December 2021 to 31<sup>th</sup> January 2022, were used, totaling 9 dataset points.

Table 1 shows the results of H<sub>2</sub> and N<sub>2</sub> reactant conversion as well as NH<sub>3</sub> yield based on the operating conditions of temperature, pressure, reactant ratio, and inert mole. The data were then plotted as a graph in Figure 1 to observe the midpoint of the dataset points based on the conditions

influencing the reactant conversion and product yield. Polynomial regression was performed on the data in Table 1 to determine the optimal relationship between temperature, pressure, reactant ratio, and an inert mole in the conversion of H<sub>2</sub> and N<sub>2</sub> into NH<sub>3</sub>.

In Figure 1, there was a convergence point of the four sets of operating conditions, which was indicated by the 6th dataset. This suggested that the optimal operating conditions affecting the NH<sub>3</sub> production process were achieved with the 6th data, namely 351.25 °C temperature, 154.32 kg/cm<sup>2</sup> pressure, 3.58 reactant ratio, and 3.57% inert mole.

Based on polynomial regression results, Figure 2 showed a similar intersection point to Figure 1, which was achieved at the 6th operating data point. This indicated the occurrence of synchronization between the factors affecting the NH<sub>3</sub> process, namely temperature, pressure, reactant ratio, and inert mole. The conversion results obtained were 32.82% conversion of H<sub>2</sub>, 35.11% conversion of N<sub>2</sub>, and 20.28% yield of NH<sub>3</sub>.

**Table 1.** Ammonia Converter Operating Conditions: Design and Actual Data

Data	Inlet Temp. (°C)	Inlet Press. (kg/cm <sup>2</sup> )	H <sub>2</sub> /N <sub>2</sub> Ratio	Inert (%mol)	Energy Gibbs (kJ/kmol)	H <sub>2</sub> Conversion (%mol)	N <sub>2</sub> Conversion (%mol)	NH <sub>3</sub> Yield (%mol)
1	349,50	151,84	3,20	3,78	-165,9	30,00	33,11	19,56
2	349,31	152,57	3,31	3,68	-165,9	30,85	34,30	19,92
3	349,34	153,40	3,37	3,63	-165,9	28,41	36,66	20,10
4	347,73	153,61	3,57	3,61	-165,6	32,91	34,15	19,89
5	347,56	155,02	3,34	3,78	-165,6	29,04	36,11	20,11
6	351,25	154,32	3,58	3,57	-166,3	32,82	35,11	20,28
7	348,42	154,45	3,55	3,68	-165,7	30,57	35,71	20,05
8	347,75	154,80	3,43	3,57	-165,6	25,00	38,66	19,78
9	349,25	154,40	3,26	3,80	-165,9	31,13	33,61	20,03
<b>Design</b>	<b>380,00</b>	<b>157,90</b>	<b>3,00</b>	<b>3,50</b>	<b>-171,8</b>	<b>32,55</b>	<b>32,44</b>	<b>20,31</b>

## Performance Analysis of Ammonia Converter in Ammonia Unit Factory

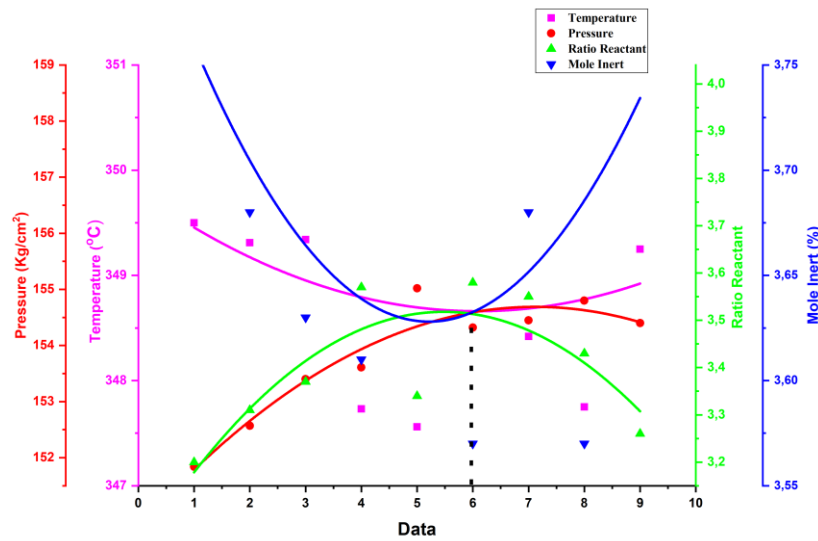


**Figure 1.** Comparison of temperature, pressure, reactant ratio, and inert mol toward operating data 1-9

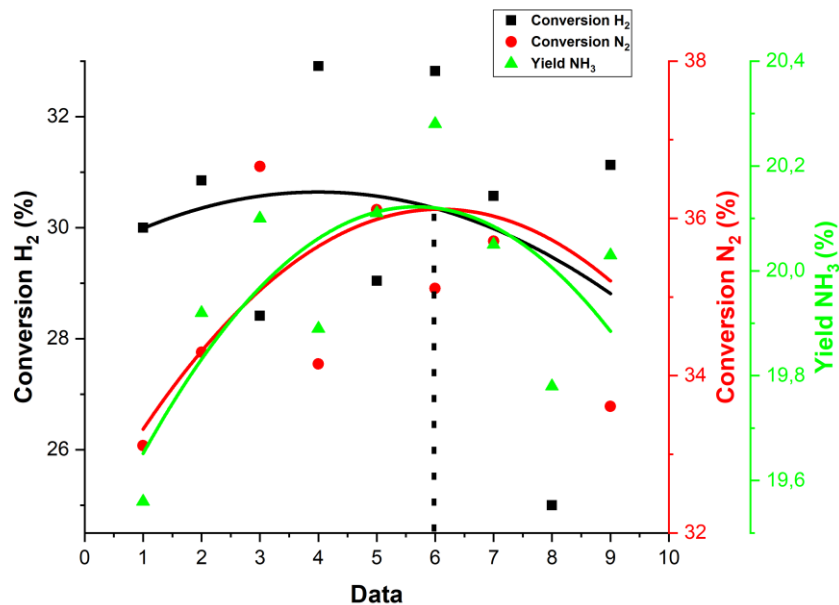


**Figure 2.** Comparison of H<sub>2</sub> conversion, N<sub>2</sub> conversion, and NH<sub>3</sub> yield toward operating data 1-9

The optimal temperature in this study was 351.25°C, leading to an NH<sub>3</sub> yield of 20.28% and an H<sub>2</sub> reactant conversion of 32.82%, which were the highest actual data. This study showed that the actual dataset results were similar to the design results, as shown in Table 1. Furthermore, high reaction temperatures could yield high reactant conversion and product yield [6]. Operations at high levels often accelerated the reaction process and increase the conversion of H<sub>2</sub>, N<sub>2</sub>, and mole NH<sub>3</sub> [7]. However, processes at high temperatures

could shorten the catalyst lifespan by causing faster saturation and decreasing the NH<sub>3</sub> equilibrium degree in the reaction [8].

Inlet temperature affected the NH<sub>3</sub> yield through two factors, including chemical equilibrium and chemical kinetics. Based on chemical equilibrium, the effect of these factors was governed by Le Chatelier's principle. The principle stated that a system in equilibrium, when affected externally, shifted to form a new equilibrium to minimize the external effect [9]. This indicated that the operating

**Performance Analysis of Ammonia Converter in Ammonia Unit Factory**

temperature in exothermic reactions was limited by chemical equilibrium. When the levels exceeded the threshold, productivity decreased, and product decomposition into reactants occurred to reach a balance [10]. Therefore, the operating temperature in the  $\text{NH}_3$  reaction must be maintained within the desired range.

The decrease and increase in  $\text{NH}_3$  yield with temperature could be attributed to the energy involved in the reaction process, specifically Gibbs energy [11]. Gibbs energy is a measure of the potential work of a reversible reaction or the maximum work possible for a system at a constant temperature or pressure [11, 12]. Furthermore, it was often used to assess the spontaneity of a reaction. Equilibrium occurred when its value was zero, and there was no reaction if the value was greater than zero. This indicated that the smaller the generated Gibbs energy, the higher the negativity, leading to increased spontaneity [13].

Factors in chemical reaction kinetics were related to the rate of reaction. Higher temperatures often led to faster reactions, leading to an increase in product formation [14]. This was because higher temperatures led to more frequent particle movement, thereby increasing collision frequency and rate [15]. Therefore, increasing the levels within the equilibrium limit could enhance the  $\text{NH}_3$  product yield. For the Haber-Bosch synthesis of  $\text{NH}_3$ , the chemical equilibrium limit occurred at a temperature of  $495^\circ\text{C}$  [13].

Decreases in yield were also affected by catalyst performance in each bed and interchanger performance. A lower inlet temperature for an ammonia converter increased the load on the interchanger to raise the level to the desired range. This was because an ammonia converter reaction

was exothermic, indicating that increased the temperature enhanced raw material yield, but decreased the  $\text{NH}_3$  equilibrium degree in the reaction [16].

Optimal conditions were achieved at the 6th data point with a pressure of  $154.32 \text{ kg/cm}^2$ . This actual value was lower compared to the design data of  $157.9 \text{ kg/cm}^2$ . The results showed that pressure affected both  $\text{NH}_3$  equilibrium and reaction rate [16,17].

The increased pressure was caused by several factors, such as the flow rate of fresh makeup gas, a decrease in converter temperature below the desired range, and changes in the gas composition of the  $\text{H}_2$  and  $\text{N}_2$  ratios. It could also be caused by an increase in  $\text{NH}_3$  content in the recycle gas, an increment in inert content, and catalyst deactivation [18], leading to a reduction in product yield. This aligned with the actual data obtained from the first data point with the lowest pressure of  $151.84 \text{ kg/cm}^2$ , which yielded the smallest  $\text{N}_2$  conversion at 33.11% and  $\text{NH}_3$  mol composition at 19.56%. However, this could not be proven for  $\text{H}_2$  conversion data due to its greater fluctuation compared to others.

The optimal reactant ratio of 3.58 was achieved at the 6th data point, which was higher compared to the design dataset of 3. Furthermore, the  $\text{H}_2/\text{N}_2$  ratio referred to the ratio of  $\text{H}_2$  and  $\text{N}_2$  inlet for each reactant. In the 6th data point, with a value of 3.58, the  $\text{H}_2$  conversion was closest to the design data. This corresponded to the highest  $\text{NH}_3$  yield obtained from the actual data at 20.28%.

The relationship between the  $\text{H}_2/\text{N}_2$  reactant ratio and  $\text{NH}_3$  yield was related to concentration. According to Le Chatelier's principle, when the equilibrium system experienced an increase in concentration on one side, the equilibrium shifted to the

**Performance Analysis of Ammonia Converter in Ammonia Unit Factory**

opposite side [19]. Therefore, increasing the raw material  $H_2/N_2$  ratio was expected to lead to an increase in  $NH_3$  product yield [20].

During the synthesis process, 3 molecules of  $H_2$  and 1 molecule of  $N_2$  were needed to form 2 molecules of  $NH_3$ . When the  $H_2/N_2$  ratio increased beyond the limit, an imbalance in the reactant ratio occurred [21]. Therefore, control of this parameter was necessary to achieve the desired product yield.

In an ammonia converter, the  $H_2/N_2$  ratio was easier to maintain compared to controlling the temperature and pressure conditions. Furthermore, it could be maintained in the reforming unit, specifically in the secondary reformer, by adjusting the air supply to maintain a close-to-3:1  $H_2/N_2$  ratio.

$H_2/N_2$  ratio greater than 3 could be controlled by increasing the airflow into the secondary reformer to increase  $N_2$  as the feed for an ammonia converter.  $H_2$  and  $N_2$  components were maintained since the reactants flowed into an ammonia converter or as fresh feed gas to be converted into  $NH_3$ .

Figures 1 and 2 showed the optimal conditions achieved at the 6th data point, with an actual inert mol of 3.57%, which was the closest to the design value of 3.5%. This inert mole gave the highest  $NH_3$  yield and was closest to the design data at

20.28%. Furthermore, the results showed that an increase in the parameter reduced the total reactant conversion. Although the inert compounds present in an ammonia converter were not catalyst poisons, the percentage of inlet and outlet inert mol increased in actual conditions [21]. The increase in the parameter reduced the amount of raw materials entering an ammonia converter. Changes in the percentage value of inert mol in actual conditions were affected by the performance of the reforming section, which supplied reactants before entering the reactor. Methane carried into the converter was obtained from the reactants in the primary and secondary reformers that were not converted into  $H_2$  raw materials.

**4. Conclusion**

In conclusion, the evaluation of the  $NH_3$  reactor performance showed optimal operating conditions, namely  $351.25^\circ C$  temperature,  $154.32 \text{ kg/cm}^2$  pressure, 3.58 reactant ratio, and 3.7% inert mol. These operating conditions gave the highest  $NH_3$  yield at 20.28%, with 32.82%  $H_2$  conversion and 35.11%  $N_2$  conversion. However, the pressure factor was difficult to evaluate due to the fluctuating and unstable data obtained.

**References**

- [1] Qian, J., An, Q., Fortunelli, A., Nielsen, R. J., & Goddard, W. A. (2018). Reaction Mechanism and Kinetics for Ammonia Synthesis on the Fe(111) Surface. *Journal of the American Chemical Society*, 140(20), 6288–6297. doi: 10.1021/jacs.7b13409
- [2] Siringo-ringo, N. O., Sari, I., & Selpiana. (2019). Evaluasi kinerja ammonia converter pabrik urea ditinjau dari konversi  $N_2$  dan  $H_2$  dengan menggunakan hysys. *Jurnal Teknik Kimia*, 25(3), 80–85. doi: 10.36706/jtk.v25i3.133
- [3] Agustria, R. M. Y., Al-Azhar., & Putri, R. W. (2019). Evaluasi efisiensi ammonia converter unit ammonia pada industri pupuk urea. *Jurnal Teknik Kimia*, 25(3), 70–74. doi: 10.36706/jtk.v25i3.130
- [4] Rahmatullah, Caesaranty, P. F., & Sari, P. F. (2019). Evaluasi performance ammonia converter

**Performance Analysis of Ammonia Converter in Ammonia Unit Factory**

- 
- Pabrik urea ditinjau dari pengaruh temperatur, tekanan, rasio  $H_2/N_2$ , dan mol inert inlet, serta perhitungan neraca massa dan neraca panas dengan simulator. *Jurnal Teknik Kimia*, 25(1), 21–30. doi: 10.36706/jtk.v25i1.17
- [5] Abdurrahman, S., & Hidayat, M. (2012). Studi Simulasi pada Unit Reformer Primer di PT Pupuk Sriwidjaya Palembang. *Jurnal Rekayasa Proses*, 6(2), 30.
- [6] Akpa, J. G., & Raphael, N. R. (2014). Optimization of an Ammonia Synthesis Converter. *World Journal of Engineering and Technology*, 02(04), 305–313. doi: 10.4236/wjet.2014.24032
- [7] Peng, P., Chen, P., Schiappacasse, C., Zhou, N., Anderson, E., Chen, D., ... Ruan, R. (2018). A review on the non-thermal plasma-assisted ammonia synthesis technologies. *Journal of Cleaner Production*, 177, 597–609. doi: 10.1016/j.jclepro.2017.12.229
- [8] Klaas, L., Guban, D., Roeb, M., & Sattler, C. (2021). Recent progress towards solar energy integration into low-pressure green ammonia production technologies. *International Journal of Hydrogen Energy*, 46(49), 25121–25136. doi: 10.1016/j.ijhydene.2021.05.063
- [9] Uline, M. J., & Corti, D. S. (2006). The ammonia synthesis reaction: An exception to the Le Châtelier principle and effects of nonideality. *Journal of Chemical Education*, 83(1), 138–144. doi: 10.1021/ed083p138
- [10] Demirhan, C. D., Tso, W. W., Powell, J. B., & Pistikopoulos, E. N. (2019). Sustainable ammonia production through process synthesis and global optimization. *AIChE Journal*, 65(7). doi: 10.1002/aic.16498
- [11] Wibowo, B. H., & Abdillah, H. L. (2014). Penentuan Tetapan Kecepatan Dan Suhu Reaksi Untuk Memilih Proses Pembuatan Butadien. *Majalah Sains dan Teknologi Dirgantara*, 9(1), 35–42. Retrieved from [http://jurnal.lapan.go.id/index.php/majalah\\_sains\\_tekgan/article/view/2051/1864](http://jurnal.lapan.go.id/index.php/majalah_sains_tekgan/article/view/2051/1864)
- [12] Ozturk, M., & Dincer, I. (2021). An integrated system for ammonia production from renewable hydrogen: A case study. *International Journal of Hydrogen Energy*, 46(8), 5918–5925. doi: 10.1016/j.ijhydene.2019.12.127
- [13] Mao, C., Li, H., Gu, H., Wang, J., Zou, Y., Qi, G., ... Zhang, L. (2019). Beyond the Thermal Equilibrium Limit of Ammonia Synthesis with Dual Temperature Zone Catalyst Powered by Solar Light. *Chem*, 5(10), 2702–2717. doi: 10.1016/j.chempr.2019.07.021
- [14] Aboelkheir, I. M. (2022). An Optimized Chemical and Mechanical Engineering Design of an Ammonia Reactor. *Cognizance Journal of Multidisciplinary Studies*, 2(1), 10–37. doi: 10.47760/cognizance.2022.v02i01.002
- [15] Badescu, V. (2020). Optimal design and operation of ammonia decomposition reactors. *International Journal of Energy Research*, 44(7), 5360–5384. doi: 10.1002/er.5286
- [16] Yancy-Caballero, D., Biegler, L. T., & Guirardello, R. (2015). Optimization of an ammonia synthesis reactor using simultaneous approach. *Chemical Engineering Transactions*, 43, 1297–1302. doi: 10.3303/CET1543217
- [17] Tripodi, A., Conte, F., & Rossetti, I. (2021). Process Intensification for Ammonia Synthesis in Multibed Reactors with Fe-Wustite and Ru/C Catalysts. *Industrial and Engineering Chemistry Research*, 60(2), 908–915. doi: 10.1021/acs.iecr.0c05350
- [18] Suhan, B. K. M., Hemal, M. N. R., Choudhury, M. A. A. S., & Mazumder, M. A. A. (2022). Optimal design of ammonia synthesis reactor for a process industry. *Journal of King Saud University - Engineering Sciences*, 34(1), 23–30. doi: 10.1016/j.jksues.2020.08.004
- [19] Hakiki, M. N., Hidayat, M., & Sutijan, S. (2017). Simulasi Pengaruh Steam-To-Carbon Ratio Dan Tube Outlet Temperature Terhadap Reaksi Steam Reforming Pada Primary Reformer Di Pabrik Amoniak. *Rotor*, 10(2), 58. doi: 10.19184/rotor.v10i2.6393
- [20] Aslan, M. Y., Hargreaves, J. S. J., & Uner, D. (2021). The effect of  $H_2:N_2$  ratio on the  $NH_3$  synthesis rate and on process economics over the  $Co_3Mo_3N$  catalyst. *Faraday Discussions*, 229, 475–488. doi: 10.1039/c9fd00136k
- [21] Cheema, I. I., & Krewer, U. (2020). Optimisation of the autothermal  $NH_3$  production process for power-to-ammonia. *Processes*, 8(1), 1–21. doi: 10.3390/pr8010038
-

# Utilization of Activated Carbon/Magnesium(II) Composites in Decreasing Organic Materials

Pemanfaatan Komposit Karbon Aktif/Magnesium(II) Dalam Penurunan Kadar Bahan Organik

Dheasi Rani Ullica<sup>1)</sup>, Titin Anita Zaharah<sup>1\*)</sup>, Imelda Hotmarisi Silalahi<sup>1)</sup>

<sup>1)</sup>Universitas Tanjungpura, Chemical Engineering, Indonesia

## Article History

Received: 11<sup>th</sup> February 2023; Revised: 08<sup>th</sup> August 2023; Accepted: 10<sup>th</sup> August 2023;

Available online: 22<sup>th</sup> August 2023; Published Regularly: June 2023

doi: [10.25273/cheesa.v6i1.15662.63-75](https://doi.org/10.25273/cheesa.v6i1.15662.63-75)

\*Corresponding Author.

Email:

titin.anita.zaharah@chemistry.untan.ac.id

## Abstract

This study aimed to determine the characteristics, adsorption capacity, and isotherm of the adsorbent AC/Mg(II) composite in decreasing organic matter in peat water. Activated carbon was produced from empty fruit bunches of oil palm containing high levels of lignocellulose. Carbon was synthesized through the carbonization process and then activated with  $\text{CH}_3\text{COONa}$ . The activated sample was composited with magnesium nitrate hexahydrate through an in-situ method under alkaline conditions using NaOH. The adsorbent AC/Mg(II) composite that had been prepared was characterized using FTIR, showing the presence of Mg-O bonds at the absorption wave number of  $403.12\text{ cm}^{-1}$ . The results showed that the moisture content of the adsorbent was lower compared to activated carbon, namely 1.30%. Furthermore, the best mass was 2 g AC/Mg(II) with an adsorption of 2.26 mg/g and an organic matter adsorption percentage of 14.41%. Furthermore, the optimum contact time was 15 minutes with an adsorption of 2.42 mg/g and a percentage of 17.15%. The mechanism occurring in the AC/Mg(II) composite with peat water organic matter followed the Langmuir isotherm equation, which formed a monolayer. The equation gave  $R^2$ , adsorption capacity ( $Q_0$ ), and adsorption constant ( $k$ ) values of 0.9994, 0.2340 mg/g, and 0.0047, respectively.

**Keywords:** Activated carbon; fruit bunches; Magnesium(II); organic matter; peat water

## Abstrak

Penelitian ini bertujuan untuk menentukan karakteristik adsorben AC/Mg(II) serta mengetahui kapasitas adsorpsi dan isoterm adsorpsi terhadap penurunan kadar bahan organik air gambut. Karbon aktif dipreparasi dari tandan kosong kelapa sawit (TKKS) yang merupakan limbah yang mengandung lignoselulosa tinggi sebagai sumber karbon. Karbon dibuat melalui proses karbonisasi kemudian diaktivasi dengan  $\text{CH}_3\text{COONa}$ . Karbon aktif dikompositkan dengan magnesium nitrat heksahidrat melalui teknik in-situ dalam suasana basa menggunakan NaOH. Adsorben komposit AC/Mg(II) yang telah dibuat dikarakterisasi menggunakan FTIR menunjukkan adanya ikatan Mg-O muncul pada serapan bilangan gelombang  $403,12\text{ cm}^{-1}$ . Kadar air adsorben AC/Mg(II) lebih rendah dari karbon aktif yaitu 1,30%. Hasil penelitian menunjukkan massa adsorben terbaik adalah 2 g AC/Mg(II) dengan daya adsorpsi 2,26 mg/g dan persentase adsorpsi bahan organik sebesar 14,41%. Waktu kontak terbaik adalah 15 menit dengan daya adsorpsi 2,42 mg/g dan persentase adsorpsi bahan organik 17,15%. Mekanisme adsorpsi yang terjadi pada komposit AC/Mg(II) dengan bahan organik air gambut mengikuti persamaan isoterm adsorpsi Langmuir yang membentuk lapisan monolayer dengan nilai  $R^2$  sebesar 0,9994, nilai kapasitas ( $Q_0$ ) sebesar 0,2340 mg/g dan nilai konstanta adsorpsi ( $k$ ) sebesar 0,0047.

**Kata Kunci:** air gambut; bahan organik; karbon aktif; Magnesium(II); tandan kosong kelapa sawit.

## 1. Introduction

Peat water is a type of surface water found in peatland areas and is characterized by its acidic nature (low pH), yellow to brown color, and high organic matter content. Furthermore, its primary organic components are humic and fulvic acids, which are primarily responsible for its properties. This resource can be treated to obtain clean water by reducing organic matter to meet the standard quality criteria. Several methods have gained widespread usage for the treatment process, including adsorption [1], membrane separation, and coagulation-flocculation [2]. Among these methods, adsorption holds a distinct preference due to its economic feasibility, ease of use, high efficiency, and ability to remove undesired compounds [3]. An extensively studied adsorbent is activated carbon derived from oil palm empty fruit bunches (EFB).

The high lignocellulose content within oil palm EFB offers a foundational resource for the production of activated carbon due to the presence of active functional groups, such as hydroxyl and carboxyl. These groups have been reported to serve as active sites for the binding of metals [4]. Despite this inherent potential, the adsorption capacity of the adsorbent is still suboptimal. This indicates that its combination with other nanoparticles is required to enhance the adsorption capability [5].

Several studies have reported the capacity of MgO nanoparticles to significantly decrease COD levels in tannery wastewater. In a previous study, the concentration dropped from an initial 2725.9 mg/L to 126.5 mg/L [6]. Furthermore, MgO exhibits the capacity to reduce the concentration of humic acid within a solution, with a maximum

efficiency of approximately 91% after a contact time of 20 minutes [7].

Ghalekhondabi et al. [8] have composited MgO with activated carbon to adsorb methylene blue organic compounds. The composite showed an impressive maximum adsorption efficiency and capacity of 97.5% and 642 mg/g, respectively. Chemical modifications have also been widely used to enhance the quality of activated carbon as an adsorbent for broader applications [9].

Activated carbon has showcased its utility in the removal of Fe(II) from peat water [10] and the reduction of organic matter [11]. The positive results obtained from the use of this adsorbent in adsorbing Fe(II) and organic matter formed the foundation for this current study to employ the Activated Carbon/Magnesium(II) (AC/Mg(II)). Activated carbon was combined with magnesium(II), where the positive charge of Mg interacted with the negative charge on the surface of the adsorbent. This interaction hinged on the connection between the hydroxyl groups on the activated carbon surface and magnesium, aiming to enhance the capacity and efficiency of organic matter adsorption in peat water.

The use of Mg offers the potential to greatly enhance the ability of the composite to adsorb organic matter due to the formation of complex compounds between organic molecules and the metal. Organic matter content reduction occurs through Mg complexation with organic substances within the pores of activated carbon. Organic compounds carrying a negative charge often bond with the positive charge of composites and vice versa [12]. Therefore, this study aimed to create activated carbon from EFB, which was activated using CH<sub>3</sub>COONa. The

## Utilization of Activated Carbon/Magnesium(II) Composites in Decreasing Organic Materials

matter was then composited with Mg(II) as an adsorbent for organic matter in peat water. CH<sub>3</sub>COONa exhibited the best performance in activating EFB charcoal compared to ammonium chloride and ammonium sulfate [13]. The adsorbent produced was subjected to characterization using FTIR to identify functional groups or bonds formed within the AC/Mg(II) composite, with subsequent comparison to the results of activated carbon. This study examined the influence of adsorbent mass and contact time to determine the optimum capacity of carbon composite for organic matter in peat water using a batch system. Furthermore, the adsorption isotherm model occurring during the process was also determined.

## 2. Research Methods

### 2.1 Tools and Materials

The instruments used in the study included Shimadzu 820 IPC Fourier Transform Infra Red (FTIR) and Shimadzu 1280 UV-Vis (Ultra Violet-Visible) Spectrophotometer. Meanwhile, the matters were peat water, CH<sub>3</sub>COONa (Merck), H<sub>2</sub>C<sub>2</sub>O<sub>4</sub>, H<sub>2</sub>SO<sub>4</sub> 98% (8 N), KMnO<sub>4</sub> (0,01 N), Mg(NO<sub>3</sub>)<sub>2</sub>.6H<sub>2</sub>O (Merck), methylene blue (Merck), NaOH (Merck), and EFB.

### 2.2 Carbonization of EFB for Activated Carbon

The EFB samples were pulverized, washed with deionized water, and dried for six days under direct sunlight. Approximately 200 g of dried EFB were then placed in a crucible, transferred to a furnace at a temperature of 350 °C for 1 hour, and placed in a closed container. Furthermore, the percentage of water loss after the carbonization process was calculated. The carbonized sample was

then ground and sieved using a 100-mesh sieve to obtain a uniform particle size.

### 2.3 Carbon Activation

A total of 61.18 g of carbon was placed in a round-bottom flask equipped with a condenser and a magnetic stirrer. Subsequently, 250 mL of 1 N CH<sub>3</sub>COONa solution was added to the flask, and the mixture was refluxed for 1 hour using a hotplate at approximately 120 °C. After the reaction mixture was cooled to room temperature, the solid was filtered and washed with deionized water [13]. The solid was then dried in an oven at 110 °C for 6 hours, leading to the production of activated carbon.

### 2.4 Preparation of AC/Mg(II) Composites

Magnesium oxide was composited with activated carbon in a 1:1 ratio. A total of 42 g of Mg(NO<sub>3</sub>)<sub>2</sub>.6H<sub>2</sub>O was dissolved in 250 mL of deionized water and stirred. In the mixture, 15 mL of NaOH 2M and 42 g of activated carbon (obtained from procedure 2.3) were slowly added while stirring gently for 60 minutes. The suspension obtained was allowed to stand for 60 minutes and slowly decanted. Subsequently, the residue was dried in an oven for 24 hours at a temperature of 80 °C and calcined at 350 °C for 60 minutes.

### 2.5 Characterization of the AC/Mg(II) Composites

The characterization of activated carbon and composites was carried out by determining the moisture content, adsorption capacity, and functional groups using FTIR.

#### 2.5.1 Determination of Functional Groups Using FTIR

Activated carbon and AC/Mg(II) composite samples were prepared, weigh-

## Utilization of Activated Carbon/Magnesium(II) Composites in Decreasing Organic Materials

ing approximately 0.5 g, and then stored in containers. Furthermore, the samples were analyzed using an FTIR at Hasanuddin University, Makassar.

### 2.5.2 Determination of Moisture Content

A total of 1 g of activated carbon was weighed and placed in a porcelain crucible of known weight (sample weight was denoted as  $W_1$ ). The porcelain crucible was then placed in an oven at 105 °C for 2 hours. After cooling in a desiccator, it was weighed until a constant weight was achieved (denoted as  $W_2$ ). The calculation formula for determining the moisture content is presented in Equation 1.

$$\text{Moisture Content} = \frac{W_1 - W_2}{W_1 - W} \times 100\% \dots\dots(1)$$

$W$  = Weight of crucible (g)

$W_1$  = Initial sample weight before oven drying (g)

$W_2$  = Sample weight after oven drying (g)

### 2.5.3 Methylene Blue Adsorption Test (SNI 06-3730-1995)

A Methylene Blue (MB) solution was prepared with a concentration of 10 ppm, and its absorbance was measured in a wavelength range of 500–700 nm using a UV-Vis spectrophotometer. A standard curve was then established based on the absorbance of standard MB solutions with concentrations of 0, 0.5, 1, 1.5, 2, 2.5, and 3 ppm at the maximum wavelength. Furthermore, a graph relating the absorbance to the concentration was plotted, and it was used to obtain the linear equation. Activated carbon and composites were tested for MB adsorption. The samples were combined with 25 mL of a 3 ppm MB solution and shaken using a shaker at 240 rpm for 15 minutes. The mixture was then filtered using Whatman No. 42 filter paper, and the filtrate was measured using a UV-Vis spectrophotometer at the maximum

wavelength to determine the final concentration. The amount of MB adsorbed was calculated using Equation 2.

$$MB = \frac{(C_{mb\ awal} \times V_{mb}) - (C_{mb\ sisa} \times V_{mb})}{W_{\text{Sample}}} \dots\dots\dots(2)$$

MB = Amount of adsorbed MB (mg/g)

$C_{mb\ initial}$  = Initial MB concentration (ppm)

$C_{mb\ residual}$  = Residual MB concentration (ppm)

$V_{mb}$  = Volume of MB solution used (mL)

$W_{\text{sample}}$  = Sample weight (g)

After calculating the adsorbed MB concentration, the surface area of activated carbon and AC/Mg(II) was determined using equation 3.

$$S = \frac{Q_t \times N \times A}{M_r} \dots\dots\dots(3)$$

$S$  = Surface area of activated carbon and AC/Mg(II) (mg/g)

$Q_t$  = Weight of adsorbed substance (mg/g)

$N$  = Avogadro's number ( $6,022 \times 10^{23} \text{ mol}^{-1}$ )

$A$  = Area covered by 1 molecule of the sample ( $197 \times 10^{-20} \text{ m}^2$ )

$M_r$  = Relative molecular mass of MB (320,5 g/mol)

### 2.6 Determination of Organic Matter Content in Peat Water Using Permanganometry Method

A total of 100 mL of the sample was placed into an Erlenmeyer flask, and three boiling stones were added. A few drops of 0.01 N  $\text{KMnO}_4$  were added to the sample until a pink color appeared. Subsequently, 5 mL of 8 N  $\text{H}_2\text{SO}_4$  was added, and the mixture was heated on an electric heater at a temperature of 105 °C  $\pm$  2 °C. The process was continued with the addition of 10 mL of 0.01 N  $\text{KMnO}_4$  standard solution, followed by boiling for 10 minutes. A total of 10 mL of 0.01  $\text{H}_2\text{C}_2\text{O}_4$  solution was added and the mixture was titrated with 0.01 N  $\text{KMnO}_4$  0,01 N solution until a pink color appeared. The

**Utilization of Activated Carbon/Magnesium(II) Composites in Decreasing Organic Materials**

volume of KMnO<sub>4</sub> used was recorded and if the value exceeded 7 mL, the test was repeated by diluting the sample. The procedure was repeated twice (duplicate), and the equivalent value of permanganate could be determined using Equation 4.

$$KMnO_4 = \frac{[(10-1)b - (10 \times c)] \times 31,6 \times 1000}{d} \dots\dots\dots(4)$$

- a = Volume of KMnO<sub>4</sub> 0,01 N required during titration
- b = Actual normality of KMnO<sub>4</sub>
- c = Normality of H<sub>2</sub>C<sub>2</sub>O<sub>4</sub>
- d = Volume of the sample

**2.7 Determination of the Relationship Between Peat Water Absorbance and Permanganate Number**

The relationship between peat water absorbance and the permanganate number was determined by creating a calibration curve between both parameters. The association was initially established by determining the permanganate number of peat water with dilution variations of 30-fold, 40-fold, 50-fold, 60-fold, and 70-fold. Subsequently, the absorbance was measured with the same dilution variations at a wavelength of 254 nm using a UV-Vis spectrophotometer. A linear equation was derived based on the curve depicting the relationship between peat water absorbance and the permanganate number. This equation was then used to determine peat water's organic matter content before and after adsorption.

**2.8 Application of AC/Mg(II) Composites as an Adsorbent**

**2.8.1 Determination of Optimal Adsorbent Mass for AC/Mg(II) Composites**

A total of 4 Erlenmeyer flasks were each filled with 100 mL of peat water. Furthermore, different variations of adsorbent mass, namely 0.5 g, 1.0 g, 2.0 g,

and 3.0 g, were added to each flask. The mixtures were stirred using a shaker at a speed of 150 rpm for 60 minutes and left undisturbed for 1 hour [14]. The solutions were filtered, and the organic matter content of peat water was determined using a UV-Vis spectrophotometer at a wavelength of 254 nm and measured for the permanganate number.

**2.8.2 Determination of Optimal Contact Time**

In this process, 5 Erlenmeyer flasks were each filled with 100 mL of peat water. The optimal adsorbent mass of 2 g was added to each flask, and stirring was carried out using a shaker at a speed of 150 rpm with varying contact times of 10, 15, 30, 45, and 60 minutes. The mixtures were then left undisturbed for 1 hour, followed by filtration. Subsequently, the organic matter content of peat water was determined using a UV-Vis spectrophotometer at a wavelength of 254 nm and measured for the permanganate number.

**2.9 Determination of Adsorption Isotherms**

The obtained data were analyzed using the Langmuir and Freundlich adsorption isotherm equations. The Langmuir isotherm determination used Equation 5, while the Freundlich isotherm used Equation 6.

$$\frac{Q_e}{C_e} = kQ_0 - kQ_e \dots\dots\dots(5)$$

- C<sub>e</sub> = Equilibrium concentration of adsorbate (mg/L)
- Q<sub>e</sub> = Total of adsorbate on adsorbent at equilibrium (mg/g)
- Q<sub>0</sub> = Adsorption capacity (mg/g)
- k = Langmuir isotherm constant

$$\text{Log } Q_e = \text{Log } kF + \frac{1}{n} \text{log } C_e \dots\dots(6)$$

- kF = Freundlich isotherm constant
- n = Intensity of adsorption

## Utilization of Activated Carbon/Magnesium(II) Composites in Decreasing Organic Materials

Langmuir and Freundlich Isotherm Models explain the formation of monolayer and multilayer adsorption, respectively. The determination of the equilibrium model for Langmuir and Freundlich isotherms was based on the coefficient of determination ( $R^2$ ), with the highest value indicating the preferred model.

### 3. Results and Discussion

#### 3.1 Oil Palm EFB Carbonization

The carbonization process of EFB was carried out in several steps. The first phases involved preparation, including size reduction, retting, water soaking, and drying. Size reduction was performed manually, followed by a retting process to separate the fiber portions since EFB was a collection of intertwined fibers. Approximately 3.10 kg of EFB fibers were soaked in hot water to remove impurities and extract any remaining oil. This was to ensure that it did not hinder the heat during the carbonization process. The EFB fibers were then drained to separate water and oil. Sun-drying was performed to eliminate any remaining moisture in the samples and reduce the raw matter's volume [15]. Furthermore, the drying process aimed to facilitate carbonization and reduce the volume of the raw matter.

The carbonization process was carried out using a furnace at 350 °C for 1 hour. At temperatures between 300 °C and 400 °C, the process was considered primary pyrolysis, which yielded charcoal, various gases, and H<sub>2</sub>O. This was due to the decomposition of wood components, such as hemicellulose, cellulose, and lignin present in EFB, leading to complete carbonization.

The yield of carbonized EFB was 204.69 g, but it was reduced to 62.21 g

after grinding, and only 50.01 g passed through the 100-mesh sieve. The carbon yield obtained from EFB was 74.01% of the original sample, accounting for the loss of 25.99%. Carbon obtained from the furnace process was then ground and sieved using a 100-mesh sieve to produce particles of uniform size and increase the contact surface area, thereby enhancing the adsorbent's ability to absorb adsorbates.

#### 3.2 Activation of EFB Carbon

This study employed chemical activation using CH<sub>3</sub>COONa as the activator. The aqueous CH<sub>3</sub>COOH species from CH<sub>3</sub>COONa salt interacted with the decomposition products generated during the carbonization process on the surface of the EFB charcoal. A 250 mL acetic acid solution was used to soak the carbon. Furthermore, the activation was aided by heating to accelerate penetration [16].

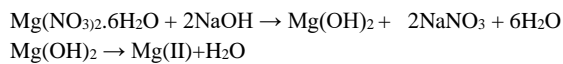
The activation process gave a yield of 97.99% or 58.94 g of the product. The process led to both physical and chemical changes in carbon. Carbon's color became slightly darker, with a smoother texture, decreased mass, and opened pores. These changes increased the surface area and affected its adsorption properties. Based on the obtained yield results, the content of compounds or impurities lost was 2.01%. The low content of non-carbon compounds or impurities lost was because the compounds that reacted with the activator had been completely consumed and transformed into soluble minerals [17].

#### 3.3 AC/Mg(II) Composites

The production of AC/Mg(II) composite was carried out using a solution of Magnesium Nitrate Hexahydrate (Mg(NO<sub>3</sub>)<sub>2</sub>·6H<sub>2</sub>O) as a precursor along with the addition of NaOH. The

**Utilization of Activated Carbon/Magnesium(II) Composites in Decreasing Organic Materials**

Mg(NO<sub>3</sub>)<sub>2</sub>·6H<sub>2</sub>O solution mixture with NaOH base solution formed a Mg(OH)<sub>2</sub> sol. The Mg(OH)<sub>2</sub> obtained was then composited within the structure of activated carbon. Furthermore, the calcination process was conducted to transform Mg(OH)<sub>2</sub> into MgO based on the reaction below [18]:



The calcination process was carried out using a furnace at 500°C for 2 hours. However, the use of high temperatures and a sufficiently long duration led to the formation of ash by composite. Consequently, the temperature of the process was adjusted to 350°C. The formation of ash was because activated carbon used in composites was derived from EFB, which were soft matter and could not be calcined at high temperatures.

The ideal condition for the formation of MgO was a temperature range of 500 – 700 °C for 1–2 hours [19,20]. Based on these results, it could not be concluded that composite matter contained MgO. However, from the characterization results,

it could be inferred that Mg(II) was composited within activated carbon. Magnesium was incorporated into activated carbon through the hydroxyl groups of Mg(OH)<sub>2</sub> on the surface of activated carbon.

### 3.4 Characterization of Activated Carbon and AC/Mg(II) Composites

#### 3.4.1 FTIR Characterization

Activated Carbon and AC/Mg(II) composites were characterized using FTIR to identify functional groups and bonds present in the adsorbents. Figure 1 (red line) showed the FTIR results of EFB-activated carbon. It was observed that in the process of producing activated carbon, absorptions occurred at wavenumbers 3419.79 cm<sup>-1</sup>, 2924.09 cm<sup>-1</sup>, 1705.07 cm<sup>-1</sup>, 1604.77 cm<sup>-1</sup>, 1379.10 cm<sup>-1</sup>, and 1246.02 cm<sup>-1</sup>. Each of these wavenumbers represented vibrations, namely stretching of –OH, CH<sub>3</sub>, and CH<sub>2</sub>, C=O stretching, C=C vibration in the hexagonal carbon structure, bending vibration of C-H, and C-O functional groups related to ethers and esters.

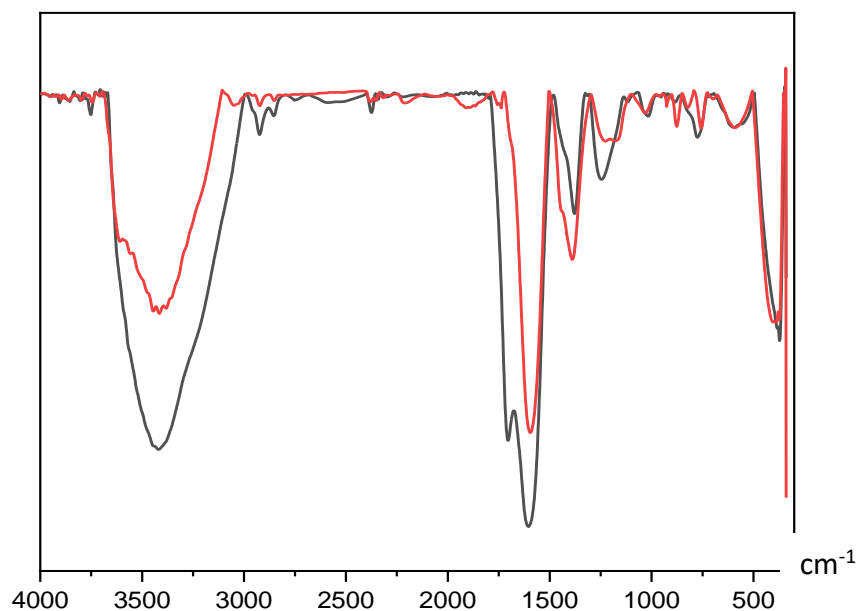


**Figure 1.** FTIR spectra of EFB activated carbon and AC/Mg(II) composites

## Utilization of Activated Carbon/Magnesium(II) Composites in Decreasing Organic Materials

The black line indicated the FTIR results for the production of the AC/Mg(II) composite. Absorptions were observed at wavenumber  $3415.93\text{ cm}^{-1}$ , indicating –OH stretching vibrations. An absorption at wavenumber  $1595.13\text{ cm}^{-1}$  indicated the presence of aromatic C=C bonds in the activated carbon structure. According to Khaleel et al. [19], the wavenumber  $1566\text{ cm}^{-1}$  signified the stretching vibration of the Mg-OH bond. The decrease in wavenumbers between activated carbon and composite in this study suggested the presence of formed Mg(II). The wavenumber  $1388.75\text{ cm}^{-1}$  indicated the bending vibration of C-H, while  $1226.73\text{ cm}^{-1}$  and  $1182.36\text{ cm}^{-1}$  showed C-O vibrations. Another bond present in the AC/Mg(II) composites was seen at wavenumber  $403.12\text{ cm}^{-1}$ , indicating Mg-O vibrations from MgO. Khaleel et al. [19] reported the presence of Mg-O vibrations in the wavenumber range of  $400\text{ cm}^{-1}$  to  $480\text{ cm}^{-1}$ . Moreover, Nga et al. [18] stated that this phenomenon was also found at wavenumber  $409\text{ cm}^{-1}$ . The shift in wavenumbers from activated carbon to AC/Mg(II) composites towards smaller values is due to the interaction of magnesium with oxide, leading to the formation of magnesium bonds. The intensity of the Mg-O vibration absorption indicated the presence of Mg(II) on activated carbon surface.

### 3.4.2 Moisture Content

The results from Table 1 showed that activated carbon and AC/Mg(II) composites had a moisture content of 8.29% and 1.30%, respectively. These values were consistent with the SNI 06-3730-1995 standard, which is specify a maximum of  $< 15\%$ . The composite process reduced the adsorbent's moisture

content due to the release of water molecules or hydration during the heating process. The lower values indicated that less residual water covered the activated carbon pores. Consequently, the pores of activated carbon became larger, leading to an increase in the surface area.

### 3.4.3 Methylene Blue Adsorption Test

Figure 2 showed that the adsorption capacity of activated carbon for MB was  $383.657\text{ mg/g}$  with an adsorption efficiency of 52.70%. In comparison, the adsorption capacity of the AC/Mg(II) composites was  $682.286\text{ mg/g}$ , with an adsorption efficiency of 92.80%. These results were consistent with Ghalekhondabi et al. [8] who stated that the AC/MgO composite could adsorb MB with a maximum efficiency and adsorption capacity of 97.50% and  $642\text{ mg/g}$ , respectively. Furthermore, the characterization results of the adsorption capacity of activated carbon and composite for methylene blue met the SNI 06-3730-1995 standard, which required a minimum of  $120\text{ mg/g}$  [18].

**Table 1.** Moisture content results for activated carbon and AC/Mg(II) composites

Sample	Moisture content %
Activated Carbon	8.29 %
AC/Mg Composites	1.30 %

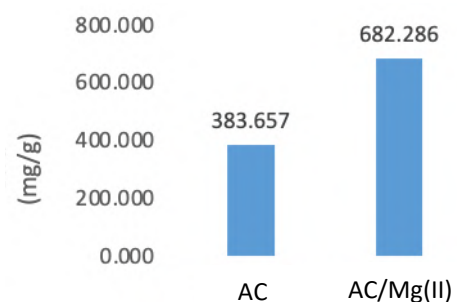


**Figure 2.** Methylene blue adsorption test

## Utilization of Activated Carbon/Magnesium(II) Composites in Decreasing Organic Materials

Another result obtained from the MB adsorption test was the specific surface area of activated carbon and AC/Mg(II). This parameter was determined based on the adsorption capacities of activated carbon and AC/Mg(II) for the MB compound, with values of 1420.38 m<sup>2</sup>/g and 2524.43 m<sup>2</sup>/g, respectively. The specific surface area of the adsorbent significantly affected its adsorption capacity. This indicated that the larger the specific surface area of the adsorbent, the greater its adsorption capability.

### 3.5 Application of AC/Mg(II) Composites as Organic Matter Adsorbent

#### 3.5.1 Relationship between Absorbance and Permanganate Number

Based on Figure 3, a relationship between the absorbance of peat water and its permanganate value was obtained with the linear equation  $y = 0.0132x - 0.2023$  with R<sup>2</sup> value of 0.9755. This equation could be used to determine the reduction in organic matter content in peat water after the adsorption process using AC/Mg(II) composite. Furthermore, the permanganate number indicated the amount of organic matter present in peat water. The higher the absorbance and permanganate number, the higher organic matter content in the sample. The relationship between absorbance and permanganate number in peat water is presented in Figure 3.

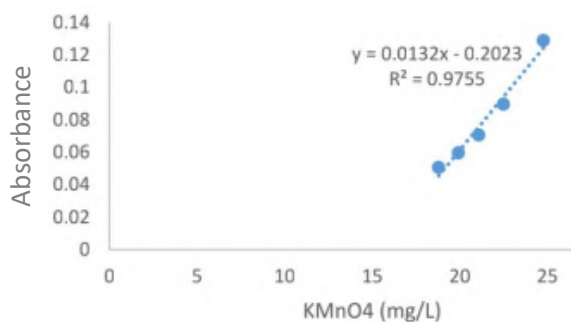


**Figure 3.** Relationship between permanganate number and adsorption

#### 3.5.2 Determination of Optimum Mass of AC/Mg(II) Composites

The optimal mass was determined to ascertain the required quantity of adsorbent for adsorbing organic matter in peat water. Based on Figure 4, it was evident that the percentage of adsorption increased with the use of adsorbent masses ranging from 0.5 g to 2 g. However, at 3 g, the adsorption percentage decreased to 11.61%. This indicated that there had been a buildup of adsorbent particles, limiting the spread of organic substances, leading to reduced adsorption onto the adsorbent surface. The reduction in organic matters content in peat water after adsorption was determined based on the percentage decrease in permanganate number. The use of AC/Mg(II) composites could reduce the percentage of permanganate by 14.41%, from the initial value of 283.28 mg/L to 242.45 mg/L.

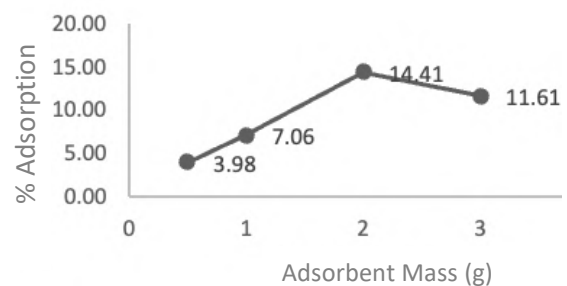


**Figure 4.** Relationship between adsorbent mass and % adsorption effectiveness

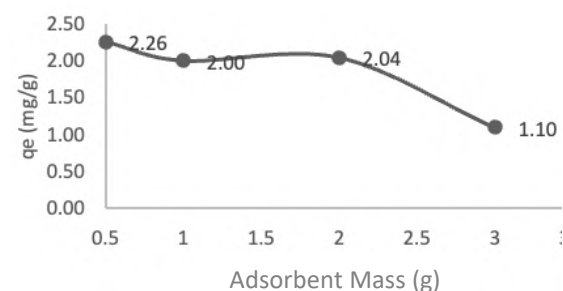


**Figure 5.** Relationship between mass and adsorption capacity

### Utilization of Activated Carbon/Magnesium(II) Composites in Decreasing Organic Materials

Figure 5 illustrated the effect of varying the mass of the AC/Mg(II) composites adsorbent on the adsorption capacity. Furthermore, adsorption capacity indicated the amount of adsorbate adsorbed per unit mass of adsorbent, and its magnitude was influenced by mass. This parameter decreased due to the addition of more adsorbent, which led to an increase in the active sites in the solution. The results showed that the adsorption time and solution concentration remained constant. This led to the need for a longer time to reach equilibrium due to the overlapping of adsorbent particles or stacking at the bottom of the container. This accumulation of particles limited the dispersion of organic matter, causing a decrease in the adsorption of organic substances onto the adsorbent surface.

#### 3.5.3 Determination of the Optimum Contact Time for Organic Matter Adsorption

Various contact times were employed, including 10, 15, 30, 45, and 60 minutes, using the optimum mass of 2 g for composite. The optimum contact time was determined to ascertain the duration required for composites to achieve maximum adsorption of organic matter.

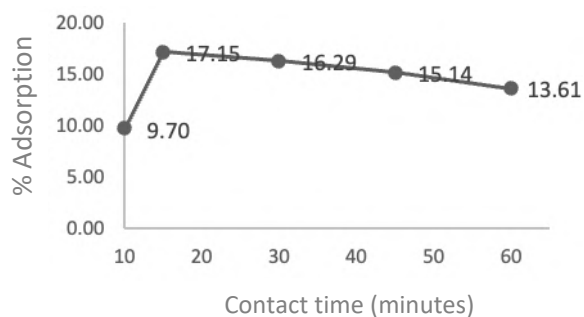


**Figure 6.** Relationship between contact time and % adsorption effectiveness

Figure 6 illustrated the amount of organic matter adsorbed by AC/Mg(II) at various contact times. Based on these results, the optimum contact time for reducing organic matter in peat water was 15 minutes.

Figure 7 illustrated the effect of varying the time for AC/Mg(II) composite at 10, 15, 30, 45, and 60 minutes, which yielded adsorption capacity values of 1.3712 mg/g, 2.42 mg/g, 2.30 mg/g, 2.14 mg/g, and 1.92 mg/g, respectively. Rahmayani et al. [20] stated that the longer the contact time used, the more frequently the adsorbent particles collided with the adsorbate, leading to increased adsorption. However, this indicated that the linearity was lower compared to the results obtained. Contact times beyond 15 minutes, such as 30, 45, and 60 minutes, showed a decrease in the percentage of organic matter absorbance in peat water, indicating the occurrence of desorption. This phenomenon often occurred when the adsorbent surface became saturated in the adsorption process. In the saturation state, the adsorption rate declined because the adsorbent had reached its maximum interaction capacity [21].

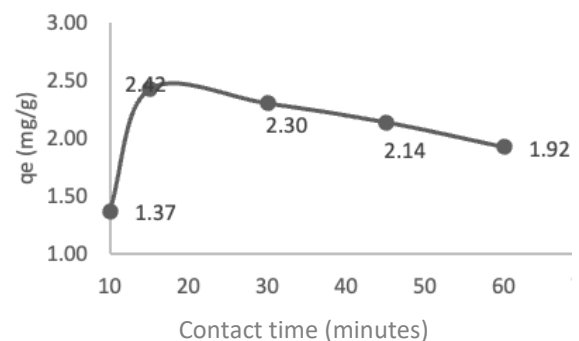


**Figure 7.** Relationship contact time and adsorption capacity

## Utilization of Activated Carbon/Magnesium(II) Composites in Decreasing Organic Materials

### 3.6 Determination of the Adsorption Isotherm Model

The determination of adsorption isotherm models was conducted to understand the adsorption mechanism. The shape of the Langmuir and Freundlich isotherm curves is presented in Figures 8 and 9, respectively.

Based on Figures 8 and 9, the adsorption isotherm model in this study followed the Langmuir isotherm with a linear equation  $y = 0.0047x - 0.0011$  and an R-squared value of 0.9994. The constant value (k) was the slope of the linear equation, which was 0.0047. Furthermore, the adsorption process of organic matter from peat water using AC/Mg(II) adsorbent derived from EFB followed the Langmuir isotherm equation. This indicated the presence of chemical adsorption that formed a single layer (monolayer). Based on the Langmuir isotherm equation  $y = 0.0047x - 0.0011$ , the adsorption capacity value was 0.2340 mg/g. The results obtained in this study did not meet the standard for clean water quality, namely 10 mg/L. However, the adsorption results were good, as they effectively reduced the organic content

from 283.28 mg/L to 234.29 mg/L. The high organic content also affected the adsorption capacity of the adsorbent. This indicated that the bonds between the groups present in the adsorbent and organic matter weakened, allowing some groups with stronger bonding to remain attached to the adsorbent.

### 4. Conclusion

In conclusion, the characteristics of the AC/Mg(II) adsorbent derived from EFB included a black color with a slight white appearance, and a lower moisture content of 1.298% compared to activated carbon. Moreover, the presence of Mg-O bonds was analyzed using FTIR instrumentation, leading to an absorption band at a wavenumber of 403.12 cm<sup>-1</sup>. The adsorption capacity of AC/Mg(II) for peat water was 2.42 mg/g, with an adsorption percentage of 17.15%. The results showed that the adsorption mechanism followed the Langmuir isotherm equation, forming a monolayer with R-squared, adsorption capacity (Q<sub>0</sub>), and adsorption constant (k) values of 0.9994, 0.2340 mg/g, and 0.0047, respectively.

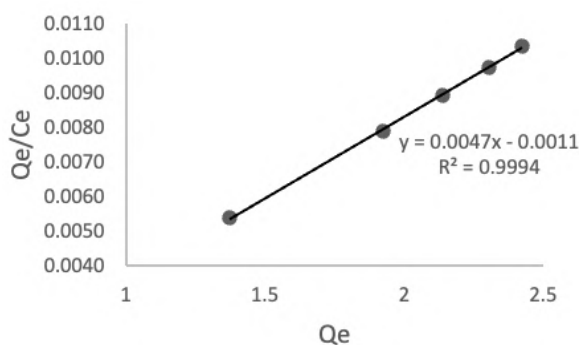


Figure 8. Langmuir adsorption isotherm curve

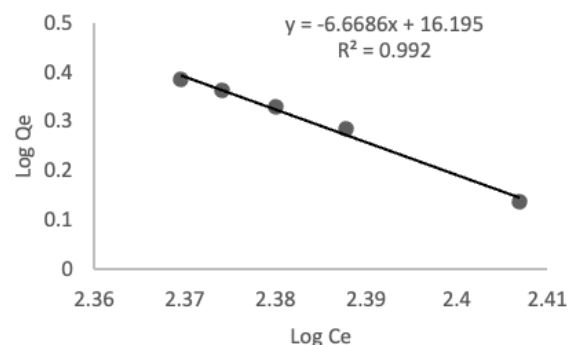


Figure 9. Freundlich adsorption isotherm curve

---

## References

- [1] Arisna, R., Titin, A.Z., & Rudiyanayah. (2016). Adsorpsi Besi dan Bahan Organik pada Air Gambut oleh Karbon Aktif Kulit Durian. *JKK*, 5(3), 31-39, <https://jurnal.untan.ac.id/index.php/jkkmipa/article/view/14912/13136>
- [2] Muthia, E., Amalia, E.P., Aulia, R., Erdina, L.A.R., Mahmud, M.C.A., Raissa, R., Dede, H.Y.Y. & Muhammad, R.B. (2021). Combination of Coagulation, Adsorption, and Ultrafiltration, Processes for Organic Matter Removal From Peat Water. *Sustainability*, 14,1, doi: 10.3390/su14010370
- [3] Endaruji, S. & Khaerul, H. (2016). Kajian Adsorpsi remozal yellow FG oleh montmorillonite-kitosan. *Integrated Lab Journal*, 4(2), <https://moraref.kemenag.go.id/documents/article/98077985952846307>
- [4] Taer, E., Mustika, W. S. & Sugianto. (2016). Pemanfaatan Potensi Tandan Kosong Kelapa Sawit Sebagai Karbon Aktif untuk Pembersih Air Limbah Aktivitas Penambangan Emas. *Jurnal Komunikasi Fisika Indonesia*, 13(13), <http://dx.doi.org/10.31258/jkfi.13.13.852-858>
- [5] Langenati, R. M., Mordiono, R., Mustika, D., Wasito, B. & Ridwan. (2012). Pengaruh Jenis Adsorben dan Konsentrasi Uranium Terhadap Pemungutan Uranium Dari Larutan Uranil Nitrat. *Jurnal Teknik Bahan Nuklir*, 8(2), <https://jurnal.batan.go.id/index.php/jtbn/article/view/812/732>
- [6] Oladipo, A.A., Olatunji, J.A., Adewale, S.O. & Abimbola, O.A. (2017). Bio-derived MgO Nanopowders for BOD and COD Reduction from Tannery Wastewater. *Journal Water Process Engineering*, 16, doi: 10.1016/j.jwpe.2017.01.003
- [7] Rasuli, L., Amir, H.M. (2016). Removal of Humic Acid from Aqueous Solution Using Magnesium(II) Nanoparticles. *University of Medical Science*, 30(1), doi: 10.3103/S1063455X16010045
- [8] Ghalekhondabi, V., Alireza F. & Keyhan K. (2021). Synthesis and Characterization of Modified Activated Carbon (Magnesium(II)/AC) for Methylene Blue Adsorption: Optimized, Equilibrium Isotherm and Kinetic Studies. *IWA Publishing : Water Science and Technology*, 83(7), doi: 10.2166/wst.2021.016
- [9] Arh-Hwang, C. & Shin-Meng, C. (2009). Biosorption of Azo Dyes From Aqueous Solution by Glutaraldehyde-Crosslinked Chitosans. *Journal of Hazardous Materials*, 172, doi: 10.1016/j.jhazmat.2009.07.104
- [10] Apriani, R., Faryuni, I, D. & Wahyuni, D. (2013). Pengaruh Konsentrasi Aktivator Kalium Hidroksida (KOH) terhadap Kualitas Karbon Aktif Kulit Durian sebagai Adsorben Logam Fe pada Air Gambut. *Jurnal Prisma Fisika*, 1 (2), doi: 10.26418/pf.v1i2.2931
- [11] Aluyor, E. A. & Badmus, A.M. (2008). COD Removal from Industrial Wastewater using Activated Carbon Prepared from Animal Hons. *African Journal of Biotechnology*, 7(21), [https://www.researchgate.net/publication/242202195\\_COD\\_removal\\_from\\_industrial\\_wastewater\\_using\\_activated\\_carbon\\_prepared\\_from\\_animal\\_horns](https://www.researchgate.net/publication/242202195_COD_removal_from_industrial_wastewater_using_activated_carbon_prepared_from_animal_horns)
- [12] Maesara, S.A. & Tresna, D.K. (2011). Penyisihan Besi dan Zat Organik Menggunakan Karbon Aktif dari Kulit Durian sebagai Media Filtrasi. *Jurnal Teknik Lingkungan*, 17(2), doi: 10.5614/jtl.2012.8.2.7
- [13] Sopiah, N., Prasetyo, D. & Aviantara, B.D. (2017). Pengaruh Aktivasi Karbon Aktif dari Tandan Kosong Kelapa Sawit Terhadap Adsorpsi Cadmium Terlarut. *J. Riset Teknologi Pencegahan Pencemaran Industri*, 8(2), doi: 10.21771/jrtppi.2017.v8.no2.p55-66
- [14] Mawaddah, D., Zaharah T.A. & Gusrizal. (2014). Penurunan Bahan Organik Air Gambut menggunakan Biji Asam Jawa. *Jurnal Kimia Katulistiwa*, 3(1), <https://jurnal.untan.ac.id/index.php/jkkmipa/article/view/5022/5141>
- [15] Hustiany, R. & Rahmi, A. (2019). *Kemasan Aktif Berbasis Arang Aktif Tandan Kosong dan Cangkang Kelapa Sawit*. Purwokerto: CV. IRDH.
- [16] Gova, A.M. & Oktasari, A. (2019). Arang Aktif Tandan Kosong Kelapa Sawit sebagai Adsorben Logam Berat Merkuri (Hg). *Prosiding Seminar Nasional Sains dan Teknologi Terapan*, Palembang: Universitas Islam Negeri Raden Fatah.
- [17] Istiana, S., Jumaeri & Agung T.P. (2020). Preparasi Arang Aktif Trembesi Magnetit untuk Adsorpsi Senyawa Tannin dalam Limbah Cair. *Indo. J. Chem*, 9:4, <https://journal.unnes.ac.id/sju/index.php/ijcs/article/view/28228/15736>

**Utilization of Activated Carbon/Magnesium(II) Composites in Decreasing Organic Materials**

---

- [18] Nga, N.K., Nguyen, T.T.C. & Pham, H.V. (2020). Preparation and Characterization of a Chitosan/MgO Composite for the effective removal of reaction blue 19 dye form aqueous solution. *Journal of science: Advanced Materials and Devices*, 5(1). doi: 10.1016/j.jsamd.2020.01.009
- [19] Khaleel, W.A., Sinan, A.S., I.A.M. Alani., M.H.M. & Ahmed. (2019). Magnesium oxide (MgO) thin film as saturable absorber for passively mode locked erbium-doped fiber laser. *Elsevier: Optic & Laser Technology*, 115, 331-336. doi: 10.1016/j.optlastec.2019.02.042
- [20] Rahmayani, I., Zaharah, A. T. & Alimuddin, H. A. (2020). Karakterisasi Adsorben Komposit Selulosa-Limbah Karet Alam untuk Penurunan Kadar COD dan Minyak Lemak LCPKS. *Jurnal Kimia Khatulistiwa*, 8(3), 2303-1077, <https://jurnal.untan.ac.id/index.php/jkkmipa/article/download/38840/75676584893>
- [21] Baloga, H., Walanda, D. K. & Hamzah, B. (2019). Pembuatan Arang dari Kulit Nangka (*Artocarpus Heterophyllus*) Sebagai Adsorben Terhadap Kadmium dan Nikel Terlarut. *Jurnal Akademika Kimia*, 8(1), 2477-5185, doi: 10.22487/j24775185.2019.v8.i1.2349



9 772614 875DD8



Kampus 3 Universitas PGRI Madiun  
Jl. Auri No 14-16 Kartoharjo Madiun  
Email: [cheesa@unipma.ac.id](mailto:cheesa@unipma.ac.id)  
<http://e-journal.unipma.ac.id/index.php/cheesa>

